DARESBURY LABORATORY

JOINT CCP4 and ESF-EACBM NEWSLETTER on PROTEIN CRYSTALLOGRAPHY

An Informal Newsletter associated with the SERC Collaborative Computational Project No.4 on Protein Crystallography and the ESF Network of the European Association of the Crystallography of Biological Macromolecules

Number 26 April 1992

Contents

Editors: Wojciech M. Wolf

Keith S. Wilson

Science and Engineering Research Council
Daresbury Laboratory, Daresbury
Warrington, WA4 4AD, England

EMBL c/o DESY
Notkestrasse 85, D-2000 Hamburg 52
Federal Republic of Germany

CCP4 installation and start up

Peter J Daly
Daresbury Laboratory, Warrington, WA4 4AD

Kim Henrick
CCPE, Hills Road, Cambridge, CB2 2QH

Eleanor Dodson
University of York, Heslington, York, Y01 5DD

March 22, 1992

1 Introduction

The CCP4 Program Suite has developed rapidly over the last twelve months and several changes have been made to the installation of the suite under both Unix and VMS and the way in which the programs themselves start up. This paper discusses the current situation and offers guidelines for others who may wish to deposit programs with CCP4.

A new version of CCP4 is about to be made available at the end of March, 1992 using the new MTZ file format (discussed elsewhere in this newsletter) and these changes will be reflected in that version.

The core programs of the CCP4 Program Suite will be available to non-profit making organisations via *anonymous-ftp* from Daresbury (see the article *"The CCP4 Bulletin Board, Info-Server and ftp"* elsewhere in this newsletter. Profit making institutions should contact the Secretary to CCP4 at the above address for the conditions of use that apply to them. Updates will, as usual, be available via the Daresbury Info-Server.

2 The CCP4 Directory Structure

It should be noted that the CCP4 Distribution Tape contains several other items of software that are not strictly part of the CCP4 Program Suite but are merely aggregated to the media since users may find such software useful. This, of course, implies that periodic housekeeping takes place and the directory structure shown in figure 1 should not be considered entirely static.

```
                |-bin-          # symbolic link to executables directory
                |-ccp4bb-       # Bulletin board messages
                |-doc-          # documentation from man pages
                |-etc-          # ccp4 shell scripts
                |-examples-     # vms and unix example files
                |-help-         # vms-like help system
      |-ccp4------|-include-     # ccp4 start up and header files
      |           |-lib--|-src-  # ccp4 library routines
      |           |      |-data- # ccp4 library data files
      |           |-man-         # man pages
      |           |-misc-        # site specific routines
      |           |-src-         # ccp4 program sources
      |           |-test-        # test files
      |
      |-corels-                  # corels    aggregated to ccp4
      |-film-                    # MOSLFM    aggregated to ccp4
-xtal-|-gilliland-               # gilliland aggregated to ccp4
      |-groningen-               # mdf format manipulation
      |-laue-                    # laue source (uses ccp4 libs)
      |-misc-                    # older unsupported programs
      |-ribbon--|-leeds-         # ribbon    aggregated to ccp4
      |-skew-                    # skew      aggregated to ccp4
      |-other_directories...     # other site dependent directories
```

Figure 1: Directory structure of CCP4

The directory structure itself is consistent under Unix and VMS and should be adhered to by any user porting the suite to another Operating System.

3 Installation

The directory include contains a startup file that needs to be edited to your local conditions. Under Unix it is called ccp4.setup; this file should then be sourced by all users wishing to use the CCP4 Program Suite in their .login files.

Under VMS it is called CCP4.COM and should be executed as part of the group login.

3.1 Under Unix

Installation of the suite is assisted under Unix by a set of Makefiles. For sites with more than one machine, it is recommended that the suite is installed on a single machine and other machines access the source code by nfs mounted disks. This is the set up at Daresbury. There is also a script cmake which helps to make the executables on the machine where the source is not installed. It assumes you can get to the source directories via the *nfs* file system.

Installation of CCP4 is complete in the following stages:

1. obtain an account called ccp4 set up the .login and .cshrc files in the home directory ~ccp4.

2. read in the tape — it is recommended that the top level directory is called /public/xtal and is separate from the ccp4 login home directory ~ccp4.

3. edit the file ccp4.setup in ccp4/include. You *must* edit the following environment variables:

```
CCP4_MASTER - top level directory for the suite
CCP4_SCR    - scratch disk for each user (use /scratch/$USER).
              Try to avoid /tmp as this is used by the system.
CCP4_BIN    - the directory for (binary) executables.
CCP4_LIB    - the directory for (binary) objects.
BINSORT_SCR - scratch directory for non-memory sort.
```

   You *may* wish to edit the following environment variables:

```
CCP4_OPEN   - set to 'UNKNOWN' or 'NEW' to stop open failures
              for files opened as NEW that already exist.
BINSORT_MEM - array size for in memory sort
MANPATH     - path for manual pages (not available on convex)
LD_PATH     - Used by linker to search for libraries (alliant only)
```

4. each user wishing to use CCP4 should then add a line to his .login file to source the ccp4.setup file. This must include the full path name since no logical names are known until this file is executed, for example, add the following line to the .login of the ccp4 id.

   source /public/xtal/ccp4/include/ccp4/ccp4.setup

   You can then, as a brief test, log out and then log back in and check the values of $CCP4_MASTER, etc.

5. *multiple machine sites only* need to do further edits to the ccp4.setup file and change the hostnames to their machine names and the appropriate environment variables. Look at ccp4.setup for further details.

6. now go and edit the top level Makefile in ccp4. In this you will need to specify the names of your Fortran and C Compilers as well as their flags. A brief table is shown at the top that covers most machines.

   The CCP4 administrator can choose to make the (binary) MTZ data files machine independent by adding the option -DCONVERT to the CFLAGS option. THis conditionally compiles in some code to make the files readable on all machines using some public domain utilities.

   You also need to specify the directory for (binary) executables and (binary) objects. For *multiple machine sites* these edits should apply to the machine that the suite is installed on.

7. You can now apply these edits to the other makefiles in the suite by typing make install.

8. *multiple machine sites only* need to do further edits to the file cmake in ccp4/bin and change the hostnames to their machine names and the appropriate environment variables.

9. go to the library source area ccp4/lib/src and check the file unix.for, in particular, the routines USTIME, UTIME and UBYTES. Also check the comment in the routine CCPOPN in ccplib.for regarding Fortran Carriage Control under Ultrix.

10. now make the binsort procedure with make binsort or *for multiple machine sites* use cmake binsort.

11. now make the library libccp4.a with make or *for multiple machine sites* use cmake.

12. goto to the library data area ccp4/lib/data and use make or cmake (as appropriate) here.

13. finally, go to the source code area ccp4/src and use make or cmake (as appropriate) here.

3.2 Under VMS

On the VMS version there are a set of command procedures (all called MAKEFILE.COM) to install the software. Just run the appropriate file in the directories [public.xtal.lib.src], [public.xtal.lib:data], [public.xtal.src]. To re-make a particular program go to the program source area and use the command procedure make.com with the target to be made as an argument.

4 Running the programs

When a CCP4 program starts up it goes through a pre-processing stage before the main body of the program is run (see figure 2). It starts by reading in a file called environ.def (in the `include` sub-directory) — this file specifies the logical names that can be expected and some information about the type of file associated with each logical name e.g. a typical line may be 'SYMOP=in.lib', which says that the logical name SYMOP is associated with a file that is input only ('in') and has a default extension of .lib; other file types are 'out' (output only) and 'inout' for both types.

After this stage, the pre-processor then reads in the file default.def, which specifies some common logical names and hence are defined for all CCP4 processes. A typical line here may be 'SYMOP=symop.lib' and means that the logical name SYMOP will be associated with the file symop.lib.

Finally, the command line arguments are parsed and the logical name / file name pairs are matched up and assigned. Here a logical name that has not been defined in environ.def causes the name to be added to its internal list and a warning issued.

Within this procedure are several devices to make running the program easier. Firstly, files without extensions have them appended using the default value. Secondly, certain files are checked for in certain directories, for example, files that end in '.lib', '.dic', '.bes', '.prt' and do *not* have a full path name have the directory $CLIBD put in front of them (so, SYMOP will actually be associated with $CLIBD/symop.lib). Furthermore, files that end in '.scr' are deemed to be scratch files and are assigned to the scratch disk.

Files of type 'in' are checked for existence and the program fails with a message if it can't find it. Output files that already exist will also cause the program to stop unless the environment variable CCP4_OPEN is set to 'UNKNOWN' in which case they will be truncated to zero, overwritten and a warning message displayed.

5 Command line Switches

The programs can take several command switches to modify the pre-processing that is done. They are detailed below.

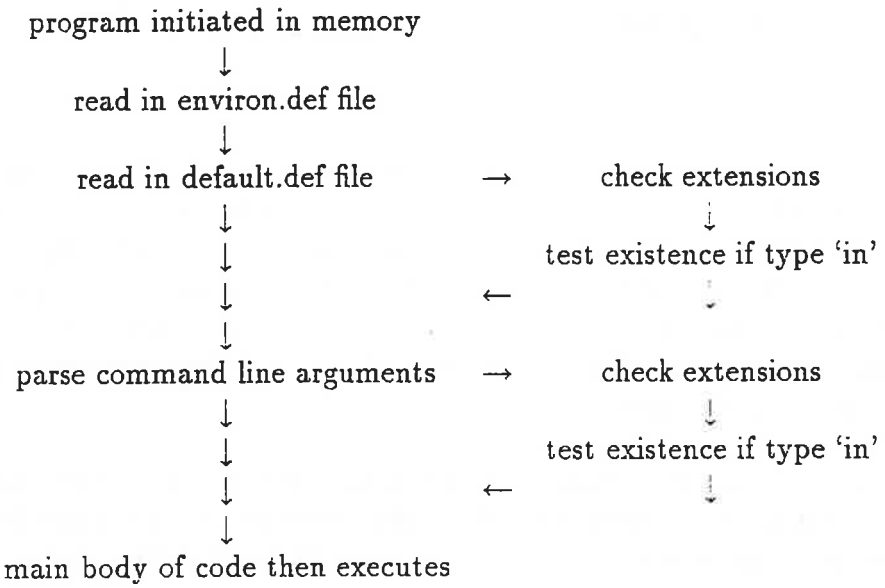

Figure 2: Description of CCP4 Program startup

-n	Do not read the global files default.def and environ.def
-v 0-9	Verbose output. Can also use -h instead of -v. Higher values give more debug information from the program, the default value is 0. An error occurs if you omit the number.
-d file	Specify an alternative to the default.def file
-e file	Specify an alternative to the environ.def file
-x exe	Use next argument as the name of the executable to use rather than the current one once all pre-processing has been completed. Can be used, for example, to specify an X-Windows version of the executable or as a front end to test programs — this option is only available under Unix.

6 example

This report is not a discussion of CCP4 so only the command line will be given, the keywords are omitted:

```
#!/bin/csh -f
sfall HKLOUT ~/test_out XYZIN BRK/test_brk \
      HKLIN  test_mtz << 'EOF-sfall'
```

```
.
.
your keywords here
.
.
'EOF-sfall'
#
```

The line `#!/bin/csh -f` is a Unix device to make the script execute in the C shell. Notice how the input is re-directed to the lines between the delimiters `'EOF-sfall'`.

The VMS example is given below and is reasonably close to the Unix one:

```
$ ASSIGN SYS$INPUT  DATA
$ ASSIGN SYS$OUTPUT PRINTER
sfall HKLOUT [sub\_dir]test_out XYZIN [.BRK]test_brk -
      HKLIN  test_mtz
.
.
your keywords here
.
.
$ EXIT
```

7 Using the Pre-processor in programs

For those who wish to use the pre-processor, the only thing you need to add to your code is a call to the routine CCPFYP as the *first* executable statement in your main program. This routine performs all of the pre-processing.

Under VMS, of course, it requires that the program is set up as a symbol so that the command line arguments are available to the pre-processor. Use something like: "program_name == "$ CCP4_BIN:program_name.exe".

For users wishing to deposit programs with CCP4 the above call is mandatory. Furthermore, there should be *no* STOP statements within the code but rather use the new call CCPERR. This has the form CALL CCPERR(num, string); where num is an exit value (0 for normal termination) and the string is a suitable message. All programs should have CALL CCPERR (0, 'Normal Termination') as the last CALL. This is used by Unix to produce user and system times.

8 Documentation

Users should be aware that *all* documentation is now expected to be in the form of Unix man pages. There is a shell script man2doc to convert this to document suitable for VMS.

9 Testing an unknown machine

If you wish to port CCP4 to a machine that has not been tested or tried before follow the steps below. After you are successful, please send the updated code back to Daresbury so it can be included into the suite for other users.

The main problem in porting CCP4 is now in the very lowest level interface and a small test program exists to test these routines. You will need the following routines in their entirely: unix.for, diskio.for, Testlib.for and library.c. You will also need the following routines from the files named in brackets: lenstr (parser.for) and ccpupc, litend, ccpfyp, fdir, froot, fextn, and setenv (ccplib.for). All these programs are in the library source area.

You may then compile them together after you have checked unix.for, particularly the routitne UTIME, USTIME and UBYTES. If your machine does not have these routines in its Fortran library you will need to re-write them in C that is Fortran callable.

Check the Fortran to C bindings in library.c (you can contact CCP4 for some help with this).

Run the test program. You can have several environment variables to change the way it runs — try the following examples:

```
a.out TESTENV test_val DISKIO disk.dft
a.out -v 3 TESTENV test_val DISKIO disk.dft
```

MTZ FILES

The new CCP4 standard format for reflection data files

Sandra M. McLaughlin
EMBL, c/o DESY, Notkestraße 85, 2000 Hamburg 52

(1) Introduction

The new version of the CCP4 program suite (available to academic users from 31st March 1992, and discussed elsewhere in this newsletter) is very different to the old one in many respects. One of the major changes which will affect every user of the suite is the fact that the reflection file format has been revised. Therefore all existing "LCF" files will have to be converted to the new format before they can be processed by the new suite. An entirely new set of routines has been developed to handle these files, and of course this will affect anyone who wishes to write even a small "jiffy" program to manipulate their files (and any existing local programs will have to be converted).

The new reflection data file format, known as MTZ, is an enhancement of the LCF format. Both types of old LCF files (standard and multi-record) have direct MTZ counterparts - "Standard-MTZ" files are used by the programs of the suite after the initial data processing stages have been completed. The MTZ file has one record per reflection, plus the header information. "Multi-record-MTZ" files are used for handling unmerged data during the initial data processing stages. In these files each reflection occupies one record which is distinguished by different batch numbers, symmetry numbers,etc., held as additional columns. These differ from standard MTZ files only in the additional header records containing the batch title and orientation data.

The major improvements/differences in the reflection data files are :

(i) More information is stored in the header records of the MTZ files (see below)

(ii) The data is all held as 4 byte REAL values (instead of 2 byte INTEGER), thus increasing accuracy

(iii) The subroutine library to handle the MTZ files has a much simpler user interface.

(iv) The S column which was present in all "standard" LCF files has been removed - values of ($4\sin^2$ theta / lamdba^2) are calculated and returned, for each reflection, by the calls to the subroutines which read reflection records from the file, and the maximum and minimum values are stored in the header of the MTZ file as REAL*4 (previously 10000*S as INTEGER*2)

(2) MTZ file format

The MTZ reflection file format uses fixed length records with, in general, four bytes for each data item (REAL*4), with a minimum of six columns (and currently a maximum of 200 columns, though this limit is imposed only by the software) of data per record. Additional information (title, cell dimensions, column labels, symmetry information, resolution range, history information and, if necessary batch titles and orientation data) is contained in labeled header records. The columns of the reflection data records are identified by alphanumeric labels held as part of the file header information. The user relates the item names used by the program to the required data items, as identified by the labels, by means of assignment statements in the program control data.

The file contains basically two classes of records - header records and reflection data records. A standard reflection data file contains the following items in the order given, not necessarily all item have to be present :

. MTZ identification record
. Reflection data
  - columns of data held as REAL*4
. A Beginning of header record
. A set of keyworded records containing
  - VERS Version of routines which wrote the file
  - TITLE File title - short identification of file
  - NCOL Number of columns, reflections and batches present in file
    if number of batches > 0, this indicates a multi-record file
  - CELL Cell Parameters
  - SORT Sort order of first 5 columns in file
  - SYMINF Various symmetry information -
    Number of symmetry operations, number of primitive operations,
    lattice type, space group number, space group name, point group name

- SYMM Symmetry operations in international tables style
- RESO Min. and max. resolution stored as $1/d^2$
- COLUMN Column label, type and min. and max. values, for each column
- BATCH batch serial numbers present in the file
  this line is not present if number of batches is 0

. End of main header card

. Up to 30 (Character*80) lines containing history information

. For multi-record files

- batch title and optionally orientation data for each batch present in the file

.End of all headers record

Column types are an extra check that the user input assignments for a requested program label is of the correct type. A full list of available column types can be found at the end of this article.

(3) Subroutines for handling MTZ files

A set of subroutines has been developed for reading and writing MTZ reflection data files. The first argument to all the subroutines calls in MTZLIB is INDEX - this should be considered as equivalent to the last character of the name of the old LCF subroutines (e.g. SRLCF1 = LROPEN(1,.....)). This allows more than one pair of MTZ files to be open for read and write at the same time, without the need for separate subroutines. At present a maximum of 6 files can be opened simultaneously (3 for read and 3 for write), but this is a restriction imposed by the software and could be easily extended.

The subroutines of an INDEX pair share an area of storage for the header data (e.g. for the cell parameters, label and title information etc.), so that when an input file has been opened, the header information is available for writing to an output file, without being explicitly copied over by the calling program. This information may be replaced of new information may be added depending on the requirements of the output file - or it may be created in the program if no input file was read.

The philosophy of the subroutines is slightly different from the old LCF routines - with LCF the call to SRLCF1 opened the LCF file and returned most of the information stored in the file header, with MTZ the call to open the file for read, LROPEN, simply opens the file and reads all the header into internal storage - other, separate, subroutines are provided to retrieve items of header information, thus the programmer can ask for only those header items which he requires, and the calls are much simpler.

All the subroutines in MTZLIB are written in ANSI standard FORTRAN 77.

A list of all the subroutines in MTZLIB can be found at the end of this article - for more details on the use of these subroutines refer to the MTZLIB documentation. These subroutines are in the CCP4 library - $CLIB/libccp4.a (Unix) or $CLIB:LIBCCP4.OLB (VMS). The documentation can be found in mtzlib.doc in the $CDOC directory. Guidelines for converting existing programs from LCF to MTZ software can be found in the files guide.doc and equicalls.doc, which are on the CCP4 distribution.

(4) Acknowledgments

The development of the MTZ files and associated software is part of the masterplan of the ESF/EACBM Working Group 2.1 for better Protein Crystallographic software for Europe. They were developed by members of this Working Group in collaboration with members of the CCP4 Working Group 2.

Appendix 1 - Column types defined in MTZ reflection data files

H	index h,k,l
J	intensity
F	structure amplitude, F
D	anomalous difference
Q	standard deviation of anything: J,F,D or other
P	phase angle in degrees
M	figure of merit (0 to 1.0)
W	weight (of some sort)
A	phase probability coefficients (Hendrickson/Lattmann)
B	BATCH number
Y	M/ISYM, packed partial/reject flag and symmetry number
I	any other integer
R	any other real

Appendix 2 - A complete list of subroutines in the MTZ package

The initialization routine for the file handling system :

MTZINI This MUST be called first

The subroutines for MTZ files which have been opened for read are :

LROPEN Open MTZ file for read

LRASSN Set up the input column assignments

LRBATS Return total number of batches, and their serial numbers from the MTZ header (for multi-record files)

LRBRES Reset batch header reading pointer

LRCELL Return the Cell dimensions from the MTZ header

LRCLAB Return the Column labels and types from the MTZ header

LRHIST Return the history information from the MTZ header

LRINFO Return general info (no.of cols, ranges etc.) from the MTZ header

LRNCOL Returns number of columns from the MTZ header

LRRSOL Return the minimum and maximum resolution from the MTZ header ($1/d^2$)

LRSORT Return the sort order from the MTZ header

LRSYMI Return symmetry information (if available) from the MTZ header

LRSYMM Return symmetry operations (if available) from the MTZ header

LRTITL Return the title from the MTZ header

LRREFL Read a reflection record in file order from the MTZ file

LRREFF Read a reflection record in Lookup order from the MTZ file

LRNREF Return the number of the reflection record last read i.e. reports on position in file

LRSEEK Move to a specific reflection record number

LRREWD Rewind an LCF file for re-read

LRCLOS Close an MTZ file which has been opened for read

The subroutines for MTZ files which have been opened for write are :

LWOPEN Open MTZ file for write

LWASSN Set up the output column assignments, new columns etc.

LWCELL Update the Cell dimensions in the MTZ header

LWCLAB Write Column labels and types to an output MTZ file

LWHIST Append line to the history information in the MTZ header

LWSORT Update the Sort order in the MTZ header

LWSYMM Update the Symmetry operation in the MTZ header

LWTITL Append to or replace the title in the MTZ header

LWREFL Write a refection record to the MTZ file

LWCLOS Close an MTZ file which has been opened for write

The (extra) subroutines for multi-record MTZ files are :

LRBAT return batch information from the header for one batch

LWBAT write updated batch header for one batch

LRBSCL return selected values from the header for one batch

LRBTIT Return the batch title from the header for one batch

LWBSCL update selected values in the header for one batch

LWBTIT write batch title & dummy orientation block for one batch

LBPRT print batch information in pretty format called by LRBAT - calls LBPRTH (does the actual print)

The next 5 are internal subroutines :

LBPRTH does the actual printing for LBPRT

RBATHD read the actual header from the file and return the data items packed into a REAL and a CHAR array - called by LROPEN

WBATHD write the batch headers to the MTZ file open for write - the batch headers are written at the end of the file called by LWCLOS

LRHDRL read one line from the header on the file (calls qread)

LWHDRL write one line to the header on the file (calls qwrite)

The utility subroutines for MTZ files are :

LKYIN These subroutines should be used by the calling program to parse any label

LKYOUT assignments (input and output) made by the user

LKYSET Similar to LKYIN except the "lookup" array is passed back to the program

LHPRT Subroutine to output data from an MTZ header mark 1

LPHIST Print the history information from the MTZ header

These last 8 are internal subroutines :

SYMFR3 These are the only symmetry subroutines called from the MTZ subroutines mark 1.

SYMTR3 They are both slight modifications of subroutines from Eleanor Dodson

SORTUP INTEGER version of indexed Singleton sort - copied from STILLS program.

LABPRT Subroutine used to output character strings (e.g. column labels) nicely across 80 character page

ADDLIN Subroutine to add a new line to a character array

NEXTLN Function to find the next empty line in a character array

LSTRSL Routine to calculate coefficients for $(\sin(\theta)/\lambda)^2$ from h,k,l for general axes

LSTLSQ Function to calculate $(\sin(\theta)/\lambda)^2$ from h,k,l - coeff's set by call to LSTRSL

The CCP4 Bulletin Board, Info-Server and ftp

Peter J Daly
Daresbury Laboratory, Warrington, WA4 4AD

March 22, 1992

1 Introduction

This article is a brief introduction to the CCP4 Bulletin Board and Info-Server and anonymous-ftp and perhaps a timely reminder for some about which address to use. There are *three* separate e-mail addresses so, please take time to appreciate them so that spurious messages are not distributed to the rest of the community.

2 anonymous-ftp

In order to reduce the number of tapes to be written the essential core of CCP4 Programs can now be obtained from Daresbury via anonymous-ftp. It should be noted, however, that this in no way relieves the end user of the need to return a licence agreement (a copy is now to be found as an appendix to the manual). Commercial users of CCP4 *must* still obtain the right to access the source from CCP4 before any transfer takes place.

The Internet address of this service is: **148.79.80.10**. Users should log in with the id ftp and the password as the host name of their machine. There is a sub-directory *ccp4*, which contains the relevant files.

The files are held as compressed, tar files to reduce the size of them. There are currently three such file: one for sources (~ 3.2Mbytes), one for the libraries (~ 1.1Mbytes) and finally the man pages (~ 0.5Mbytes). There are some other files here as well in plain ascii format: the manual as a latex file Install.tex and a README file.

A typical ftp session may go like this; not all output from ftp is shown but the general idead is given (italics are your input):

ftp 148.79.80.10
Connected to 148.79.80.10
Name : *ftp*
Guest login ok, send ident as password
Password: *dlpx1*

Guest login ok, access restrictions apply
ftp> *cd pub/ccp4*
ftp> *binary*
ftp> *get src.tar.Z*
ftp> *get libs.tar.Z*
ftp> *bye*
Goodbye.

You then need to uncompress and untar the files as follows (example shown for one of the files only):

uncompress src.tar.Z
cd $CPROG
tar xvof src.tar

3 The CCP4 Bulletin Board

The *CCP4* Bulletin Board is intended to be a forum for discussion, to query aspects of the CCP4 Program Suite, to publicise or announce meetings, etc. or to ask the user community for help. Messages may be sent to the Bulletin Board by *anyone*, and the system re-broadcasts it to a list of *known* subscribers. The address to send messages to the Bulletin Board is:

`CCP4BB@DARESBURY.AC.UK`

It is simply a mail forwarding system and digests of the messages sent to the Bulletin Board are kept in the directory ~/xtal/ccp4/ccp4bb. Each message has a message number and missing numbers are either job advertisments of announcements of meetings, which are soon out of date and so are not kept.

4 The Bulletin Board Subscriber Service

In order for you to *receive* messages from the Bulletin Board, you must first inform the system that you wish to subscribe to a particular list (a brief table of the lists available to subscribe to, and an indication of the number of subscribers is given at the end of this article, it is interesting to note that CCP4 is the largest group currently subscribing to any of the lists). In its simplest form send the message 'SUB CCP4BB' to:

`CCP4BB-REQUESTS@DARESBURY.AC.UK`

Note: take care with the address to manipulate your access to the list it is *CCP4BB-REQUESTS*, a common error is to send the message to CCP4BB, which results in the user community getting the message and no action taken by the system.

Messages to ccp4bb-requests are processed sequentially, blank lines are ignored and all commands are treated case *insensitive*. Your e-mail address will be worked out by the server. This address can be changed with the RETURN-PATH command. A brief guide to the commands follows:

SUB LIST-NAME [e-mail-address] Use SUB to put yourself on a list. Specify the list you want to submit to after the SUB command. For example to put yourself on the CCP4 Bulletin Board send:

```
SUB CCP4BB
```

The SUB command also recognises an e-mail address as an optional argument. If an address is given then this will be the one added to the list rather than the one appearing in the header of a message, eg:

```
SUB CCP4BB CCP4@UK.AC.DARESBURY
```

A sign-on message will be sent to anyone who is added to a list.

UNSUB LIST-NAME [e-mail-address] Use UNSUB to delete yourself from a list you have previously SUB'd to. Specify the list you want removing from after the UNSUB command. For example to remove yourself from the CCP4 list send:

```
UNSUB CCP4BB
```

The UNSUB command also recognises an e-mail address as an optional argument. If an address is given then this will be the one added to the list rather than the one appearing in the header of a message, eg:

```
UNSUB CCP4BB CCP4@UK.AC.DARESBURY
```

A sign-off message will be sent to anyone who is removed from a list.

INFO Use the INFO command to ask the server for a summary of the lists it supports and your current status with the server. For example, the output from an INFO command is:

```
CCP4BB              --> "Your Address" subscribing.
```

GREP SEARCH-STRING [LIST-NAME] is a case *insensitive* search through all the servers known mailing lists for the SEARCH-STRING supplied. This feature will be useful to anyone who knows they are on a list, but cannot remember what machine/address they used to subscribe. For example, the output from an GREP command is:

```
*GREP pjd

The string "pjd" appears in the following lists:
```

```
<CCP4BB>          pjd@uk.as.daresbury.cxa

End search.
```

The GREP command takes an optional list name to restrict a search to the one specified.

SEND-LIST LIST-NAME SEND-LIST will send back a list of the current subscribers to the named bulletin board

```
SEND-LIST CCP4BB
```

will return a list of known CCP4 subscribers

QUIT QUIT halts further processing by the server, ie nothing past this point is processed. This is provided so that people who have signatures, etc automatically appended to outgoing mail messages can stop the server from trying to interpret them.

HELP Send this help file. GUIDE is an alias for HELP.

RETURN-PATH e-mail-address changes the e-mail address the server uses for submission and unsubmission to lists. It also applies to any messages it sends back to you. The new return path you give the server must be valid from the JANET network, ie if you're on the INTERNET the return path must include NSFNET-RELAY.

The server automatically works out what relays to use so you should not normally have to use the RETURN-PATH command. If you don't get responses from the server and you suspect its because of problems encountered working out how to get mail back to you the best bet is to send a message to the server administrator (address given at the bottom of this file) asking for manual assistance.

Note: If you SUB after changing your e-mail address using the RETURN-PATH command you will need to respecify your return path when you UNSUB.

5 The Info-Server

It is worthwhile describing how the info server works before discussing the details of obtaining fiiles from it. The info-server itself is a unix machine that has a large disk capacity. The unix version of the CCP4 Program Suite is linked directly to these disks using the *nfs* file system and is thus indistinguishable from other info-server software that is available. The VMS version of the software is held on a VAX and a global index is pulled across each night by the info-server, users requesting VMS sources have their file requests checked against this index and, if appropriate, they are then the transferred from the VAX to the info-server for subsequent mailing. This is more limited service.

The *Complete Guide to the Daresbury Info-Server and Database* is also available in /Bootstrap/info-server-doc.ps.uue. Note that it is held as a uuencoded PostScript file.

Users may request printed copies from the library or by sending an e-mail message with your snail-mail address to the info-server manager at POSTMASTER@UK.AC.DARESBURY.

The e-mail address of the info-server is:

```
INFO-SERVER@DARESBURY.AC.UK
```

The Subject field of the message is **not** to be used. You should receive a message acknowledging the request in addition to the requested file — this extra file is for accounting purposes at Daresbury.

5.1 Examples

A vast range of free and public domain software is available using the Unix filenames. In the examples below the left side shows a request for the code from the unix machine and the right from the VAX computer that holds the VMS version of the software.

To get an index of a particular directory (for recursive index use rindex) ,but note that only the top level index exists on the VAX machine:

```
REQUEST: index
TOPIC: /CCP/xtal/lib/src
REQUEST: end
```

```
REQUEST: crystal
TOPIC: index
REQUEST: end
```

To get source files:

```
line-limit: 950
Coding: off
REQUEST: sources
TOPIC: /CCP/xtal/src/sfall.for
REQUEST: end
```

```
line-limit: 950
Coding: off
REQUEST: crystal
TOPIC: [public.xtal.src]sfall.for
REQUEST: end
```

The *line-limit* option specifies the largest file before the source is split and sent as a series of parts. The *coding* option specifies that the source is not encoded before transmission — the default is to send files in Unix uue format.

There is a program recon.c that will reconstruct your program from the mail message parts - also available on the info-server in /Bootstrap/recon.c as a plain file, but beware, some mail gateways mess up the curly brackets used in C code.

6 Bulletin Board Lists at Daresbury

List Name	Number of subscribers	List Use
Sun-Academic-News	12	newsletter for academics distributed by Sun
GPC	9	Genes Proteins and Computers programme committee
SCUD	4	Seqnet CCP11 Documentation Group
CCP4BB	**219**	**Collaborative computing project number 4**
CCP5	1	Collaborative computing project number 5
CCP6	1	Collaborative computing project number 6
ARCUser	159	Advanced Research Computing
Archimedes-Users	10	A list for users of the acorn Archimedes
STPBB	2	Software through pictures
VMEUser	20	A list for VME users
SunSpots	4	Sun spots digest in its entirety
TOCSunSpots	5	Sun spots digest table of contents
InfoMac	5	Info mac digest in its entirety
TOCInfoMac	1	Info mac digest table of contents
InfoUnix	2	Info unix digest in its entirety
TOCInfoUnix	2	Info unix digest table of contents
UnixWizards	1	Unix wizards digest in its entirety
TOCUnixWizards	1	Unix wizards digest table of contents
Atari	3	Discussions of everything atari
info-ibmpc	2	Info IBMPC digest
info-electronics	25	A list for the disemination of information & comments on Electronic Hardware.

LOCAL

Local Scaling Program for Heavy Atom Derivatives

Ian J. Tickle

Department of Crystallography, Birkbeck College, London WC1E 7HX

The purpose of this program is two-fold:

1. To scale or re-scale isomorphous heavy atom derivative data to the native.
2. To re-scale the Friedel-related amplitudes, where they have been kept separate, in order to improve the anomalous scattering information.

If both operations are required, then two runs of the program will be necessary. Normally the isomorphous scaling will be done first, the anomalous scaling being less critical.

The program consists of two main sections, either or both of which can be executed. The first section scales the reflection amplitudes conventionally with an overall scale and anisotropic temperature factor, and the second re-scales the amplitudes by the "local scaling" technique. (Mathews, B.W. & Czerwinski E.W., *Acta Cryst.*, (1975), **A31**, 480-487).

The first section of the program is normally required to put the data on the correct relative overall scale (if this has not already been done), since it is possible to judge the effectiveness and reliability of the "local scaling" only from such a starting point. Statistical data is produced by the program to allow a critical evaluation of this procedure. In the light of this evaluation the user may decide to reject the "local scaling" results and use only the overall-scaled data.

The principle of "local scaling" is as follows: for each reflection an *individual* scale factor is calculated, based on the average relative scale in the local neighbourhood of reciprocal space. In practice, a sphere in reciprocal space, whose radius is defined such that it contains (approximately) a specified number of reflections, is centred on each reflection in turn. The reflections within the sphere are used to calculate the local scale factor of the central reflection, each reflection in the sphere being given a weight which decreases with the distance in reciprocal space from the centre. The central reflection itself is given the highest weight; this helps to reduce the bias in the squares of the differences arising from random errors.

The Minimisation Function

The scaling is done by least-squares, by minimising:

$$\sum_h w(tF_1 - F_2)^2$$

where: w is a weight and t is the scale factor to be determined. For isomorphous scaling $F_1 = F_{Derivative}$ and $F_2 = F_{Native}$; for the anomalous scaling $F_1 = F_+$, $F_2 = F_-$.

w is calculated from the supplied standard deviations in F_1 and F_2. These are normally based only on counting statistics for diffractometer data and therefore the program has provision for including a contribution from the fractional error in the measured intensity arising from other sources.

Thus:

$$\sigma^2(I) = \sigma_c^2(I) + (aI)^2$$

or:

$$\sigma^2(F) = \sigma_c^2(F) + (0.5aF)^2$$

Here a is the "instability factor", typically 0.05 to 0.1. The least-squares weight:

$$w = (t^2\sigma_1^2 + \sigma_2^2)^{-1}$$

For overall anisotropic scaling;

$$t = g \cdot exp(\mathbf{h}^\tau \beta \mathbf{h})$$

and the parameters g and β_{ij} determined in the usual way by iterative least-squares.

For local scaling the minimisation function is:

$$\sum_{\mathbf{h}'} f_{\mathbf{h}'} w_{\mathbf{h}'} (t_{\mathbf{h}'} F_{1\mathbf{h}'} - F_{2\mathbf{h}'})^2$$

where the $\mathbf{h}'$ subscript denotes only the reflections within a sphere radius s_o in reciprocal space centred on reflection $\mathbf{h}$. $f_{\mathbf{h}'}$ is an attenuation factor:

$$f_{\mathbf{h}'} = exp(-s^2_{\mathbf{h}'}/s^2_o)$$

where $s_{\mathbf{h}'}$ is the distance in reciprocal space of $\mathbf{h}'$ from h . Since the weight w varies with t, the minimisation function is not quadratic; hence the usual Taylor expansion in terms of powers of the change in t (initially $= 1$) is required. Only one iteration is performed, however, since the data is assumed to be on the correct overall scale. The shift in t is:

$$\delta t_{\mathbf{h}} = \frac{\sum_{\mathbf{h}'} f_{\mathbf{h}'} w_{\mathbf{h}'} v_{\mathbf{h}'} (F_{2\mathbf{h}'} - F_{1\mathbf{h}'})}{\sum_{\mathbf{h}'} f_{\mathbf{h}'} w_{\mathbf{h}'} v^2_{\mathbf{h}'}}$$

where:

$$v = \frac{F_2\sigma_1^2 + F_1\sigma_2^2}{\sigma_1^2 + \sigma_2^2}$$

The shift is "accelerated" to compensate for the non-linearity, and the final value of t is $(1 + 0.5\delta t)/(1 - 0.5\delta t)$.

Statistics

Statistics are tabulated before and after each scaling operation to allow critical evaluation of the results and also to point up "rogue" data; the user must therefore examine this output carefully to achieve the best results.

The data are sampled according to h, k, l, resolution, rms F_D and (for isomorphous scaling only) rms F_N. Columns labelled **A** to **N** in the output contain the following information:

A: Root weighted mean ratio;

$$\sqrt{\sum wt^2 F_1^2 / \sum wF_2^2}$$

This should be near 1 for all values of h,k,l and resolution. It will vary with rms F_D and F_N.

B: Mean difference;

$$n^{-1}\sum(t^2F_1^2 - F_2^2)$$

This should be small relative to column **C** (say $< 10\%$) for all values of **h, k, l,** and resolution. It will vary with rms F_D and F_N .

C: RMS difference;

$$\sqrt{n^{-1}\sum(t^2F_1^2 - F_2^2)^2}$$

Increase with h, k, l, or resolution would indicate lack of isomorphism. In theory it should be independent of rms F_D and F_N, but will probably not be in practice, owing to random errors.

D: RMS fractional intensity difference;

$$\frac{\sqrt{n\sum(t^2F_1^2 - F_2^2)^2}}{0.5\sum(t^2F_1^2 + F_2^2)}$$

E: Root weighted mean square residual;

$$\sqrt{\frac{\sum w(tF_1 - F_2)^2}{0.5\sum w(t^2F_1^2 + F_2^2)}}$$

This should decrease after scaling.

F: Weighted mean square deviation;

$$n^{-1}\sum w(tF_1 - F_2)^2$$

This is the minimisation function, and must therefore decrease after scaling. In addition, it should not vary strongly with rms F_D or F_N, and large deviations would indicate inappropriate weights. Increasing the instability factor(s) will reduce it for larger values of F_D and F_N.

G: Root mean variance of local scale factor;

$$\sqrt{\sum_h [\frac{(\sum f_{\mathbf{h}'} w_{\mathbf{h}'} \triangle^2_{\mathbf{h}'} - t \sum f_{\mathbf{h}'} w_{\mathbf{h}'} v_{\mathbf{h}'} \triangle_{\mathbf{h}'})}{(n-1) \sum f_{\mathbf{h}'} w_{\mathbf{h}'} v^2_{\mathbf{h}'}}]}$$

where:

$$\triangle = F_2 - tF_1$$

H: Root mean deviation of local scale factor;

$$\sqrt{n^{-1} \sum (t-1)^2}$$

This should not be significantly less than the variance in column **G**, otherwise the scaling is unlikely to have any useful effect.

I: Average number of neighbours in local zone;

N: Number of common reflections in this bin.

Recent changes to the MOSFLM package for processing film and image plate data

AGW Leslie, MRC Laboratory of Molecular Biology, Hills Rd., Cambridge, CB2 2QH,UK

Over the last year substantial changes have been made to the MOSFLM program for measuring rotation data collected either on film or image plate. These changes were driven by two requirements:-

1) To obtain a version of the software that could be run under Unix as well as VMS.

2) To merge the existing versions for processing films and image plates so that any algorithm improvements would only need to be made to one set of software.

The first requirement was achieved by running the film processing version of the software through the TOOLPACK program at Daresbury, which incidentally revealed a number of small bugs. I am extremely grateful to Kim Henrick for the considerable effort he expended in converting the MOSFLM package, especially as some of the conversion was far from straightforward. The TOOLPACKED version served as a starting point for making the changes necessary to allow both film and image plate data to be processed. The essential difference lies only in the format of the stored images. In the case of film data, the optical densities are stored as bytes, while for the image plate data the individual pixel values are stored as I*2 variables. Thus the great majority of the code is applicable to either type of detector, and only those parts which deal with handling individual pixel values need to be distinct. In practice this has been achieved by maintaining the detector independent code in the main library, and having separate libraries for the image plate and film versions of the detector specific code. The main library is thus linked with the appropriate detector library to give the required version of the program. To simplify software maintenance, all common blocks and parameter statements are stored in a separate text library, and are incorporated with the code using the FORTRAN INCLUDE statement. Unfortunately one of these common blocks (the one actually holding the pixel values of the image) is also detector specific. This means that the appropriate version of this common block must be placed in the common block text library prior to compiling any modules of either the main library or the detector specific libraries, but command procedures have been set up to do this automatically. Another problem which had to be overcome arises because Unix machines do not all store variables with the same byte order within a word: in some the first byte is the most significant (big-ended eg ESV, Convex, Silicon Graphics, Alliant FX40/80) while in others it is the least significant (little ended eg VAX, Ultrix, Alliant FX2800). A specially written subroutine (due to Phil Evans) automatically determines the "endedness" of the machine and if necessary byte-swaps the stored image when it has been read into memory.

Algorithm Improvements

A number of improvements have also been made to the algorithms employed in the program. These fall broadly into three categories: (1) those affecting refinement of detector parameters, (2) those affecting reflection integration, and finally (3) those allowing refinement of crystal orientation and, in favourable cases, cell parameters, as an integral part of the MOSFLM program.

1) Refinement of detector parameters

In the original version of the program, the refined parameters were the centre of the diffraction pattern (camera constants CCX and CCY) the orientation of the detector around the X-ray beam (CCOMEGA), the crystal to detector distance (XTOFD), the detector tilt and twist (rotations of the cassette about a horizontal and a vertical axes respectively), the bulge of the film in the cassette and a parameter (YSCALE) to allow for the non-equivalence of the pixel sizes in the X and Y directions for films scanned on a rotating drum scanner. These parameters were found to be inadequate for the refinement of data collected on image plates, and two additional parameters ROFF and TOFF were introduced, while the bulge parameter was removed as inappropriate for the image plate. ROFF and TOFF are acronyms for Radial

OFFset and Tangential OFFset and are required to allow for mechanical misalignment of the scanner. It is assumed that the radius of the outermost pixel in the scanned image is known exactly. This position is determined mechanically by a limit switch, and if this is not set correctly the effect is to produce a constant radial offset in the actual position of all pixels. This offset can be quite large (0.5mm in the case of the LMB scanner, 0.2mm for the scanner at Daresbury), giving rise to significant deviations from the predicted positions, but should be constant for a given scanner (variation of this parameter in increments of 150μ suggests that the limit switch is not functioning reproducibly - such effects have been seen in images recorded at Daresbury). The second assumption in determining the position of a given pixel is that the scanning direction is exactly radial, that is, it is exactly in line with the centre of rotation of the image plate. If this is not the case, the distortion introduced can, to a very good approximation, be described in terms of a constant tangential offset in the position of every pixel (this would not be true for the innermost pixels if the minimum radius was much less than 10mm). This parameter should also be constant for a given scanner, and has a value - 0.23mm for the scanner at Daresbury. In practice there is a significant correlation between this parameter and CCOMEGA.

With these additional parameters in the refinement the positional residuals are very low (~20μ) for strong images and small spot sizes (~6-7 pixels) providing accurate cell parameters (eg from IDXREF) are available. For weaker images the residual is inevitably larger as the position of the centroid of the spots is less well determined.

Another minor change to the software forces the program to find at least 50 reflections for the final positional refinement. The I/σ(I) threshold for selection of refinement spots is lowered automatically until 50 reflections are found, although it will not be lowered below 2.0. A practical note is that the user should not set this threshold too low, (REFINEMENT IMIN are the pertinent MOSFLM keywords...keywords will be given in parentheses where appropriate in the following text) or the refinement may use poorly defined weak reflections even if stronger reflections are present in the image.

In the initial stages of positional refinement, only spots in the central part of the image are used, and in order to increase the radius of convergence the peak/background mask is not used to determine the centroid. Instead, the background constant is determined from the pixels with the lowest values, and this constant is subtracted from all pixels prior to determining the centroid. The disadvantage of this procedure is that it gives rise to a impoverished signal to noise ratio, and if the spot separation is such that an adjacent spot intrudes into the "background" region of a spot being evaluated the resulting centroid will be seriously in error. In these circumstances the user can request (REFINEMENT USEBOX) that the peak/background mask is used even in the initial stages refinement, and an improved background rejection algorithm (see later) should reject any adjacent spot which intrudes into the background. This of course requires and accurate knowledge of the camera constants if the refinement is to succeed.

Under normal circumstances partially recorded and overloaded reflections are excluded from positional refinement. However in some instances it may be necessary to include partials if the crystal has an unusually large mosaic spread and there are not enough fully recorded reflections present to permit refinement (REFINEMENT INCLUDE PARTIALS). This will inevitably lead to a higher positional residual, and it may be necessary to increase the maximum allowed residual (REFINEMENT RESIDUAL) in order to achieve a "successful" refinement. Overloaded reflections can also be included in refinement in the unusual case when almost all reflections in the central area are overloaded (as occasionally occurs with film data collected at a synchrotron).

2) Reflection Integration

a) Background plane definition

The most significant change in reflection integration is in the determination of the background plane. This has been modified to improve the rejection of background pixels

which deviate significantly from the true plane due to the intrusion of an adjacent spot into the background region. An initial estimate of the background plane parameters is derived from a fraction (typically one half,but this is under user control, BACKGROUND BGFRAC) of the background pixels which have the lowest pixel values. The constant component is corrected to allow for the systematic error introduced by selecting only the lowest pixels, and the modified plane constants are then used to reject any background pixels which lie more than N*sigma from this background plane (N is typically 3, but can be set by the user BACKGROUND BGSIG). The sigma value is derived from counting statistics and the plane constant (rather than from the rms fit to the plane). This procedure is also applied to the standard profiles, which are derived by adding together all fully recorded reflections above some threshold intensity in a localised region of the detector. Because typically hundreds of reflections contribute to each standard profile, the counting statistics errors are proportionately much smaller than for a single reflection, and this therefore allows "bad" pixels to be identified with much greater confidence (N in this case is set by PROFILE BGSIG). By default background pixels rejected in the standard profiles ("starred" in the printed profiles listed in the logfile PROFILE PRINT) are also rejected when evaluating individual reflections (PROFILE CHANGEMASK). In fact for reasonably strong images the counting statistics errors are sometimes so small that rejection of pixels deviating by more than three sigma will lead to the rejection of a whole constellation of pixels surrounding the peak region. This is almost certainly due to the finite point spread function of the detector, which gives rise to weak "tails" in the true profile of every spot. Normally these tails are lost in the counting statistics noise, but for hundreds of summed reflections this is no longer the case. It is not due to positional errors as these are very much less than one pixel (typically 20-30μ rms errors for strong images). For pragmatic reasons (i.e. retaining a reasonable number of background pixels) it may be necessary to increase the sigma cutoff in such cases from 3 to 4 or even 5 (PROFILE BGSIG).

b) Profile fitting

The evaluation of the standard profiles has not been changed significantly (apart from internal scale factors to improve the effective dynamic range of the profiles). A separate standard profile is still evaluated for each different size of measurement box, and the measurement box expansion is determined automatically by the program on the basis of the size of the peak region, the obliquity of the diffracted beam on the detector, and the detector thickness. Whereas the "thickness" of the detector is well determined in the case of film, in the image plate it will depend on the depth of penetration of the X-rays (which will depend on the wavelength) and the power of the incident laser light when scanning the image. A default value of 0.2mm has been chosen, and this gives a sensible number of profiles (typically 9 in all) under most conditions. However when processing low resolution data (i.e. at a large crystal to detector distance and hence low obliquity) this can result in a single profile being used across the entire detector, which is not satisfactory. While the best solution to this problem is to allow user-defined regions for evaluation of the profiles, this is not yet implemented. A pragmatic solution currently available is simply to increase the notional detector thickness (THICKNESS) for example up to 1mm. The only effect this will have is to force expansion of the peak region of the mask (which when using profile fitting will not significantly affect the quality of the data) and give as many standard profiles as the user deems appropriate.

A new feature is the possibility of calculating a separate profile for each reflection. The profile used for evaluation is calculated as a weighted sum of the standard profiles for the area surrounding the reflection being evaluated. The actual value of the profile is calculated from the contributing profiles using a linear interpolation procedure based on the detector co-ordinates of the reflection and the coordinates of the standard profiles (which in turn are calculated as the intensity weighted mean of all reflections contributing to the profile). For most reflections, a weighted mean of four surrounding profiles is used, but for reflections near the periphery of the image only 3 or 2 profiles will be used, or in some cases no sensible interpolation can be performed. This procedure should provide a more accurate modelling of the way in which the reflection profile varies across the face of the detector, and in test datasets collected on the LMB scanner the variable profiles do give a modest reduction in the overall R_{merge} (From 5.9% to 5.6% for a 2Å resolution dataset comprising 48 images).

Other options that are now available are (1) Estimation of the intensity of overloaded reflections by profile fitting (PROFILE OVERLOAD). (2) Estimation of the intensities of reflections where up to half of the measurement box lies outside the scanned area by profile fitting (PROFILE EDGE).

Additional criteria have been added to allow rejection of individual reflections (REJECTION). The criteria now applied are (1) Excessive variation in the background plane (BGRATIO) - this is rarely observed now because of the improvements to the algorithm for determining the best background plane. (2) Poor fit of the reflection profile to the standard profile (PKRATIO - only applied to fully recorded reflections). (3) Excessive gradient in the background plane (GRADMAX). (4) Too many background pixels rejected (MINBG). There is the option to print the pixel values of all rejected spots (PLOT).

The current software will cope with pixel values of up to 65535 (stored as unsigned I*2 variables). For the Mar Research scanner pixels with counts greater than this are written to the end of the image file, but no use is made of this information at present.

3) Refinement of crystal orientation, mosaic spread, beam parameters and cell parameters.

When processing film data, the program POSTCHK has been available for the refinement of crystal orientation, mosaic spread, beam divergence and, in favourable cases, cell parameters. This program uses the principle of post-refinement; that is using the observed distribution of the intensities of partially recorded reflections between successive oscillation films to optimise these parameters assuming a model for the rocking curve. The disadvantage of POSTCHK is that it is first necessary to process the data, then run POSTCHK, and if there are any significant shifts in any of the parameters the data must be reprocessed, POSTCHK run again and if necessary the whole procedure repeated until convergence is achieved. This is very tedious, particularly if the crystal was slipping slowly during data collection.

The fact that the Mar scanner is a fixed origin detector has been exploited to allow post-refinement to be carried out on every image allowing continual updating of the crystal orientation and mosaic spread (the latter may change as a result of radiation damage). Because of the fixed origin, one can guarantee that any given (partially recorded) reflection will lie on exactly the same pixels on both images on which it is present (reflections spanning more than two images are not used). Thus, by storing 2 images in memory at the same time, it is a straightforward matter to integrate both halves of a partially recorded reflection occuring at the end of the oscillation range of the first image and the start of the second. This information is used in post-refinement at the end of every image, and the updated parameters are used to generate the reflection list for the following image.

Refinement of cell parameters can only be relied upon if the crystal symmetry is trigonal or higher, as for lower symmetries one or more of the cell parameters will be poorly determined from a single pair of images. The option to allow the information from several pairs of images to be accumulated, permitting a more meaningful refinement of cell parameters, is envisaged but not yet implemented.

In practice the refinement appears to be very stable, including refinement of the mosaic spread (see Table 1) and can easily follow slight crystal slippage.The ability to process a complete dataset in a single generate file, avoiding continual manual updating of crystal orientation and multiple generate files, greatly simplifies the processing of image plate data, and is probably the most useful improvement over earlier versions of the software. Unfortunately, because the origin of film images will depend on how the film is placed on the scanner and will also be affected by variability of camera constants, the same approach is not possible with film data. However since the image plate seems destined to replace film for the great majority of data collection this is not seen as a serious drawback. It remains to be seen whether the same approach can be used with the Rigaku R-axis detector, which has two image plates which may not share an exact common origin.

If the refined missetting angles for a given image deviate by more than some preset limit (POSTREF MAXSHIFT, usually 0.05°) from the values used in generating the reflection list for that image, then the reflection list will be recalculated and the image measured again. This will be repeated until convergence is achieved. If the post-refinement residual exceeds a preset limit (POSTREF MAXRESIDUAL) then processing is terminated.

4) The addition of partially recorded reflections over adjacent images

As explained in the previous section, it is possible to add together the pixel values of partially recorded reflections on two successive images and thus generate the equivalent fully recorded reflection. The option to do this, and hence treat all reflections as if they are fully recorded, is available (ADDPART). In fact this option will allow the integration of reflections spanning up to 3 images, although reflections spanning 3 images will still be treated as partials (the first part corresponding to the first image on which the reflection occurs, the second part to the sum of the second and third images on which it is present). In most cases these reflections, will lie close to the rotation axis and have large Lorentz factors (whose value will depend critically on the exact crystal orientation) and it is questionable whether they will add significantly to the overall data quality. However if the crystal has an unusually large mosaic spread (eg as a result of flash-freezing) this option may be useful. It should be realised that the method assumes that the exposure time and the incident flux for each image is the same, which may not necessarily true for a synchrotron source. Tests with a laboratory data set gave an identical R_{merge} for data processed with and without partial summation (as expected).

Practical Details

1) The necessity of "still" images

Although the autoindexing program REFIX (Kabsch, 1988) is generally very successful in determining crystal orientation, it cannot provide accurate cell constants from a single image (particularly for symmetry lower than trigonal) and two orthogonal stills are essential in order to determine cell parameters accurately. A second problem is that REFIX refines cell parameters against the observed reflection co-ordinates, and consequently any error in the crystal to detector distance will give an error in cell parameters. (This is in contrast to post-refinement /IDXREF where the cell parameters are insensitive to errors in crystal to detector distance providing this is sufficiently accurate to allow correct indexing of the reflections). Although the parameters determined from REFIX may be adequate to allow processing of images collected over a fairly narrow angular range around the image used for autoindexing, in general they will not be adequate for large angular ranges (eg greater than 10-15°).

The orientation matrix determined by REFIX can be input as an initial orientation to IDXREF when refining the cell parameters, which circumvents the problems of estimating the missetting angles from the stills themselves.

2) Post refinement of crystal orientation

It should be realised that it is implicit in the post-refinement option that successive images have identical exposure times and incident flux. Fortunately the refined parameters are in fact rather insensitive to the changes of up to 10% in the overall scale of the second image relative to the first, so beam decay will not normally introduce a significant error although a change in exposure time by a factor of 2 certainly will! The procedure also assumes that images with sequential pack numbers are indeed sequential in rotation angle. Thus if two separate wedges of data are collected from the same crystal, the first image of the second wedge should NOT be given a pack number that follows on from the last image of the first wedge, or else it will be used in the post refinement of that last image with unpredictable results.

3) Coordinate systems

It is an unfortunate fact that the Mar scanner software adopts a different convention when displaying the image to that adopted by MOSFLM. In the scanner display software, the

image is displayed as viewed from the crystal looking towards the detector, while in MOSFLM the view is from behind the detector looking towards the source. Thus an image displayed with the MOSFLM graphics display option will appear to be inverted left to right when compared with the scanner display software. This is dealt with internally in the MOSFLM software, and the only point at which this is really visible to the user is in the definition of the direct beam position (BEAM in MOSFLM, CENTRE in IMSTILLS). The co-ordinates of the direct beam are given in mm with respect to the lower left hand corner of the image, with the X-axis horizontal and the Y-axis vertical. However the lower left hand corner of the MOSFLM image is equivalent to the lower right hand corner of the image displayed by the scanner software. Since the direct beam co-ordinates are generally determined from the scanner version of the image (either by locating the co-ordinates, in pixels, of the right and left sides, and top and bottom of the wax rings, or by running the Daresbury program WAX) in order to avoid confusion both MOSFLM and IMSTILLS expect the co-ordinates to be given relative to the Mar scanner software origin. The X co-ordinate is then changed to (Image width -X) internally in the IMSTILLS/MOSFLM software to allow for the change in origin. In the MOSFLM output, the parameters XCEN and YCEN define the position (in 10 micron units) of the direct beam in a co-ordinate frame with X horizontal, Y vertical, origin at lower left pixel of image in the MOSFLM view, and for the Mar scanner these will therefore be (Image width-X_{input})*100, Y_{input}*100 where the image width is 180mm.

Future Developments

The implementation of a more flexible method of assigning the areas on the detector to be used for the evaluation of the standard profiles is the immediate objective, together with some features meantioned above as not yet implemented (eg post-refinement of cell parameters using data from several images). Minor improvements in profile fiting are also anticipated. The package would also greatly benefit from more sophisticated graphics options, and the possibility of using John Campbells XDLVIEW X-windows package is being investigated although this would only be available in the Unix version

Availability

VMS and Unix versions of the software are available. The VMS version is distributed on Exabytes or standard 9 track tapes, the Unix version on Exabyte, QIC or standard tape or by anonomous FTP. Please contact the author (E-mail ANDREW@UK.AC.CAM.MRC-LMB) for further details. The software is distributed subject to the condition that bugs are reported.

Warning

The first authentic release of this software is version 4.2. Versions earlier than this will not handle pixels with values greater than 32767 correctly, do not have the postrefinement option, and do not invert the image right to left and will therefore give rise to anomalous differences with the incorrect sign. They also contain a number of bugs which can give integer overflow problems in some instances. Versions prior to 4.22 will also give integer overflow for strong images.

Acknowledgements

I am very grateful for many valuable discussions on various aspects of this software with Jan Pieter Abrahams and Phil Evans. Several users have also been very helpful in locating bugs in the early versions of the software, particularly Howard Terry (Hamburg) and Stephen Cusack (EMBL, Grenoble). Peter Daly (Daresbury) assisted with the conversion to Unix and together with Dave Edwards at York in getting the package to run on Silicon Graphics machines.

References

Kabsch, W. (1988) J. Appl. Cryst. 21, 67-71.

TABLE 1

Summary file from MOSFLM for a series of 2A resolution images collected at LMB. These show the stability of the refinement of both the positional parameters (first half of table) and the orientation, cell parameters (Space group R32) and beam divergence parameters. Note the tracking of the small slippage in PHIY.

PACK	CCX	CCY	CCOM	XTOFD	YSCALE	TILT	TWIST	ROFF	TOFF	RESID	NR	NFULL	NPART	NOVR	NNEG	BGR	SIGMA	BAD	RF	RP	PKR	NBGR	SCF
18	-20	-6	0.780	10025	1.0000	2	2	-52	-20	1.7	60	709	922	13	118	0.9(1.1)	414.0	6	5.1	10.5	0.8(1.2)	0	0.14
19	-19	-6	0.770	10016	1.0002	0	3	-50	-19	1.8	58	691	864	25	105	0.9(1.1)	391.1	5	5.6	11.1	0.8(1.2)	0	0.13
20	-20	-5	0.764	10022	0.9999	2	3	-52	-19	2.4	60	675	907	13	138	0.9(1.1)	415.6	3	5.4	10.3	0.8(1.2)	0	0.15
21	-19	-6	0.776	10012	1.0002	0	4	-50	-19	2.5	59	689	889	17	123	0.9(1.1)	396.8	7	5.3	10.8	0.8(1.4)	0	0.15
22	-19	-5	0.780	10014	1.0003	1	3	-50	-19	2.1	57	653	921	13	115	0.9(1.1)	402.7	5	5.1	10.1	0.8(1.4)	0	0.15
23	-19	-5	0.768	10016	1.0001	1	3	-50	-18	2.3	60	701	932	15	140	0.9(1.1)	392.5	5	5.3	9.2	0.8(1.3)	0	0.14
24	-19	-5	0.767	10019	1.0001	3	3	-50	-19	1.9	57	643	912	25	121	0.9(1.1)	388.7	3	5.3	10.5	0.8(1.0)	0	0.13
25	-19	-5	0.752	10015	1.0002	1	2	-50	-17	2.3	57	719	930	17	136	0.9(1.1)	383.2	6	5.0	11.1	0.8(1.2)	0	0.15

RESULTS OF POSTREFINEMENT

Cell parameters are being refined

Beam parameters are being refined but input values will be used

Image	PHIX	PHIY	PHIZ	A	B	C	ALPHA	BETA	GAMMA	EPS	DIVH	DIVV	Resid	NR
18	-0.22	-0.11	0.19	107.70	107.70	123.70	90.00	90.00	120.00	0.00	0.15	0.15	0.032	219
19	-0.22	-0.11	0.19	107.72	107.72	123.69	90.00	90.00	120.00	0.00	0.18	0.18	0.039	204
20	-0.21	-0.10	0.18	107.63	107.63	123.71	90.00	90.00	120.00	0.00	0.19	0.19	0.035	234
21	-0.21	-0.10	0.18	107.66	107.66	123.73	90.00	90.00	120.00	0.00	0.18	0.18	0.041	203
22	-0.21	-0.10	0.19	107.70	107.70	123.71	90.00	90.00	120.00	0.00	0.18	0.18	0.040	267
23	-0.21	-0.09	0.19	107.71	107.71	123.74	90.00	90.00	120.00	0.00	0.20	0.20	0.042	208
24	-0.21	-0.09	0.19	107.68	107.68	123.71	90.00	90.00	120.00	0.00	0.17	0.17	0.037	278
25	-0.21	-0.08	0.19	107.67	107.67	123.73	90.00	90.00	120.00	0.00	0.19	0.19	0.037	212

CRYSTALLOGRAPHIC STUDIES OF THE CHIMAERIC FAB' FRAGMENT B72.3

R.L. BRADY & R.J. TODD.

The crystal structure of a monoclonal chimaeric Fab' fragment has been determined. In addition to being the first structure of a chimaeric Fab' fragment and anti-tumour antibody reported, the structure determination has employed a number of recent developments in experimentation in both hardware and software.

Monoclonal antibodies have great potential as diagnostic and targeting reagents for viruses or diseased cell lines. One example is the murine monoclonal antibody, B72.3, which recognises and binds to a tumour-associated mucin-like molecule, TAG72, found on human colorectal, breast and lung carcinomas. A chimaeric form of the Fab' fragment of B72.3 has been constructed which contains the murine light and heavy chain variable domains of B72.3 fused to a human κ and $\gamma 4$ first domain respectively. "Humanization" improves the potential clinical application of the chimaeric antibody as the molecule becomes less prone to recognition as "foreign" when used in humans, and hence gives rise to fewer immune responses.

Crystals of the chimaeric B72.3 belonged to the space group $P2_12_12_1$, a = 67.5Å, b = 93.2Å, c = 208.8Å, with two molecules per asymmetric unit. Although diffraction could be observed to 2.6Å resolution at the SRS, acute radiation sensitivity rendered these crystals unsuitable for data collection using conventional film methods. Data were therefore collected on the Weissenberg camera at the Photon Factory Synchrotron, Japan, which utilizes image plates and a finely collimated beam (0.1mm), but even then

radiation sensitivity limited the resolution of recordable data. However a complete data set (to 3.1Å resolution) was obtained from a single crystal and recorded as a set of twelve images. These data were processed in York using the WEISO8 package adapted to run on a Silicon Graphics computer. Data processing was greatly facilitated by the image plate display programme IPD written for a Silicon Graphics Iris by M. Hartshon at York (available to academic users).

These data were then used to determine the chimaeric B72.3 structure by molecular replacement using a known Fab structure. The model used was the Fab portion of the HyHel-5 structure, chosen because it exhibited the greatest sequence similarity with B72.3. The programme package XPLOR (version 2.1) was used to perform the cross-rotation search. The highest 200 peaks from this search were subjected to the Patterson Coefficient (PC) refinement. This procedure gave a solution with a single maximum, which was interpreted as the two molecules being oriented almost identically in the asymmetric unit (a result expected from the calculation of a native Patterson which contained a large non-origin peak at (0, 1/2, 1/8)). In addition the rigid-body refinement procedure in XPLOR changed the elbow-angle of the model by some 18° from the of the HyHel-5 structure. The correctly oriented model was then submitted to the translation function search in XPLOR. The two highest peaks from this search were separated by the translational vector (0 0.5 0.125) which satisfied the non-crystallographic symmetry evident in the native Patterson. A point to note is that this procedure could not be repeated so easily with the programmes available through CCP4 (ALMN and TFSGEN) most probably because of the absence of a PC refinement stage, which in this case quite dramatically changed the elbow-angle between the domains of the search model.

At this stage the two molecule model was submitted to a round of simulated annealing (SA) refinement within XPLOR keeping strict non-crystallographic symmetry (NCS) constraints applied. The R-factor decreased from an initial 0.408 (15-3.1Å), rms-bonds = 0.067Å, rms-angles = 5.76°, to 0.212, rms-bonds = 0.030Å, rms-angles = 5.1°. A 2Fo-Fc map was calculated and the density for the two molecules "skewed" (SKEW programme, CCP4). The model for B72.3 was manually rebuilt within FRODO from this "skewed and averaged" map and segments of chain absent in the original search model (such as the hypervariable loop and elbow regions thought likely to possess differing conformations and consequently left out) were inserted. A further round of SA refinement with strict NCS constraints gave an R-factor of 0.188. A final rebuild and round of refinement gave a final model with R-factor of 0.179 (15-3.1Å), rms-bonds = 0.017Å, rms-angles = 3.71°.

A predicted main-chain model for the structure of B72.3 has been constructed (D.J. Edwards and R.E. Hubbard, unpublished results) based on the canonical structures approach suggested by Chothia *et al.* (Nature, **342**, 877-883, 1989) . It was interesting to note that the loop structural assignments agreed well for five out of the six hypervariable loops. The one predicted conformation that disagreed was for the H3 loop, where no recognised canonical structures exist. In the B72.3 structure this loop is unusually short and tucks in at the base of the epitope-binding region formed by the CDR loops.

QUANTA plot created on Tue Nov 26 1991 12:02:27 by user: todd

FIGURE : B72 (THICK) VS. HYHEL-5 (THIN) OVERLAID ON C-DOMAIN

Abstract - A program to abstract 3 dimensional coordinates from stereo diagrams

T.J. Oldfield, R.E. Hubbard, P. Murray-Rust (Glaxo)

Introduction

With the rapid pace of modern methods of macromolecular structure determination, there is an increasing number of research articles describing the three dimensional structure of proteins. One of the frustrations in reading these articles is that often the coordinates on which diagrams are based are unavailable for local study, comparison and modelling. The Brookhaven laboratory (Bernstein et. al.) acts as a central repository for protein structural information, and coordinates for most proteins eventually appear in the database. However, this can take some time. In most cases, the coordinates are caught up the process of being deposited, validated and published in the database. Occasionally, the coordinates are unavailable for commercial reasons or because a research group wishes to exploit the structure further.

These problems were recognised many years ago by Michael Rossman, who produced a computer program for generating a three dimensional structure from the information contained in an alpha carbon stereo diagram. This involved measuring or digitising the two dimensional coordinates from a stereo diagram, and from these refining a consistent three dimensional model.

This abstract, we present a novel technique for generating dimensional coordinates from stereo diagrams. The main advantages of the procedure are that it results in low errors for coordinates, and is robust and rapid.

Procedure

Figure 1 is a flow diagram showing the basic steps of the procedure. The left and right eye views of the diagram are digitised and transferred to a workstation. The digitising is carried out using an Apple Macintosh Scanner using Applescan software at a resolution of 300dpi in line art mode. These images are stored in TIF (Daveport & Vellon) format, and then transferred to the workstation.

The images are displayed on the workstation with the left eye image at the top of the screen and the right eye image at the bottom of the screen. The images are continuously displayed and hence must be placed in write protected display memory, or isolating a particular set of bit planes with a write mask.

The most novel aspect of this technique for abstracting coordinates exploits a particular feature of the hardware used to produce dynamic stereo in modern

graphics workstations. If the left eye view of a image is drawn in the top half of the screen and the right hand view of the image in the bottom half with the monitor running at 120Hz, then the individual images are lengthened in the y direction and the two images appear every 1/60th of a second. The appearance of the two images can be synchronised with a pair of liquid crystal glasses so that when the left image is displayed this is seen with the left eye, and when the right image is displayed this is seen with the right eye. This produces a very effective dynamic stereo perception with only a reduction in the y resolution.

The images are first aligned by identifying equivalent positions in the left and right eye view. Typically, the N terminus and an atom as far as possible away from the N terminus in the horizontal screen axis. Once the left and right eye images are aligned, they can be viewed in stereo to give a static stereo view of the alpha carbon diagram. (Unless explicitly stated, the remainder of the procedures are performed while viewing the screen in stereo).

Before building the alpha carbon trace, it is necessary to define the scale and stereo angle of the left and right views. Although the two parameters are in theory independent of each other, in practice they can have similar effects on the perceived stereo, particularly when they are close to the correct values. Small errors in the scale and stereo angle can make the building of an alpha carbon chain of reasonable geometry difficult. The program therefore has a facility to display a piece of beta sheet or alpha helix with idealised geometry which can be modelled and rotated. This can be scaled and the stereo angle adjusted so that the idealised section of structure aligns with a section of local structure within the stereo image.

The main part of the program consists of building an alpha carbon backbone into the displayed image. In general, the manipulation of the images and molecular structure is performed with a three-button mouse in conjunction with an on-screen cursor. In addition, some options in the program are accessed by single letter keyboard commands.

The first stage is to identify the N-terminus using a three dimensional cursor. Consecutive atoms are then added one at a time and manipulated into position defined by the stereo image. Each atom is represented by a ball connected to the previous atom by a bond of 3.8Å. The position of the atom currently being fitted to the stereo image is manipulated by changing the Ca-Ca-Ca internal angle, and the Ca-Ca-Ca-Ca pseudo torsion angle. After accepting the built atom, the program provides the user with the next alpha carbon and this is fitted in the same way. When complete the final poly peptide chain can be written out as a protein databank format file and used in 3 dimensional analysis.

The building process for an atom is aided in the following ways:-

1) An enlarged few of the region being fitted is displayed in the corner of the screen.
2) The elevation of the new atom (above or below the z position of the previously fitted atom) is represented by the colour.
3) The orthogonal view of the growing peptide chain is displayed to indicate the z-coordinated interpretation.
4) A contoured plot of allowed regions for the Ca-Ca-Ca internal angle, and the Ca-Ca-Ca-Ca pseudo torsion angle is displayed (in preparation) and the current values of the moving atom is marked by a pointer. The position of each atom is therefore restricted by the bond length, angle and pseudo torsion to other atoms.
5) A very much enlarged view can be used to adjust the atom position to align with the stereo image without any geometrical constraints. This display also shows bump distances between atoms.

At any stage in the building process the secession can be halted and the current status of the program automatically saved. The program, when restarted, continues at exactly the same point.

Conclusions

This abstract has described a novel approach to building an alpha carbon trace from a stereo image. For a protein of about 200 residues, the overall RMSD from the actual coordinates is around 1.4Å, and can be built in under 2 hours by an experienced user. It has been found that after building a polyalanine model structure (in preparation) it is possible to use the model coordinates as a search molecule in a rotation function.

The program is still under development and future features should include the general rotation of the built molecule within the program and addition of standard fragments of structure such as residues or complete helices.

This work has been funded by Glaxo Research.

References

Bernstein, F.C., Koetzel,T.F., WIlliams,G.J.B., Meyer.E.F., Brice,M.D., Rodgers,J.R., Kennard,O., Shimanouchi.K. & Tasumi,M.j. (1977) J.Mol.Biol **112**, 535-542

Davenport, T. & Vellon M. (1987) Aldus Corporation and Windows Marketing Group, Microsoft Corporation.

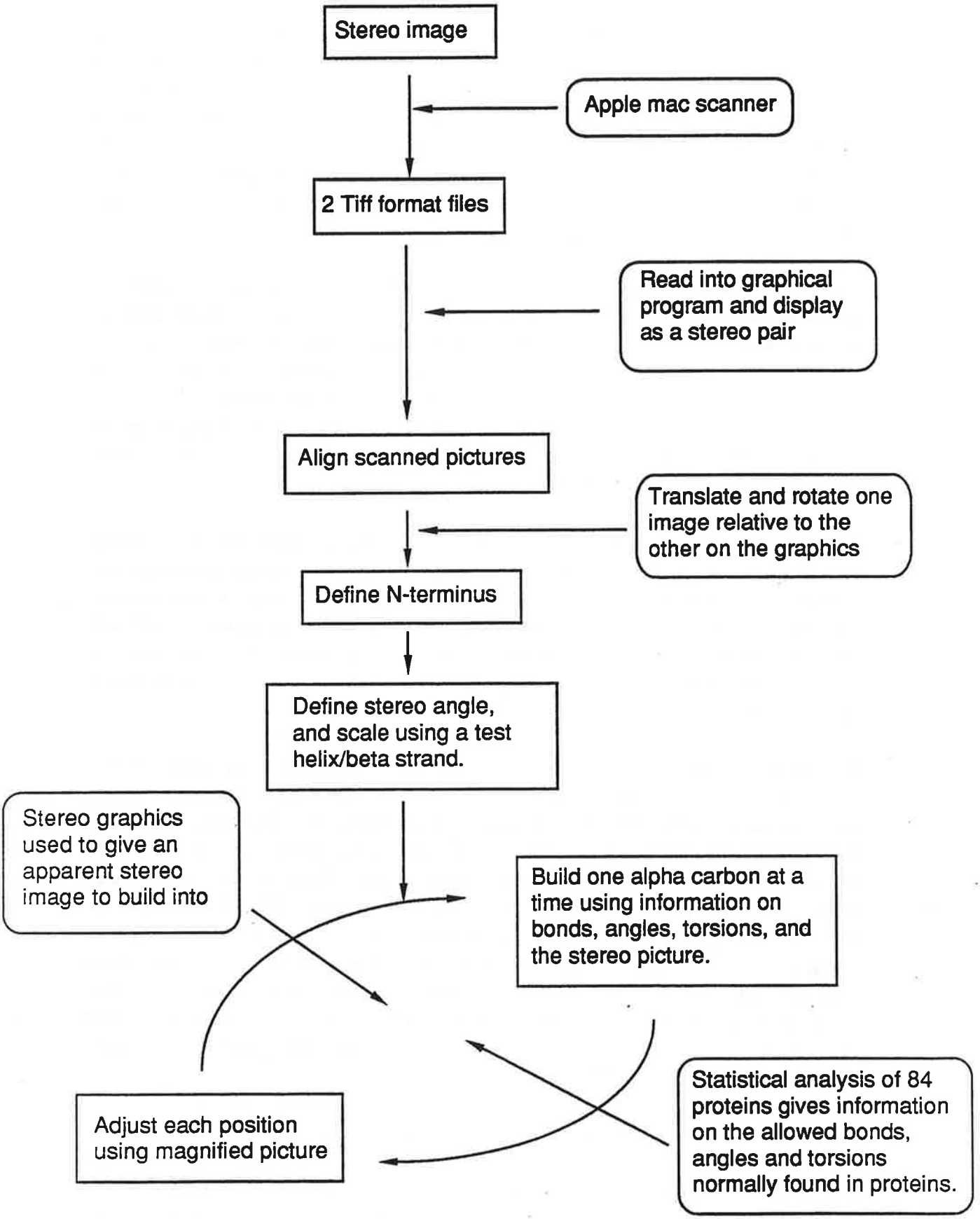
Stereo image
Apple mac scanner
2 Tiff format files
Read into graphical program and display as a stereo pair
Align scanned pictures
Translate and rotate one image relative to the other on the graphics
Define N-terminus
Define stereo angle, and scale using a test helix/beta strand.
Stereo graphics used to give an apparent stereo image to build into
Build one alpha carbon at a time using information on bonds, angles, torsions, and the stereo picture.
Statistical analysis of 84 proteins gives information on the allowed bonds, angles and torsions normally found in proteins.
Adjust each position using magnified picture

PROTEIN CRYSTALLOGRAPHY AT I.M.B.B. CRETE, GREECE

In its fourth year of existence the Protein Crystallography group at IMBB is focussing on projects where the fundamental aspects of protein structure can be used to develop the full potential of biotechnology and protein engineering.The data collection for most of the following projects are or will be carried out in EMBL-Heidelberg (use of the Xentronics area detector)and/or EMBL Hamburg (use of the imaging plate detector on a Sychrotron beam-line).

Understanding of the structural principles of a tertiary class of proteins (the 4-alpha-helix bundle proteins) by a combination of theory and experiment and use this knowledge as the basis for engineering novel functions (our model systems are ROP and ferritin). Finally, apply this method to the production of specific prototypes of engineered functional proteins. Functions to be engineered include metal binding sites, enzyme inhibitors, peptide hormone analogues etc.

Determination of the three-dimensional structures of important functional classes of proteins as a first step towards rational re-designing of their properties for industrial and other applications. Presently we are working on restriction enzymes (PvuII endonuclease) and its companion methylase from E. coli and on copper containing enzymes (nitrite reductase, pseudoazurin from Alc. faecalis S-6) involved in electron transfer.

Purification and crystallisation of the plasmid encoded beta-lactamase cephalosporinase (TEM-5). This new project is a collaboration with Dr. E. Scoulica and Prof. I. Tselentis of the department of Medicine (Univ. of Crete). The beta-lactamases are enzymes that cleave beta-lactam antibiotics. They offer significant resistance of bacteria to this group of antibiotics. The TEM-type (1 to 7) beta-lactamases are plasmid-coded, class A enzymes synthesized by gram-negative bacteria. The TEM's are the most widespread type of beta-lactamases and are specific for hydrolysing the cephalosporins (e.g. cefotaxime, cefmenoxime and ceftazidime). We concentrate our efforts in the purification and crystallisation of the TEM-5.

Determination of the stucture of adamantyl-triazine derivatives. This project is a collaboration with Dr. S. Hamodrakas, Dr. P. Tsitsa and Dr. E. Antoniadou-Vyza (University of Athens). Dihydrofolate reductase, an enzyme which reduces dihydrofolic to tetrahydrofolic acid, is a protein of central importance in

biochemistry and medicinal chemistry. It is used as a target for several antibacterial and antineoplasmic (antitumor) drugs. The activity of these drugs is due to selective inhibition of the enzyme from species to species. The discovery that diamino-s-triazines interfere with folic acid metabolism triggered research on the antifolate activity of this class of compounds and has shown promise in cancer chemotherapy. A series of possible DHFR inhibitors have been synthesized as antitumor, antibacterial and antifungal agents. In order to understand the observed variation in biological activity and compare structure and binding with other antifolate ligands, crystal structure determination and conformational analysis of both active and inactive lipophilic compounds is under way. At I.M.B.B. the structure of 2-Amino-4-(tricyclo[3.3.1.1.3,7]decyl-1)-6-dimethyl-amino-1,3,5-triazine was determined from triclinic crystals.

Determination of the three-dimensional structure of Photosystem II (in collaboration with Prof. D. Ghanotakis of the chemistry department of the Univ.of Crete), which will provide most crucial information relevant to energy technology and agriculture. Characterize the herbicide binding site and design novel herbicides with improved properties. An extermely important breakthrough was achieved recently with the first crystallization of a Photosystem II complex.

Protein Crystallography in Galway, Ireland

A group of chemists based in University College Galway are in the process of starting up the first Protein Crystallography Group in Ireland. Prof. Pat McArdle, Dr. Des Cunningham and Dr. Tim Higgins are all inorganic chemists. Their crystallography experience began when they purchased a secondhand Hilger and Watts Y290 4-circle diffractometer from Prof. George Ferguson at the University of Guelph in 1978. That diffractometer loaded its program from and output its data to paper tape. It was not unknown then for a data set to be read into the processing DEC20 upside down and backwards. One of the first tasks undertaken was to replace the paper punch with a microcomputer and to write random indexation software. This certainly made life easier. The PDP8 computer controlling the instrument died 4 years ago, by that time the few hundred structures solved had created a justification for a new Enraf Nonius CAD4 diffractometer. The CAD4 works around the clock 300 days per year collection data.

A few years ago the group looking for new challenges approached Prof. Guy Dodson for advice on the feasibility of tackling protein. Following Guys encourgement all 3 Galway staff and their first postgraduate student in protein crystallography Martin Walsh spent periods of time in York. Prof. Dodson and Dr. Tony Wilkinson both also visited Galway to assist.

The Galway group have been lucky to initiate a collaboration with Dr. Steve Mayhew of University College Dublin. Steve is a biochemist/microbiologist and has worked on redox proteins for many years.

The groups first project is an investigation of the stereochemical environment of the flavin in flavodoxin from *Desulfibrio vulgaris*. The interactions between protein side chains and the nucleotide are being probed by site directed mutagenesis. Flavodoxins are a group of small flavoproteins (molecular weights 15,000 - 23,000) that have been isolated from microorganisms. They contain a single molecule of flavin mononucleotide (FMN) and they function as electron carriers in low potential oxidation-reduction reactions, such as nitrogen fixation, hydrogen formation and photosynthesis, in which they transfer electrons between other redox proteins. In some organisms they are synthesized in place of ferredoxin in response to iron deficiency. Crystal structures have been determined for flavodoxins from four species; the anaerobic bacteria *Clostridium beijerinckii* (aka *Clostridium* MP) and *Desulfovibrio vulgaris* (a sulphate-reducing organism), the cyanobacterium *Anacystus nidulans*, and from the alga Chondrus *crispus*. Protein-flavin interactions that stabilize the semiquinone, that increase the pK values of the quinone and decrease the pK of the hydroquinone, and which dramatically change the affinity of flavin and protein with redox state have been suggested from the known crystal structures. This previous structural work and some molecular modelling is being used to select appropriate

mutations. The results of redox and other thermodynamic studies are being used to select mutants for crystallization experiments.

Data has already been collected (on the Daresbury synchrotron) for the wild type protein in oxidized and semireduced states as well as for 3 mutants. This data is at present being processed.

Unfortunately the mutants are not crystallizing as easy as the native protein did and many long hours of trials have to be set up. Those mutants already crystallized are not occurring in the original space group, making molecular replacement necessary to solve the structure. The group is also at present isolating and purifying a range of proteins from *Megasphera elsdenii* with a view to crystallization trials, these include electron transfer flavoprotein, D-lactate dehydrogenase and butryl CoA dehydrogenase. Preliminary work is also underway on a cellulase enzyme and a fatty acid binding protein.

The CAD4 4-circle diffractometer is the only data collecting device in Galway. It is hoped to collect data to low resolution on this and travel for the high resolution data until the work can justify more purchases. The group has been able to attract industrial support for computing and molecular graphics and is reasonably equipped in this area. The availability of molecular software (CHEMX) and the presence of a staff colleague, Dr. John Simmie, with an interest in this has also lead to the group developing in this area.

ESF MEETING CRYSTALLOGENESIS

December 19-20 1991

Centre Educatif B. Frachon

Gif sur Yvette - France

A meeting on crystallogenesis was held in Gif sur Yvette (France) on 19-20 December 1991, on behalf of the European Science Foundation (ESF) and the ESF network of the European Association of the Crystallography of Biological Macromolecules (EACBM). This workshop was organized by Arnaud Ducruix and his groups from ICSN-CNRS in Gif. This two-days meeting focused on robotic for the first day and nucleation and crystal growth for the second day. It was attended by 22 people from various levels (post-docs, graduate students, technicians). It is clear that although protein crystal growth became a scientific field, crystallization is involving many technicians which need access to this kind of meeting. Because the number of people was limited, the organisers had to select only one per group of research from different countries in Europe (Denmark, France, Germany, Italy, Portugal, Sweden, Switzerland, U.K.) A few travel grants were allocated to graduate students. It is to be acknowledged that registration fees, full board and lodging were taken in charge by ESF.

The program included 15 lecturers. Many speakers came from french laboratories. In fact it does reflect the important biophysical-chemistry effort which is done by the French community in the field of protein and nucleic acids crystal growth. In replacement of Keith WARD who had to cancel his participation at the last moment, a general overview of the field was given by Richard GIEGE from Strasbourg. It was followed by a lecture given by C. CARTER from UNC in Chapel Hill (USA) on efficient screening and quantitative analysis of crystal growth conditions. Factorial experiment design was discussed with a new "response surface" design for optimization in difficult cases. A new Macintosh version of the corresponding program called INFAC developed by C. Carter was given to all participants. In the afternoon some of the robots developed in Europe by some groups were presented. Naomi CHAYEN from Imperial College presented results obtained by IMPAX, a robot designed by Douglas Instrument. Using a computer controlled microdispenser crystallization samples are produced as droplets under oil. Anita BENTLEY described TAOS, a 5-axis prototype robot developed at Orsay. J. Fontecilla from DIEP-Grenoble gave a first description of AUTOCRYS, a prototype developed by his group. Rolf HILGENFELD made a comparison of different pipeting stations and robots used in his department at Hoechst Cie. This was followed by a general discussion in form of buyer's guide. This was followed by a general discussion in form of buyer's guide. In the evening, an animated discussion followed an introduction to a practical approach of crystallization given by Madeleine RIES-KAUTT from Gif.

On the second day nucleation and crystal growth were discussed with short talks. Richard GIEGE presented new results using light scattering to follow nucleation. Magali JULLIEN from Orsay described a prenuncleation study of ribonuclease A by fluorescence anisotropy and its use to monitor prenucleation in the presence of different types of precipitating agents. Arnaud DUCRUIX presented new crystallizing agents and a solution study using small angle X-ray scattering to characterize the influence of salts on protein/protein interactions. Marie-Claire ROBERT from Paris gave new results obtained in her group concerning crystal growth in gels and the influence on the rate of nucleation and protein crystal growth. Membrane proteins were discussed with a talk given by Françoise REISS-HUSSON from Gif on the selection of detergents and one on the crystallization of porin given by Andreas KREUSCH from G. Schulz group in Freiburg.

Youri TIMSIT from D. Moras group described the analysis of the intermolecular packing contacts found in different structural forms of DNA and how it can be a good starting point for understanding the correlation between the oligonucleotide sequence, the molecular assembly and the crystallization conditions. Jean-Luc EISELE from the Pasteur Institute explained the advantages of the use of bacterially expressed antibody fragments for crystallographic studies with examples from R. Poljak's group.

Professor Jan DRENTH organized a general discussion on the needs and future of the field. The perspective and possible further meetings were debated as crystallogenesis is a rapidly moving field. Finally, Professor Jan DRENTH gave his humorous concluding remarks which gave the final touch to this workshop.

TWO MEETINGS FOR SYNCHROTRON RADIATION USERS.

David A. Waller
Department of Biochemistry and Molecular Biology University of Leeds, Leeds, LS2 9JT, England

In July two meetings were held about synchrotron radiation which were of particular interest to protein crystallographers. The meetings were the third ESRF users meeting in Grenoble and the SRI-91 satellite meeting "Synchrotron Radiation Instrumentation and Macromolecular Crystallography".

The previous ESRF users meetings had helped in the preparation of the Foundation Phase Report and advised on the priorities for beamlines. This third meeting was designed to inform potential users of the ESRF's new facilities about progress with the building work, construction of the machine and the design of the first beamlines. Andrew Miller opened the meeting with a brief description of the present status of the ESRF and the happy news that work is presently six months ahead of schedule and on budget.

The presentations which followed described the parameters of the bending magnets and insertion devices and the designs of the first seven beamlines, which were discussed in detail. The two beamlines which the ESRF itself is building that are of interest to the protein crystallographic community are BL3 and BL4.

BL3 is a white beam (5-60keV) derived from a multipole wiggler. Its principal applications will be for Laue diffraction from protein crystals and energy dispersive scattering from materials under high pressure although this station will also be available in monochromatic mode for protein crystallography. BL4 is a high flux line derived from an undulator. The tunable range of the line will be from 5keV upwards with a peak brilliance at 12keV. The applications on this beamline will be small angle scattering and protein crystallography.

Beamline control, data acquisition and general computing, all of which are envisaged on an integrated network of Unix platforms, were discussed briefly.The method of beam-time allocation, which will be based on the proposal system already used by the

neighbouring Institut Laue Langevin and the establishment of an independent ESRF users group were also described in outline.

Two things emerged from this meeting; first although the construction of machine and beamlines is well advanced one area lags behind, that is the matter of detector development. Scientists at the ESRF and elsewhere are now putting considerable effort into the development of detectors which will allow full use to be made of the brilliance of third generation synchrotron radiation sources.Second the facilities provided by the ESRF for protein crystallography appeared to be limited given the number of users who already use various synchrotron sources. However, the situation is not as bad as it may have appeared since the ESRF has agreed that beamline 19 (based on a bending magnet) will be a dedicated MAD line developed in conjunction with EMBL and beamline 20, sourced from an undulator, will be a dedicated protein crystallography line, this represents an additional one and a half lines because when BL20 comes on-line BL4 will be given over entirely to small angle scattering. In addition, a number of Cooperative Research Groups are planning stations on the bending magnets which will have potential for protein crystallography.

The second meeting was organised by Prof John Helliwell and entitled"Synchrotron Radiation Instrumentation and Macromolecular Crystallography" as a satellite of the fourth International Conference on SRI. This meeting reiterated some of the information about the ESRF beamlines given in Grenoble but also provided updates about development of the DORIS-Bypass in Hamburg and the Advanced Photon Source at Argonne. The EMBL Outstation in Hamburg will gain a new wiggler beamline in addition to the resiting of beamlines X11 and X31 in the new Hasylab V experimental hall with increases in both the available beamtime and intensity. Work at Argonne is progressing well: the development of stations is the responsibility of Cooperative Access Teams, a number of which are interested in developing a variety of macromolecular crystallography stations.

A second theme at this meeting concerned progress with new detectors. Talks included a report by N.Allinson on his group's work with CCD detector systems. He emphasized the basic properties of these devices and the rapidity with which their performance is improving. Perhaps the most encourgaging development is the increasing size of CCDs. D.W.J.Cruickshank's description of how theoretical considerations are providing guidelines for the specification of new detectors for Laue diffraction concluded with an outline of an on-line energy resolving system with good

spatial resolution and high count rate handling -- unfortunately this is, as yet, only a specification!

The final futuristic talk was provided by Prof. G. Kulipanov who described preliminary studies which may lead to a compact synchrotron source which even a university will be able to accommodate and afford!!

BIOZENTRUM
DER UNIVERSITÄT BASEL

Prof. J.N. Jansonius
Abt. Strukturbiologie

CH-4056 BASEL /SWITZERLAND
Klingelbergstrasse 70

Tel. 061/267 20 80
FAX 061/267 21 09

The DEPARTMENT OF STRUCTURAL BIOLOGY of the BIOZENTRUM, University of Basel, Switzerland

seeks to fill a position of

ASSISTANT PROFESSOR (Projektleiter/In)
in Protein Crystallography

We would welcome candidates who are interested in membrane proteins. The position also involves teaching.

Applications including a Curriculum Vitae, a list of publications, reprints of three representative papers and a synopsis of past and proposed research activities should be sent before March 31, 1992 to:

Prof. J.N. Jansonius
Department of Structural Biology
Biozentrum, University of Basel
Klingelbergstrasse 70
CH-4056 Basel, Switzerland
Tel. 061 - 267 2080
FAX 061 - 267 2109

For further information, please contact
Prof. J.N. Jansonius or Prof. J. Rosenbusch, tel. 061 - 267 2110

RESEARCH ASSOCIATE OR SENIOR RESEARCH ASSOCIATE POSITION
IN PROTEIN CRYSTALLOGRAPHY AT SSRL

The Biotechnology Group at the Stanford Synchrotron Radiation Laboratory (SSRL) has an opening for a Ph.D. scientist with research interests and experience in protein crystallography and crystallographic computing. SSRL has a vigorous program in protein crystallography using synchrotron radiation from the dedicated storage ring SPEAR. Facilities have been developed for the collection of multi-wavelength diffraction data using a multi-wire area detector, and for routine high-speed photographic data collection using a rotation camera mounted on a high intensity wiggler beam line. The RA/SRA will have the opportunity to participate in the further development of multiple-wavelength anomalous dispersion phasing techniques to solve macromolecular structures, the development of white beam Laue diffraction techniques for time-resolved studies, data collection at extreme low-temperatures, the use of novel x-ray detectors (such as imaging plates and CCD's), and the development of methods to facilitate data collection from microcrystals. SSRL offers an RA/SRA 50% of his/her time to pursue individual and collaborative research projects. Funds for materials/supplies and capital equipment, as well as staff priority beam time, are also provided. For the other 50% time, the RA/SRA will advise and assist visiting user groups and participate in beam line and experimental facility (and methodology) development projects related to protein crystallography. A willingness to provide good quality user support is considered to be a very important part of this staff position. A strong background in protein crystallography is essential. Experience in software development on VAX systems in "C" and Fortran, and in real time instrument control would be very desirable. Salary and appointment period will be determined by experience. The position includes full Stanford University staff benefits. Interested applicants should send a CV, a list of publications and the names and phone numbers of three referees, together with a brief description of their research interests to Dr. Paul Phizackerley, SSRL, Stanford Linear Accelerator Center, P.O. Box 4349, Bin 69, Stanford University, California 94309, USA. Application deadline is 1 February 1992. Stanford University is an Equal Opportunity Employer.

Post Doctoral Position
Université de Paris Sud
is available for crystallographic studies of
ANTIGENIC VARIATIONS OF INFLUENZA HEMAGGLUTININ

The outstanding characteristics of influenza is their ability to cause frequent epidemics of respiratory diseases; each outbreak is caused by an antigenically distinct virus. The component primarily involved in the variation is the hemagglutinin (HA), a membrane anchored protein with which neutralizing antibodies react. A distinction has been established between two kinds of antigenic variation, according to their extent. Antigenic drift involves the mutation of a few aminoacids and allows the annual occurrence of influenza epidemics. Antigenic shift is much more extensive than antigenic drift (about 40% of the sequence is altered); it has occurred three times since the isolation of influenza virus and is associated with more severe outbreaks; the corresponding HAs belong to subtype Hl (1933-1957 and 1977-present), H2 (1957-1968) or H3 (1968-present).

Whereas the hemagglutinins of subtype H3 have been extensively studied from a structural point of view, no such data is available on other subtypes. We now reproducibly obtain crystals of a subtype H1 HA. strain Weiss/43. These should allow comparison of the structures of H1 and He HAs, and an understanding of the way of Ha structure accommodates such extensive sequence variations. Since H1 HAs presently cocirculate with H3 in the human population, any attempt towards rational drug design will have to take an H1 structure into account.

Our group shares laboratory facilities with Prof. J. Janin and his associates. The laboratory is well equipped with a computer network. two graphic systems. two rotating anode generators and an image plate area detector. We are located very close to the LURE synchrotron and have easy access to its facilities.

The position is funded by an EEC grant and applicants should be citizens of one of the EEC countries, except France. For further information write or contact M. Knossow, Laboratoire de Biologie Physicochimique. Bat. 433, Université de Paris Sud, 91405 Orsay Cedex. France Tel.: **-33-1-69416180. FAX: **-33-1-69853715. Bitnet: KNOSSOW@FRLURE51.

ESF Workshop on Synchrotrons and Detectors Hamburg 13th - 14th December 1991

The rest of the newsletter is made up of the report and contributions to the above meeting. The time table of the meeting is also included.

Report on Synchrotron and Detector Meeting

Hamburg 13-14th December 1991

The meeting began with an extensive survey of the facilities and plans at the SR centres in the USA and Europe (including Russia). There was as well a series of papers on experience with detectors and their development. A number of issues were identified:

1) The importance of coordination and collaboration between the EMBL and ESRF.

2) The priorities of the PX community for the beamlines at the ESRF which had been agreed last year in Paris were confirmed.

3) The impressive progress with the construction of the ESRF was noted. It was hoped that this progress would allow the beamline development also to be accelerated by permitting early trials and implementation. At the same time it was appreciated that an advance in the timing could generate pressure on the engineers and those responsible for developing the beamlines.

4) The need for detector development remains paramount. It was recognised that the experimental needs of the SR community will not be met by one kind of device. Thus resources need to be found to develop and exploit the different technologies which are all being developed in Europe. It was hoped that there could be some coordination of detector development that could be linked to defined experimental requirements.

   The experimental requirements for PX detector defined in the Aussois meeting were discussed by Roger Fourme (LURE, Paris). This report will be extremely helpful and will be circulated separately.

5) CSG and the public beam lines
   It was generally considered that demand for SR time was not being met by existing national facilities [(1 eg) Uppsala with 43 scientists got 400 hours (pa. and needed 800 + hrs pa)].

The size of the European PX community implies that the national SR centres and the ESRF will be needed. It is essential to coordinate usage and to define clearly the specific needs for the ESRF.

It was noted that the best use of PX resources would be to have singly committed beamlines serving the whole community. It was agreed that the initiatives starting in the individual PX communities in Europe for CRGs should be coordinated. Initial discussions were planned which would it was hoped would lead to some specific proposals which could then be considered by the PX community.

There was a unanimous view that the EMBL would be the obvious agency to coordinate and submit the CRG proposals.

Guy Dodson
Chemistry Department
York University
England

Synchrotron and Detector Meeting December 13 - 14th 1991

Speakers	Title
Friday, December 13th	
Chairman K.S. Wilson	
14:00 Paul Phizackerley SSRL, Stanford/USA	PX Facilities at Stanford
14:30 Sigrid Bernstorff Sincrotrone Trieste/Italy	A high-power beamline for macromolecular crystallography at ELETTRA
14:55 Alexander Popov Academy of Sciences, Moscow/USSR	Facilities in Russia
15:20 Colin Nave Daresbury Laboratory/UK	Facilities at Daresbury Laboratory for PX, present and future
15:45 Roger Fourme LURE, Paris/France	Two new instruments at LURE
16:10 *Tea*	
Chairman R. Fourme	
16:30 Tseneyuki Higashi Rigaku Corporation, Tokyo/Japan	Weissenberg camera and facilities at the Photon factory
17:00 Jacob Pijpelink EMBL Hamburg/FRG	PX facilities at EMBL, Hamburg; present and future.
17:25 Hans-Dieter Bartunik MPG Hamburg/FRG	The MPG/GBF beam-line in Hamburg
17:45 Mogens Lehmann ILL, Grenoble/France	PX with long wavelength radiation: the S and P edges

18:00	Uli Arndt MRC Cambridge/UK	Ideas on sources and detectors: present and future
	Dinner	

Chairman A. Leslie

20:30	Felix Frolow Weizmann Institute, Rehovot/Israel	Cryogenic Studies
21:00	Ada Yonath MPI, Hamburg/FRG	SR and Crystallography of large bio assemblies
21:30	Dave Stuart Oxford University/England	Virus structures with Synchrotron Radiation

Saturday, December 14th

Chairman J.R. Helliwell

9:00	Steve Ealick Cornell, University, Ithaca/USA	Current and future facilities at Chess
9:30	Jules Hendrix EMBL Hamburg/FRG	Imaging Plates
10:00	Andrew Leslie MRC Cambridge/UK	Experience with the Image Plate Scanner, and software developed
10:30	Zbyszek Otwinowski Howard Hughes Medical Institute Yale University, New Haven/USA	DENZO software for processing of image plate data
	Coffee	

Chairman P.R. Evans

11:30	Nigel Allinson York University/UK	CCD detector development
12:00	Roger Fourme LURE, Paris/France	The Aussois detector meeting: A Summary
12:30	Zbigniew Dauter EMBL Hamburg, FRG	Data collection with imaging plate using short wave length radiation on both synchrotron and conventional sources
	Lunch	

Chairman G. Dodson

14:00	John R. Helliwell	A report on the progress of the ESRF machine construction in Grenoble
14:15	Stephen Cusack EMBL Grenoble, France	Current plans for collaboration between EMBL and ESRF
14:30	Peter Bösecke ESRF, Grenoble/France	Beamline 4 of the ESRF: A High-brilliance Beamline for macro-molecular Crystallography and Small-angle X-ray Scattering
15:00	Andy Thompson EMBL Grenoble /France	The MAD beam-line at ESRF
15:20	Phil Pattison Universite de Lausanne/Switzerland	The Swiss/Norwegian CRG at ESRF
15:40	Michel Roth CEA, Grenoble/France	IBS use of SR in Grenoble and progress report on D2AM beam-line construction at ESRF
	Tea	
16:00	Jochen Schneider HASYLAB/FRG	A beam line on the PETRA ring?
16:15	Carl Ivar Branden Uppsala University/Sweden	Current use and future needs for synchrotron radiation at the Biomedical Centre in Uppsala

Followed by general discussion led by C.I. Branden

PROTEIN CRYSTALLOGRAPHIC FACILITIES AT THE STANFORD SYNCHROTRON RADIATION LABORATORY

Paul Phizackerley
SSRL, P.O. Box 4349, Bin 69, Stanford University, California 94309, USA

Background to SSRL, and SPEAR Storage Ring Parameters

The Stanford Synchrotron Radiation Laboratory (SSRL) is a National Facility that provides synchrotron radiation for research in the fields of biology, chemistry, medicine, materials science, physics and other scientific fields. Approximately 30% of all the research proposals are in the biological sciences. SSRL is supported by the Department of Energy, Office of Basic Energy Sciences and Office of Health and Environmental Research and also by the National Institutes of Health, Biomedical Resource Technology Program, Division of Research Resources. Some of the protein crystallographic equipment was developed or purchased with funds from the National Science Foundation.

The laboratory originated in 1973 and now has a total of twenty-two experimental stations on nine beam lines on the storage ring SPEAR. Two of these stations (BL1-5AD and BL7-1) are dedicated to protein crystallography and two others (BL1-5 and BL10-2) are available for protein crystallography part time. Until 1991, the SPEAR run schedule for synchrotron radiation research was strongly influenced by the availability of the Stanford Linear Accelerator Center's electron injector, used for high energy physics research. However, SSRL has now built its own 3 GeV electron injector, incorporating a 120 MeV linac and a 133 m circumference booster synchrotron, allowing SSRL to run independently. We expect, therefore, that the amount of beam time available in future years will increase significantly - maybe eventually up to nine months per year. Intensive commissioning of the new injector/SPEAR complex started in February 1991 and was completed mid September 1991 with user beam time available during half of that time. During commissioning, injection rates of ~20 mA minute^{-1} were typical and during the last 10 days of the run a low emittance lattice, reducing SPEAR's horizontal emittance from 511 nm.rad to 129 nm.rad at 3 GeV, was tried and performed well. It is hoped that SPEAR will routinely be run in this new low emittance mode in the future. Unfortunately, the 16 GeV low emittance PEP storage ring, on which SSRL has two beam lines, is no longer functioning and is not likely to be run again in the foreseeable future.

The SPEAR ring is typically operated at 3 GeV with an initial beam current after injection of ~80 mA. Beam lifetimes in excess of 20 hours are frequently obtained. Occasionally SPEAR is run in timing mode to permit time-resolved experiments to be conducted. When operated in this mode, four equally spaced single bunches of electrons are stored (there are 280 possible electron "bunches" around the circumference) producing a radiation pulse of the order of 300 psec every 195 nsec. In this mode, the maximum total current is limited to about 60 mA and the ring is usually operated at either 3.3 GeV or 3.5 GeV. Beam position monitors have been installed on each of the beam lines and are used to control the vertical height of the emitted photon beam. This system works very well and beam stability is normally excellent.

Area Detector Facility for MAD (Beam Line 1-5AD)

This facility, which was opened to users in the spring of 1982, incorporates a single multi-wire proportional counter (MWPC) area detector and has been built specifically for multi-wavelength anomalous dispersion (MAD)

phasing studies in macromolecular crystallography. It is permanently in place at the end of the unfocused bending magnet beam line 1-5. The wavelength of the incident x-ray beam is tuned by a two-crystal monochromator and currently, the beam line does not include a mirror. Higher energy harmonics in the beam are eliminated by slightly detuning the monochromator, by rotation of the water-cooled first crystal with respect to the second crystal, with a piezoelectric adjustment. One milli-radian of radiation is available at the experimental station. However, since we have not yet installed focusing optics, because of spatial constraints within the beam line, only a fraction of this fan of radiation is used. Consequently, the intensity of the beam is no higher than is available from conventional x-ray sources, which has been a severe problem for weakly diffracting crystals. The installation of focusing optics, to increase the beam intensity, is going to be given a high priority during 1992.

The area detector currently being used in this system was purchased from San Diego Multiwire Systems in December 1988. It has an active area of 288 mm x 290 mm, with a spatial resolution of 2 mm and 1.133 mm, respectively, and is filled with ~70% Xe and ~30% synthetic air at a pressure of 1 atmosphere. The entrance window is made of beryllium (0.75 mm thick) and the absorption depth in the gas at normal incidence is 10.7 mm. No absorption edges are present due to the detector fill gas or entrance window over the range of x-ray wavelengths we use for MAD experiments. The detector is mounted on an optical bench connected to the 2θ circle of a 5-circle single-crystal Huber diffractometer, which is mounted on its side because of the horizontal polarization of synchrotron radiation. The crystal-to-detector distance can be readily varied from 19 cm to 81 cm. Two ion chambers mounted between collimators on the diffractometer input arm are used to measure the intensity of the incident x-ray beam and to measure x-ray absorption edges from elemental foils that can be placed between them for x-ray energy calibration. Due to the positional stability of the x-ray beam from SPEAR and the mechanical stability of the beam line monochromator, the tuned x-ray energy within a given storage ring fill, and between separate fills, is maintained to better than 0.5 eV at 10 keV. Since we have beam line shutters both upstream and downstream of the monochromator, the temperature of the monochromator crystals can be kept equilibrated even during access to the experimental enclosure (which is the size of a small room). To determine the optimal x-ray wavelengths for data collection, x-ray fluorescence spectra from the anomalously scattering element(s) within the sample crystal itself can be measured using a scintillation counter. This counter can be mounted in two different orientations so that effects due to x-ray dichroism can be measured. In one position, normal to the x-ray beam in the horizontal plane, two orthogonal orientations of the sample crystal can be measured. In the second mounting position, normal to the x-ray beam in the vertical plane, the third orthogonal orientation of the sample can be measured. The fluorescence signal has been found to be adequate with the counter positioned ~1 cm away from the sample crystal and no Z-1 filters have been found to be necessary.

The complete system is controlled by a MicroVAX II GPX colour workstation which is also used to process the measured data. Software for system control and data reduction was written by Ethan Merritt when he was a scientific staff member of SSRL. Special data collection control software has also been written to overcome intensity errors due to count rate losses that become significant when a strongly diffracting sample crystal, with a very low mosaic spread, is rotated in a quasi-parallel x-ray beam. Raw diffraction images are stored on internal disks and later transferred to an 8 mm Exabyte tape for archival purposes. The MWPC area detector system produces very good quality data, but typically a three wavelength data set takes many days of beam time.

Four-Circle Diffractometer (For Use on Beam Line 1-5)

The bending magnet branch line 1-5 in fact has two experimental stations in tandem. The end station (BL 1-5AD) is occupied by the area detector system described above. The other experimental station, upstream of the area detector, is called BL 1-5 and is a general purpose station. An Enraf Nonius CAD4 diffractometer, mounted on its side because of the horizontal polarization of synchrotron radiation, can be temporarily installed at this station. The system has been available since 1977 and has been used for initial experiments on anomalous scattering phasing methods, for the determination of anomalous scattering factors, and for the investigation of dichroic effects and beam polarization. Although available, in recent years it has not been used for protein crystallographic studies. In 1988, the diffractometer was upgraded by the Enraf Nonius Corp. to incorporate new microprocessor-based control and readout electronics and control software, and interfaced to a MicroVAX II computer system.

Rotation Camera Facility (Beam Line 7-1)

An Enraf Nonius rotation camera is permanently installed on the 8-pole 1.8T wiggler side station (beam line 7-1). The experimental station has been equipped with an enclosure for radiation protection that is the size of a small room. This facility has been open to users since the spring of 1984 and has been in very strong demand by the user community. It has primarily been used for the rapid collection of high quality diffraction data to high resolution and for the investigation of smaller and also radiation-sensitive crystals. It has also been used for data collection at LN_2 temperatures.

The intense beam available from the wiggler is focused by x-ray optical elements in both the horizontal and the vertical planes. An asymmetrically cut and cylindrically bent triangular Si(111) or Ge(111) crystal monochromator is used to focus ~1 milli-radian of radiation in the horizontal plane. The monochromator is followed by a 58 cm long platinum-coated fused-silica x-ray mirror which is inclined to the incident x-ray beam to reject the higher energy harmonic components in the beam. The mirror can be bent to focus the beam in the vertical plane.

The rotation camera is equipped with two ion chambers to measure the intensity of the incident beam, a motorized backstop so that an attenuated exposure of the direct beam can be made on each film, and a film carousel capable of holding up to 8 flat 5 inch x 5 inch film cassettes or 4 high resolution angled film cassettes. Currently, the maximum crystal-to-film distance is 42 cm, however, space is available to increase this if desired. The camera and associated equipment is mounted on an optical bench which can be rotated about a vertical axis positioned directly below the monochromator crystal to permit the x-ray wavelength to be readily changed over a limited range. A larger change of x-ray wavelength can be obtained only by interchanging the monochromator crystal. The system is normally used at a wavelength of either 1.08Å or 1.5418Å (Cukα) for extended periods of time to accommodate the maximum number of user proposals. The wavelength 1.08Å was chosen because it was the lowest wavelength that could be reached before running into the Pt L_{III} edge. Wavelengths lower than the Pt L_{III} edge are not accessible because of spacial constraints (due to beam line shielding) on the minimum angle 2θ to which the optical bench can be set. A maximum x-ray flux of ~2×10^{10} photons sec^{-1} is available (at both the standard x-ray wavelengths used and the normal SPEAR emittance) through the 200μm collimator that is chosen by most user groups.

The motions of the beam line optical elements, the rotation camera

alignment table and the camera phi axis and film carousel are under computer control and software has been written for system alignment and data collection that is both flexible and straightforward to use. Furthermore, provision has been made to rotate the crystal phi axis at a speed determined by the incident x-ray flux, thereby making the intensity of the recorded diffraction patterns independent of beam intensity fluctuations. An elemental foil can be remotely interposed between the two ion chambers for x-ray wavelength calibration. The beam line optics and experimental apparatus is very rigidly constructed and the user is protected against inadvertently missetting critical alignment motions by software protection. Consequently, in all but a few cases, users have been able to rely on the camera being optimized for the duration of their data collection.

An FTS systems crystal cooling device provides temperature control at the sample position down to just below $0^{\circ}C$. A low temperature cryostat based on the design developed by Håkon Hope at the University of California at Davis, and capable of rapidly cooling the sample crystal down to ~$100^{\circ}K$, is also available.

Fiducial marks can be recorded on the film packs after exposure using a specially adapted x-ray generator located near to the rotation camera. A large well equipped darkroom, also close to the camera, has temperature controlled processing tanks with N_2 burst capability. No film densitometer is available at SSRL for film scanning and consequently no data processing software for rotation photographs has been supported to date.

During the next two months we plan to upgrade the rotation camera facility. A Mar-Research Imaging Plate X-Ray Data Collection System, incorporating a single-crystal goniometer and an imaging plate recording camera/scanner controlled by a VAXStation 3100 model 76, has been purchased and is currently being installed on the beam line. Our plan is to incorporate the system in such a way as to retain the capability of recording data on x-ray film, until this capability is no longer required by users. We hope that within the next year, the Mar-Research system will be used exclusively at a wavelength of 1.08Å so that camera and wavelength changes are no longer required. This will maximise the beam time available to users and the scientific productivity of the facility.

White Beam Laue Diffraction Camera (For Use on Beam Line 10-2)

During the past year, the high intensity 31-pole 1.45T (λ=7 cm) wiggler beam line 10-2 has been modified to provide a white light capability so that Laue diffraction studies can be performed at SSRL. The beam line incorporates Be windows totaling 660 µm in thickness and a carbon filter which is 76 µm thick. The beam line also incorporates a 70 cm long Pt-coated fused quartz bent cylindrical x-ray mirror which focuses ~2.3 milli-radians of beam to produce a 1 mm x 4 mm (VxH) focal spot size with 1.4 W/mA in the beam. ~1 milli-radian of beam is available without the mirror, with a spot size of 3 mm x 20 mm (VxH) and with 1.5 W/mA in the beam.

A Laue diffraction camera for protein crystallography and associated experimental apparatus has also been designed and built that is capable of recording diffraction patterns on x-ray film on the time scale of a few tens of milli-seconds. This camera, which is still under development, incorporates a water cooled tungsten pre collimator with adequate lead shielding to reduce background scattering to a minimum, a high speed tungsten focal plane shutter, a goniometer with a motorized Ø-axis and a motorized sample translation along the Ø-axis, and a high magnification crystal mounting telescope fitted with a colour CCD TV camera and display monitor. The Ø-axis can also be inclined

through an angle μ to the direct beam. The entire camera is under computer control and can easily be aligned to the x-ray beam using orthogonal motorized adjustments.

During initial trials on the beam line in May 1991, good quality Laue diffraction data were collected. Typically, only a 60 ms film exposure was found to be necessary to record each diffraction exposure at a SPEAR current of 40 mA. In the near future, using imaging plates as a recording medium and with SPEAR operating at maximum current and in a low emittance mode, it should become possible to record such diffraction patterns on the milli-second time scale. Although not used during our initial trials, the use of the focusing x-ray mirror would provide an even further reduction in exposure time with the loss of some x-ray bandwidth. Trials with this mirror are planned during the next run. Unfortunately, beam time is severely limited on BL 10-2. The line belongs to the University of California/National Laboratories participating research team (PRT), and only one third of the time is available for SSRL general users and it is significantly oversubscribed.

During the development of our Laue camera at SSRL, we have benefited significantly from experience gained with the method at the Daresbury Laboratory with Janos Hajdu, Vilmos Fülöp and Ian Clifton of the University of Oxford.

Chemical and Biochemical Laboratory

The chemical and biochemical laboratory at SSRL includes two stereo microscopes (one with a magnification sufficient to view microcrystals down to 10 μm in size), a Supper optical analyzer, wax melters, fiber optics light sources and adequate bench space for crystallographers to mount sample crystals. The laboratory is also equipped with an ultracentrifuge (1000-65000 rpm), a microfuge, a UV-VIS spectrometer, an inert atmosphere glovebox, ultrafiltration cells, a convection oven (225^{o}C max.), a pH meter, analytical balances (0.001 - 400 gm), a water purifier, a refrigerated circulator (-30 to 100^{o}C), a refrigerator/freezer, an ice machine, a dishwasher, a vortex mixer and an ultrasonic cleaning bath. There are also a number of common chemicals and a selection of basic laboratory glassware. A cold room will be installed in 1992.

Computer Resources

The central computer at SSRL, which is used both for experimental data analysis and for administration purposes, is a DEC VAX 8810. It is linked via Ethernet to DEC MicroVAX II/GPX workstations on each experimental beam line. Each workstation typically has 5 MBytes of memory, a 70 MByte hard disk and a 90 MByte tape drive. The central VAX 8810 and all beam line computers are being run exclusively under the VMS operating system and provide FORTRAN 77 and 'C' compilers. The SSRL computer network is connected to the worldwide HEPnet. Communication to the outside world is also possible using BITnet. A DECserver based dial-in telephone modem (1200 Baud) with 8 lines can also be used to gain access to any SSRL VAX computer from outside the laboratory.

Proposed Future Developments

A Fuji BAS 2000 stand-alone (off-line) imaging plate scanner has been ordered and should arrive at SSRL in February 1992. This scanner will be used for white beam Laue diffraction studies and will also be available to users of the rotation camera facility for very high resolution crystallographic studies and/or for recording diffraction patterns from very large unit cells. A fast changing recording camera will be designed and built in the near future for

Laue diffraction experiments (with either individual imaging plates or with a long roll of imaging plate material if such material can be procured), and a large format recording camera will be built for high resolution monochromatic studies.

As mentioned above, we plan to instal focusing optics on the existing MAD beam line (BL1-5AD) as soon as possible. Although it is likely that we will choose to use a conventional x-ray mirror, or mirrors, we are also going to investigate the use of an asymmetric Kumakhov lens, since the capture and transmission efficiencies are relatively high. After the beam line has been focused, it is almost certain that the MWPC will be replaced by some type of imaging plate detector system for MAD phasing studies, which will eliminate the count rate (and count rate loss) problem, and will provide a higher spatial resolution so that with favorable space groups we can measure Bijvoet related reflections out to the resolution limit at approximately the same time. We are also closely following the development of CCD detectors since they may also prove to be adequate for this application in the near future.

In response to a recent new funding initiative proposed and being investigated by the DOE - Office of Health and Environmental Research, SSRL has requested funding to build a dedicated Structural Molecular Biology Beam Line with four individual experimental stations. These stations would provide facilities for multi-wavelength anomalous dispersion phasing and white beam Laue diffraction in protein crystallography, XAS and SAXS. Although we have not yet heard whether funding for the beam line will be made available, we are encouraged by the fact that the DOE-OHER, through this new initiative, has provided the funding for two additional staff scientists in the SSRL Biotechnology group headed by Keith Hodgson. One of these new positions will be in protein crystallography. Currently, there are only three staff scientists at SSRL working in the field of protein crystallography - Henry Bellamy, Michael Soltis and myself. If funds for this new beam line become available, it will be based on a multi-pole permanent magnet wiggler. We are investigating the possibility of incorporating switchable dipoles within the wiggler so that the radiation can be directed either exclusively to one of the two tandem end stations (to be used for MAD and Laue diffraction) or to one of these stations and also to side stations for XAS and SAXS. This would have the advantage of being able to increase the x-ray intensity to the end stations when required and also to make more efficient use of the fan of wiggler radiation, by reducing the lost radiation generated between individual branch lines. We are also seriously thinking of incorporating a large imaging plate Weissenberg camera of the type that has been developed and used with great success by Prof. Sakabe and his group at the Photon Factory.

User Access to SSRL

To obtain access to beam time and facilities at SSRL, a research proposal must be submitted which is then subjected to peer review. Based on scientific merit, the proposal is assigned a rating by a Proposal Review Panel and beam time is later assigned based on that rating. However, it is sometimes possible to obtain a small amount of beam time without review based on a letter of intent. A special scheduling procedure has been implemented to provide easy access to the rotation camera facility. Beam time is obtained through the submission of a very short application form which is reviewed by the Biology Subpanel of the Proposal Review Panel and given a rating. These ratings are only used to schedule the line in periods when it is oversubscribed. If the line is not oversubscribed, beam time is assigned on a first-come first-served basis. Applications for use of the rotation camera may be submitted at any time. There is no charge for beam time or for the use of SSRL owned facilities.

A MACROMOLECULAR CRYSTALLOGRAPHY BEAMLINE FOR ELETTRA

S. Bernstorff, E. Busetto, M. Colapietro[+] and A. Savoia
SINCROTRONE TRIESTE, Padriciano 99, Trieste, Italy
[+]Dipartimento di Chimica, Univ. "La Sapienza", Rome, Italy

The construction of the storage ring ELETTRA is now in progress. It will be a new third generation source for synchrotron radiation (SR) with a very low emittance (7×10^{-9} m×rad at 2 GeV). The ring will contain up to 11 insertion devices, the electron energy will be 1.5-2 GeV and electron currents of up to 400 mA will be stored. ELETTRA is scheduled to start operation in 1994.

One of the insertion devices will be a permanent magnet wiggler consisting of three segments with 19 poles each. With a peak magnetic field of 1.55 T it will have a critical energy of 4 keV (at 2 GeV) and thus produce a usable photon flux up to photon energies of 25 keV (≈0.5Å) (see figure). The total power of this wiggler will be about 10 kW emitted into a solid angle of about 0.5 (vertically) x 9 (horizontally) $mrad^2$. This power can be reduced by "switching off" one or two wiggler sections; and the emitted SR-spectrum can be shifted to lower energies by decreasing the magnetic field. Only the central part of the wiggler fan will be used for the crystallography beamline, the lateral wings are foreseen for two SAXS beamlines.

The beamline optics is designed to meet several requirements. Both monochromatic and white light must be available. For experiments requiring a low beam divergence the unfocussed beam will be used. Otherwise a higher flux on the sample can be obtained by using a toroidal mirror to focus X-rays up to 25 keV both horizontally and vertically. This mirror will have a grazing angle of 3 mrad, a length of 1.5 m and thus will collect ≈3 mrad horizontally and most of the vertical divergence. Its demagnification factor will be 1.5, which gives an image of the required horizontal size. In the vertical plane the image would be to small, which would not allow a sufficient homogeneity of the flux over the sample area. However the fact that a 1.5m long mirror can hardly be manufactured with the required accuracy can be exploited. The mirror will therefore be composed of three identical toroidal segments with a length of 500 mm each. By slightly moving these mirrors from there ideal position, an image

with an almost constant intensity over the sample area can be obtained.

Upstream of the mirror the SR can be monochromatized in the range 4-25 keV (0.5-3 Å) by a fixed-exit double-crystal monochromator with the crystals in a nondispersive antiparallel setting. By using Si(111) or Si(220) crystals an energy resolution of about $\Delta E/E = 1.3\times10^{-4}$ or 5.3×10^{-5} (at λ=1.542 Å), respectively, will be obtained.

The first monochromator crystal absorbs almost all of the incoming radiation power, i.e. up to 3 kW (for 2 GeV electron energy, 400 mA beam current and 3 mrad horizontal acceptance) with a peak power density of up to 7 W/mm^2. Therefore the first crystal must be cooled efficiently to avoid melting. A cooling scheme with rectangular cooling fins and water or liquid Gallium as a coolant is foreseen. The second crystal will be warmed up to approximately the temperature of the first one in order to minimize the difference in lattice constants which would lead to a movement of the exit beam due to slightly different Bragg's angles. Because of the 18 m long distance to the sample this movement could produce intolerable shifts of the focal spot. During energy tuning the two crystals will be kept parallel within 1 arcsecond by means of a feedback system containing a four-quadrant autocollimator and acting via piezoelectric transducers onto the second crystal. This fine alignment drive will also allow to move the second crystal slightly out of its parallel position with the first one in order to further compensate for small thermal detuning effects or to suppress higher harmonics. For this the intensity of the emerging beam will be monitored with a detector and its output will be used as a signal for the feedback loop.

The segmented mirror will be downstream of the monochromator in order not to impair its resolution. There it needs not to be cooled. However when the focussed white beam is required, the first monochromator crystal will be removed from the beam and the mirror will be translated vertically in order to compensate for the shift in the beam height. Then it is subjected a huge power load. In order to keep the total energy deposited on the mirror, the beamline exit window and also on the sample (on which, neglecting losses, up to 3 kW/mm^2 would arrive) within safe limits, the cooled beam shutter of the beamline will be let open only for the required short measuring times. In addition a rotating shutter can be used to chop the beam.

The experimental station will be build similar to the station at the wiggler beamline of ADONE in Frascati, which is currently used by us as a prototype. However for the ELETTRA diffraction station a Huber 6 circle diffractometer will be chosen with the χ-circle having a diameter of 40 cm. The diffractometer will again be mounted vertically in order to avoid intensity losses due to the horizontal polarization of the SR. The motors of the diffractometer will be controlled with highly reliable switching actuator cards which allow to achieve a resolution of 0.001° in the angular position of each circle. The diffractometer can be controlled either via an operator keybord or automatically by a computer using the CS-program system developed for and currently tested at the ADONE station.

Photomultipliers with NaI(Tl)-scintillator, an image-plate detector and an area-detector based on a CCD in combination with fluorescent optical fibers (pixel size down to $20*20\mu m^2$) will be used to collect the diffracted intensities in the monochromatic or in the narrow bandpass Laue method.

For the data analysis and the presentation of the results the SIR-CAOS software will be used.

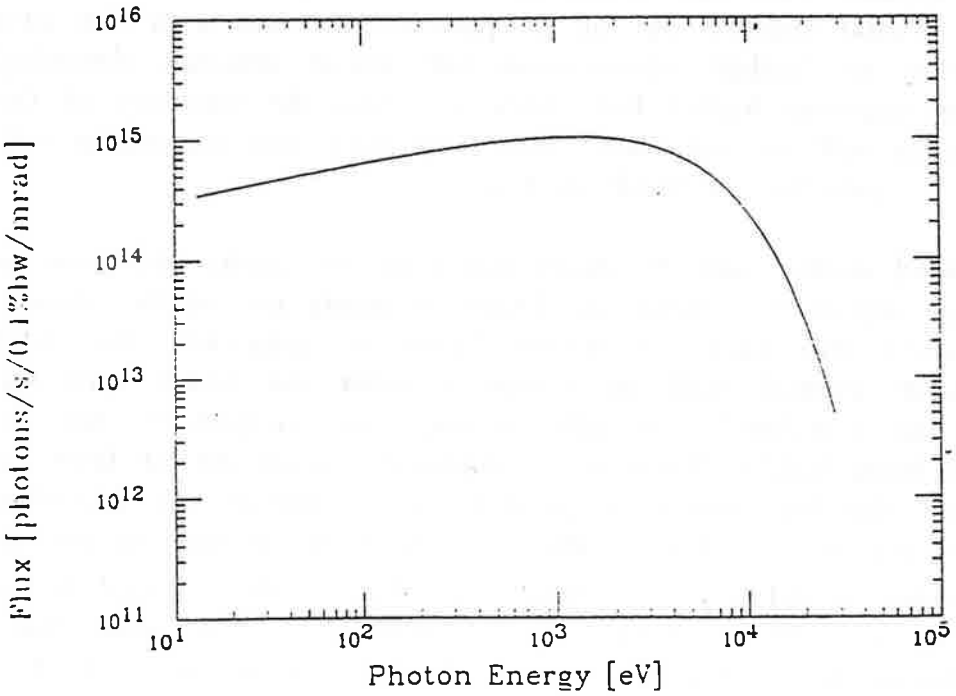

Spectral photon flux of the Elettra 57-pole wiggler at 2 GeV 400 mA.

THE CRYSTALLOGRAPHY WORKSTATION FOR X-RAY STRUCTURAL INVESTIGATIONS OF SINGLE CRYSTALS AT THE TNK STORAGE RING

A.N.Popov, D.M.Kheiker, E.H.Harutyunyan

Institute of Crystallography of the USSR Academy of Sciences
Moscow, USSR

1. INTRODUCTION.

At the Institute of Crystallography, Moscow, a new instrument has been constructed for structure investigations of single crystals at the SR source. The station is intended for work at the TNK storage ring in the town of Zelenograd. Though a wide range of structure investigations is supposed to be carried out, the investigation of protein crystals structure is considered as the main task.

2. THE TNK STORAGE RING.

The TNK storage ring in Zelenograd about [illegible] km from Moscow [illegible] developed at the [illegible] Institute [illegible] Novosibirsk, is [illegible] dedicated SR source intended to solve problems encountered in [illegible] [illegible] investigations [illegible] The source comprises [illegible] [illegible] radiation. [illegible] two superconducting [illegible] The crystallography station [illegible] superconducting wiggler. The main parameters of the TNK and [illegible] are presented in tables 1 and [illegible] The [illegible] radiation source [illegible] collimation. The [illegible]

from the wiggler "S" angle is uniformly distributed among five users channels, with 0.8 mrad radiation for each channel. The distance from the source to the instrument monochromator is 15 m.

Table 1.

Parameters of the dedicated SR source TNK

Energy	- 1.2; 1.6; 2.0 GeV
Emittance	- 27 nm-rad
Stored current: total	- 300 mA
single bunch	- 100 mA
Lifetime	- 10 h

Table 2.

Parameters of the superconducting wigglers

Undulator parameter	- 230
Number of poles	- 8
Length	- 130 cm
Maximum field	- 40 kGs
Interpole gap	- 2 cm

Energy	1.2 GeV	1.6 GeV	2.0 GeV
σ_x, mm	0.2	0.36	0.48
σ_z, mm	0.13	0.43	0.54
σ'_x, mrad	0.1	0.11	0.12
σ'_z, mrad	0.07	0.07	0.09
Γ, mrad	0.02	0.02	0.03
Power, kW	0.5	44	93

4. WORKSTATION COMPONENTS

The radiation is monochromatized and focused by a horizontally deflecting triangular cut Si monochromator prepared from perfect Si single crystals. In front of the monochromator the slits are placed that restrict the white beam. Focusing in vertical

direction as well as cutting of high harmonics is provided by a segmented mirror that is positioned behind the monochromator. The monochromator and the mirror are followed by the slits to eliminate the background and for collimation. To carry out experiments with the crystals under study a special four-circle diffractometer was constructed with a horizontal axis of scanning ω, point scintillation detector and area detector. In front of a changeable collimator of the diffractometer there is a high-precision ionization chamber to monitor the beam. All units of the workstation following the monochromator are placed on the bench that can be turned around the axis, which coincides with that of the monochromator, within 11°-45° range relative to the white SR beam. A special high-precision carriage is used to adjust the diffractometer. The possibility of fine adjusting the distance from the monochromator to the investigated crystal within the range 3-4 m is also envisaged.

4. OPTICAL SYSTEM.

The monochromator design is similar to that of an automatic goniometer head that allows to make adjusting rotations and displacements, bend the triangular crystal-monochromator as a round cylinder and to turn it around the vertical axis by 0.4" steps. Using of a set of crystals Be (111), Si (220) with various asymmetry cut angles [illegible] and the possibility to change the distance [illegible] provides Guinier focusing with the resolution [illegible] reaching $4\cdot10^{-4}$ in a wide wavelength range 0.4-2.5 Å, the intensity of the beam being high. The calculated horizontal size of focal spot is near 300, 380 and 350 μm for Be (111), Si (111) and Be (220) correspondingly. Using of Be instead of Si provides more than two times gain in total intensity, the flux density increasing by only 10-20 %. The mono-

chromator is placed within cylindrical vacuum chamber that can be filled with helium to prevent heating effects.

The vertical size of the beam is about 4 mm at a distance 16 m from the source. The mirror comprises eight planar segments made of polished glass, each measuring 200×80×25 mm^3. The segments are positioned to form a surface imitating an elliptical cylinder. Tuning the mirror to the grazing angle of 2.4 mrad ($\lambda_{min} \approx 0.9$ Å) leads to vertical focusing of the whole beam to 0.5 mm. Such a geometry will allow to work in the wavelength range 2.5-0.95 Å without readjusting the mirror when changing λ. To focus more hard radiation one will need plates with heavy metal coating. The evaluated density of the radiation flux for 0.15 A current is 10^{12}-10^{13} photons/(s mm^2) in the focus point.

5. DIFFRACTOMETER.

All four diffractometer axes are supplied with absolute angledetectors that allow to measure angles to 0.005° precision. Discreetness of rotation around all axes is not worse than 0.002°.

As an area detector a multiwire proportional chamber is used with a drift gap 100 mm long, constructed at the Joined Institute for Nuclear Research, Dubna. The detector is filled with Ar, Xe and methane gas mixture under the pressure 4 atm. Passive getter inside the detector provides long-time gas purity without refilling. The entrance window of de[illegible] mm thick imitates part of the spherical surface of 120 mm radius and has the diameter 130 mm. Correcting drift electrodes practically eliminate parallax. The data is collected by fast delay-lines, counting rate being 10^6 Hz at 20 % losses. The number of pixels is 300×300, the pixel size - 0.25 mm, the detector resolution - [illegible] mm. Differential non-linearity does not exceed [illegible] %. The detector allows to work in a wide wavelength range

from 0.8 Å to 1.8 Å with detecting efficiency not worse than 80 % .

The area detector is fixed on a special carriage that allows both its rotation by 45° around horizontal axis coinciding with ω axis of the diffractometer and changing the distance from the crystal under study to the detector from 100 mm to 800 mm.

6. CONTROL SYSTEM.

All the controlling and detecting units including the electronics of the area detector are manufactured according to CAMAC standards. As a controlling computer a PC AT is used.

REFERENCES

1. A.G.Valentinov et al. - Preprint INP 90-129, Novosibirsk, 1990.
2. G.N.Kulipanov - Synchrotron Radiation News, 1991, Vol.4, N°1, p.17-20.

PROTEIN CRYSTALLOGRAPHY AT THE SRS

Colin Nave
SERC Daresbury Laboratory, Warrington WA44AD, UK

The SRS is a 2GeV electron storage ring with a $\lambda_c = 3.9$Å and circulating currents of 200-300mA with a lifetime of over 30hrs. A 5 Tesla superconducting wiggler is used as a wavelength shifter to give $\lambda_c = 0.9$Å. The machine was upgraded in 1987 to give a reduced source size of 2.4mm fwhm horizontal and 0.3mm vertical. The SRS runs at high currents for approximately 5000 hours each year. During the past 10 years four facilities for protein crystallography have been developed. Each facility is optimised for a particular type of data collection. However, particularly in the earlier beamlines, some flexibility was built in to gain experience of different types of experiment. The facilities are used for routine data collection where the demand exceeds the time available. In addition, less routine experiments, such as anomalous scattering and Laue diffraction are being undertaken. All the protein crystallography groups in the UK, as well as many from abroad, use the facility. Agreements with the Medical Research Council, Sweden and the EEC provide access for users not supported by the SERC. These agreements are used to fund some of the developments of the protein crystallography facilities.

The SRS is currently in a 6 month shutdown to install a new 6 Tesla Wiggler (with no protein crystallography beamlines!). Beam should be available again in May 1992.

Each station is briefly described below. The intensity for each station is quoted for 200mA current taking into account losses in the beamline. Measured values are in reasonable agreement with these figures.

Station 7.2 - Monochromatic
Bent triangular Ge(111) monochromator with 4mrad horizontal acceptance giving 9:1 horizontal focusing at 1.488Å.
$\Delta\lambda/\lambda = 0.0004$
Fused quartz mirror 1:1 vertical focusing
Focal spot size 0.5mm x 0.3mm HxV
Intensity $6X10^{11}$ photons/sec/mm^2
Arndt Wonacott oscillation camera and film data collection.

This was constructed in 1980 to use radiation from a bending magnet. It is available for approximately 75% of the time for protein crystallography.
Some wavelength tunability was incorporated into this station. However, it is now operated at a fixed wavelength of 1.488Å for routine data collection from protein crystals. There are no resources at present to develop this facility any further, although an obvious improvement would be the installation of a detector system other than film.

Station 9.6 - Monochromatic
Bent triangular Si(111) monochromator with 3mrad horizontal acceptance giving 8:1 horizontal focusing at 0.895Å. The source is a 5 Tesla Wiggler.
$\Delta\lambda/\lambda = 0.0004$
Platinum coated fused quartz mirror 1:1 vertical focusing
Focal spot size 0.5mm x 0.3mm HxV
Intensity $1.3X10^{12}$ photons/sec/mm^2
Arndt Wonacott oscillation camera and film data collection.
Upgraded Enraf Nonius FAST TV detector - resolves 80 diffraction orders?
R-Axis II Image Plate System - resolves > 200 diffraction orders?

This station on the wiggler has also been used for developing multiwavelength techniques and also focused Laue. It is now operated routinely as a fixed wavelengtn station at 0.895Å. The reduced wavelength on this station (compared with station 7.2) gives reduced absorption errors, a reduction in radiation damage, and enables higher resolution data to be collected.

For a long time, this was the worlds most intense source for protein crystallography at 0.9Å. This is exemplified by its use for FMDV (with perhaps the lowest diffracting power of any solved structure) and SV40 (perhaps the largest object whose structure has been solved). Both of these projects used film for data collection. Nowadays, multipole wiggler sources available elsewhere (e.g. Cornell) provide more intensity. However, improved detector systems on 9.6 should mean that the facility will be very useful for the majority of crystallographic projects. The FAST TV detector is being upgraded with the DEP image intensifier. This should enable data collection from small to medium unit cells with a minimum of dead time. It will be complementary to the R-Axis II image plate system which would be used for data collection from large unit cells. Both of these systems will be available after the present shutdown of the machine.

Station 9.7 - Laue
Wavelength range 0.2-2.6Å.
10^{10} photons/sec/mm^2 in $\Delta\lambda/\lambda = 0.00015$ at 1Å
Modified oscillation camera with film data collection
Shutter opening times down to 20 msec

This station is available approximately 25% of the time for protein crystallography. It is the preferred station for those Laue experiments which require wavelengths of less than 0.5Å.

Station 9.5 - Focused Laue and Tunable Monochromatic
Wavelength range 0.45-2.6Å.
Water cooled channel cut Si(111) monochromator.
$\Delta\lambda/\lambda = 0.00015$
Platinum coated fused quartz toroidal mirror.
Aperture 1.4 mrad horizontal, 0.1mrad vertical
Focal spot size 1.5mm x 0.4mm HxV
Calculated intensity $3.6X10^{11}$ photons/sec/mm^2 at 1Å within $\Delta\lambda/\lambda = 0.00015$
Modified Arndt Wonacott oscillation camera and film data collection.
Shutter opening time down to 50 microseconds
Marresearch image plate system now installed and collecting data routinely.

This station is constructed via a collaboration with the Swedish research council. The station has been commissioned for the Laue experiments and gives the expected reduction in exposure time compared with station 9.7. Laue data collected using the image plate system is now being processed. Several MAD data sets are also being evaluated and the station is operating routinely for conventional monochromatic data collection with the image plate system. This includes data collection from virus crystals at 3.5Å resolution.

Other Facilities
Cooling to -20C and down to near liquid nitrogen temperature
Microdensitometer for film scanning
Microscopes
Biochemistry Laboratory
Computing facilities
Software Development - CCP4, Laue

Future Developments

The facilities described above are a result of many years effort in the development of X-ray beamlines optimised for protein crystallography. The hoped for acquisition of detectors to replace film has now occurred. Facilities for on line processing of the data will be implemented as confidence in the detectors and the data processing software is gained.

The stations on the SRS will continue to be useful, for the majority of protein crystallography projects, for the foreseeable future. A facility on an ESRF bending magnet will have characteristics which are only slightly better than those of the SRS Wiggler stations. The multipole wiggler and undulator beamlines of the ESRF will have a major advantage, particularly for small crystals, large unit cells and time resolved experiments.

A review of synchrotron radiation in the UK will take place in 1992. Proposals to be submitted to this review include one to build a replacement for the SRS. This might be a 3-4 GeV machine optimised for the high flux available from multipole wigglers. For protein crystallography this should provide approximately 20 times the intensity of station 9.6 on the SRS. A national source of this type should provide state of the art facilities for all routine protein crystallography experiments. MAD experiments are now becoming routine and of course the ability to collect the most accurate high resolution data should be routine. Points to consider for future protein crystallography facilities are -

1) What wavelength?

The experience is that going from 1.5Å to 0.9Å wavelength improves crystal lifetime significantly. The mechanism for this is still not clear. For a 300 micron crystal, the number of absorbed photons per scattered photon decreases significantly when the wavelength is reduced. However, there is only a small increase in the absorbed energy per scattered photon and this criteria might be a more reasonable one. In any case, the improvement in lifetime one gets in practise is often greater than would be expected if either absorbed energy or absorbed photons are the relevant factor. The temperature rise due to absorbed radiation in a crystal is significantly greater at 1.5 Å wavelength than at 0.9Å wavelength and this might be a factor in the increased lifetime at shorter wavelength. In order to resolve these issues, there is a need for a systematic study of radiation damage as a function of wavelength at both room temperature and liquid nitrogen temperature.

2) What intensity?

The experience of using more intense sources is that it has often been possible to collect more data from a protein crystal. This is presumably because of the time required for chemical processes to destroy the crystal. By cooling the crystal to near liquid nitrogen temperature, it is possible to reduce or halt these processes and obtain enhanced crystal lifetimes. However, primary radiation damage will still occur. The experience from cryoelectron microscopy is that there is an upper limit to the dose. If this dose is translated to an X-ray dose, it would correspond to a few days exposure on an existing monochromatic synchrotron beamline (R.Henderson, Proc.R.Soc. London Ser.B241, 6, 1990). Experiments at liquid nitrogen temperature with the more intense focused white beam on station 9.5 give a crystal lifetime of a few minutes, in agreement with the prediction given by Henderson. The implication is that cooling to liquid nitrogen temperature will not allow a complete data set to be collected from a single crystal of small size. A typical protein crystal might require 2 hours exposure on present X-ray beamlines to collect a good data set. Many data sets could be collected at liquid nitrogen temperature before radiation damage occurred. However, if each dimension of the crystal was reduced by a factor of 10, it would only be possible to collect a fraction of a data set before radiation damaged occurred. If this surmise is correct, there will be a limit to the size of crystal from which it would be possible to collect a complete data set on the more intense undulator sources. This might be an argument for using some of the increased brilliance of these sources to obtain better angular collimation as well as more intensity.

3) What detector

The detector requirements for protein crystallography vary somewhat from sample to sample. The image plate systems are making a big difference to protein crystallography data collection. Their large size, and ability to record high count rates with a large dynamic range means that they can be used for essentially all the protein samples that are being studied with monochromatic radiation. The dead time associated with the scanning is not a serious problem apart from the fact that it makes fine phi slicing of the data impractical on a synchrotron. Although detectors with a poor count rate capability or significant dead time might appear to have a limited use on the more intense sources, this would not be the case if they were used for looking at more weakly diffracting specimens. There seems little point in developing detectors that would enable entire data sets to be collected in a few seconds unless time resolved studies are contemplated. Detectors with an ability to collect the best quality data in a few hours with fine phi slicing would be very useful. A detector with the following characteristics is (tentatively!) suggested.

i) Speed - Images every 5 secs. This is necessary for fine phi slicing on a synchrotron source and corresponds to the shortest time routinely used with the FAST TV detector on station 9.6 at the SRS.

ii) Resolution - At least 200 diffraction orders adequately resolved across the detector face.

iii) Size > 150mm. This is necessary, as the protein crystals themselves often define the size of the diffraction spots. Smaller detectors with better spatial resolution will have limitations in this respect.

iv) Dynamic range > 10^3 with a high DQE over this range. A range of 10^3 is superior to that obtainable with a pack of 3 films. The image plate systems can make measurements over a dynamic range of 10^5. This is extremely useful, especially for high resolution studies. However, their DQE at higher intensities is limited by errors other than photon statistics.

v) Global Count Rate >10^6 cps. This value is approximately 3 times that obtainable with the Mark II spherical drift chamber at Lure. It has been demonstrated (e.g. Weis et.al., Science, **254**, 1608, 1990) that the Lure detector can collect high quality diffraction data with an exposure time of 30 secs per 0.1° frame.

vi) Local count rate >10^3 cps for each diffraction spot.

vii) Wavelength capability - 0.9Å or less.

It should be possible to develop a detector of this type by improvements of present systems rather than using radically new and expensive technology. All detectors are a compromise so each individual specification above is relatively modest. The local count rate and dynamic range of the above might be considered the most limiting. However such a detector would represent a worthwhile improvement over present systems for many applications.

Such a detector would not properly exploit the highly parallel beams from undulator beamlines. For these beamlines, where the diffraction spots could have small angular divergence, a much larger detector placed at a large distance would give a better peak to background ratio. In addition, it would be advantageous to be able to collect data in 0.01 degree phi slices to retain compatibility with the beam divergence. This implies the ability to collect up to 10,000 images per data set. The local count rate capability would have to be higher because each diffraction spot would only be in the reflecting position for a shorter time interval. To properly exploit the highly parallel beams from undulator sources, a much more ambitious detector system needs to be developed.

EQUIPMENT FOR BIO-CRYSTALLOGRAPHY AT LURE

R. Fourme, R. Kahn, A. Lewit-Bentley & J.P. Benoit,
LURE, bat. 209D, Université Paris-Sud, 91405 Orsay Cédex, France

At LURE, the synchrotron source used for biological crystallography is called DCI. This machine is a 1.85 GeV positron storage ring with a fairly high emittance and a circulating current of 320 mA just after injection. As the beam lifetime is at least 60 hours, there is no reinjection during the course of a shift, except in case of an accidental beam dump, a situation which is very favourable for accurate data collection. A 5 pole superconducting wiggler, shifting the critical wavelength of the sychrotron radiation emission from 3.4 Å to 1.1 Å, is a source of intense and short wavelength X-rays. The planned schedule, starting from end of march 1992 after a 4 month shutdown for a *jouvence* of the ring, includes 124 user shifts of 22 hours, usually from Tuesday to Friday every week.

Facilities for protein crystallography have been developed by the local staff for the last 15 years. Initial instruments used films. Then, in parallel, several diffractometers based on spherical drift multiwire proportional chambers (MWPC) were constructed. After a major effort extending over the last three years, we are now completing a new generation of four instruments, with each of them optimised for a particular type of data collection. Two instruments are fully operational. The others will be opened to external users by september 1992.

Regular users have been primarily French groups and a few groups from foreign countries (essentially from the UK and the USA). Our capabilities will be quite significantly improved this year by the new instruments and longer sessions.

Beam time is allocated by a Programme Committee which has a meeting in February every year. Proposal forms can be obtained from Mrs Le Monze (Fax 33-1 64464148), after a contact with one of the local contacts.

A short description of each instrument is given below.

Station DW32 (wiggler line)

This setup is 100% dedicated to fast collection of diffraction and diffuse scattering data using monochromatic radiation between about 0.7 Å and 1.6 Å. The most frequently used wavelength is around 1 Å.

Double focussing optics

The optical system is designed for high intensity and slow tunability. It includes two Bragg reflectors. The first reflector, a curved crystal, selects the desired wavelength (and higher order harmonics) and focusses the beam in the horizontal plane. The second reflector, a curved layered synthetic microstructure (LSM), is used for harmonic rejection and focussing in the vertical plane. With a 8:1 demagnification, the fwhm beam dimensions at the focus are about 1.2 mm (H) x 0.6 mm (V).

curved crystal: shaped to a triangle (208 mm x 42 mm) with the profile corrected to provide elliptical curvature. Three crystals (one Ge(111) and two Si(111), optimised resp. for λ = 1.4, 1.0 and 0.7Å): Each crystal is mounted on a water-cooled copper plate with heat transfer by helium. Max. aperture: 3.9 (resp. 2.9) mrad at λ = 1.40 (resp. 1.00) Å.

LSM: rectangular plate (200 mm x 5 mm x 3 mm) with 200 Si/W bilayers, total period 37Å. Designed to reject $\lambda/3$ radiation. Elliptical bending. Reflectivity about 60% at 1.4Å. Max. aperture: 1.9 (resp. 1.3) mrad at λ = 1.40 (resp. 1.00) Å.

Optical bench

Two orthogonal axes in coincidence with resp. to the 2θ rotations of the monochromator and of the LSM.

Diffractometer stand

Stand with 4 degrees of freedom intersecting at the entrance pinhole of the collimator. Manual or automatic alignment of the diffractometer with respect to the X-ray beam, using a microprocessor in a VME crate. Focussing is optimised at the detector location by observing the X-ray beam with a phosphor-coated fibre optics and a CCD.

Goniometer

Modified from an Enraf-Nonius rotation camera. Single axis with 0.002° steps. CCD microscope (Fort, Japan) for continuous observation of the sample on a colour monitor outside the hutch.

Low temperature equipments

(i) a commercial equipment (FTS, USA) used with a heated reflector for frost-free operation down to -40°C with a standard goniometer head.

(ii) a laboratory-made equipment for cryo-crystallography, providing a laminar flow of dry cold nitrogen (from RT to - 165°C); the goniometer head is protected by a heated deflector.

Area detectors include:

(i) films on a caroussel

(ii) an image plate system in normal-beam geometry, built by J. Hendrix and A. Lentfer from the EMBL Outstation (Hamburg). The crystal-to-detector distance can be adjusted between 100 and 600 mm. The detector can be translated vertically by up to 100 mm. The sensitive surface is a disk, diameter 180 mm, pixel size 0.15 mm x 0.15 mm. Integration box: edge 10-13 pixels (typical, providing up to 120 adjacent boxes per diameter). Range

and residual noise per pixel (in ADC units): resp. 7 and 65536. Simple mapping function. Correction of the intensity per pixel using a flood-field table. Computer hardware: a VaxStation 3100 model 38 (16 MO CPU), a Winchester disk and backup on 8mm video tape (up to 2.3 GO/tape). Minimum elapsed time per frame: about 130 s. Range of exposure times (to get an idea): from about 5 s/degree at λ = 1.40 Å for a good crystal with a medium-sized unit cell, to a few minutes/degree at λ = 0.95Å for a poorly diffracting sample with a very large unit cell. Off-line data analysis software: MOSFLM package (version produced by A. Leslie, MRC Cambridge). Usual $\Delta\omega$ per frame: 1 degree (due to the relatively long cycle time). Rsym (on intensities, per sample) typically 4-6 %.

local contacts : R. Fourme and J.P. Benoit.

Station D23 (bending magnet line)

This setup is dedicated half-time to biological crystallography, and especially multiwavelength anomalous diffraction measurements (MAD), between 0.95 and about 1.8Å. It includes a tunable monochromator and a diffractometer with a MWPC (MARK II instrument).

Single focussing optics

Tunable two crystal monochromator Si(111), or Si(220) for shorter wavelengths; sagittal bending on the second crystal. Fixed position exit slit. Max. horizontal aperture: 1.5 mrad. Two position-sensitive ion chambers for beam position monitoring. Adjustment of X-ray beam focussing with a CCD detector (like DW32).

Goniometer

(4 +2) axis goniometer (Huber, Germany) with an horizontal ω-axis; 0.001° steps; beam monitor on the collimator, with charge integration during the exposure of each frame.

Detector

Large counting area detector mounted on the 2θ-arm of the goniometer. MWPC and electrostatic optics with two spherical electrodes for parallax suppression and randomisation of the pulsed time-structure of the synchrotron beam. Fixed crystal-to-detector distance (580mm). Disk-shaped useful sensitive area, diameter 486 mm, 185,500 pixels of 1mm x 1 mm. Digital position encoder, max. count rate 350,000 c/s with 20% losses. Point spread function (PSF): gaussian, fwhm 1 mm. Detection quantum efficiency (DQE): 0.75 at λ = 1Å. Integration boxes: 5 pixels x 5 pixels (up to 97 adjacent boxes par diameter). Maximum count per pixel: 65536. Average detector noise per pixel 0.01 c/s. Mapping function: simple

expression giving an rms agreement between observed and calculated positions of 0.3 mm. No further correction for spatial distortion. No flood-field table.
Current upgrade of data acquisition hardware with VME electronics. Backup on standard magnetic tapes, and soon on 8 mm video tapes.
Low temperature apparatus
Commercial equipment (FTS, USA).
Data analysis software
Off-line. MADNES package (from J. Pflugrath and A. Messerschmidt; version produced by the EEC Workshop on Position Sensitive Detector Software, dir. G. Bricogne).

As the crystal-to-detector distance is fixed, the unit cell parameters that can be handled by this instrument are proportional to the wavelength of the X-ray beam (to fix ideas, good data sets have been collected on crystals with a unit cell parameter of 250 Å at $\lambda = 1.38$Å). $\Delta\omega$ per frame is usually 0.05°, with exposure time of 15 seconds per frame at $\lambda = 1$Å; dead time between frames is about 1 second. Rsym (on intensities and per sample) range typically from 2.5 to 3.5%.

Local contact: R. Kahn .

Station D41 (bending magnet line)

This station, which will be full-time dedicated to biological crystallography, features a four-circle diffractometer equiped with a MWPC (Mark III instrument) and the curved crystal monochromator which was formerly used with a rotation camera. It will be devoted to accurate and high resolution measurements using wavelengths between about 1 and 1.8 Å. With respect to the Mark II, the capability to handle crystals with large unit cell parameters is increased.
Current status: the MARK III is installed and has produced good diffraction images. Software implementation is in progress.

Single focussing optics
Triangular, asymmetrically cut Ge(111) crystal. Max. horizontal aperture: 3 mrad. Slow tunability.
Goniometer
4-circle goniometer (Huber, Germany) with a vertical ω-axis. Beam monitor like D23.

Detector

Spherical drift MWPC on air-pads. Position in the horizontal plane controlled by the 2θ-arm of the goniometer which is on air-pads. With respect to the Mark II detector, new position encoder with fast calculation of the centroid of the cluster of impulsions on both cathode planes, built in VME technology; max. total count rate 200,000 c/s with 20% losses. Disk-shaped sensitive surface with about 742000 pixels, 0.5 mm x 0.5 mm. PSF : 0.15 mm fwhm. Integration box edge: typically 3 to 3.5 mm (up to 162 adjacent boxes along a diameter). Detector noise 0.01 c/s. Maximum count per pixel: limited in practice only by exposure time. Mapping function as for the Mark II detector. No correction for DQE variation.

Computer hardware

VaxStation 3200 (16 MO CPU), Winchester disk, backup on 8 mm video tape.

Data acquisition and data analysis software

MADNES package (see D23 setup)

Local contact: A. Lewit-Bentley.

Station DW11 (wiggler line)

The DW11 station, which is adjacent to the DW32 station (on the opposite side of the same line), is dedicated to the use of the non-focussed white radiation emitted by the wiggler. The basic equipment of the hutch (cooled slit systems, supports etc...) will be shared between diffraction experiments under high pressure (using energy dispersive measurements) and the Laue method.

The equipment for the Laue method is currently being constructed in collaboration with the IBS in Grenoble (M. Roth). It will include a multi-axis goniometer with a translation along the ϕ-axis and a CCD microscope. Detectors will include films, mounted on a film caroussel with an horizontal axis, and an image plate system with an external scanner (Molecular Dynamics). The goniometer and the detector will be installed on a remotely controlled stand, sharing the VME electronics of the DW32 experiment.

Weissenberg Camera and Facilities at the Photon Factory

by Tsuneyuki Higashi

Rigaku Corporation,
3-9-12 Matsubara-cho, Akishima-shi, Tokyo 196, Japan

The Photon Factory, KEK, Japan, is the first facility dedicated to research work using synchrotron radiation. Current operating conditions are 2.5 GeV and 350 mA. For protein crystallography, the beamlines BL-6A2 and BL-14A are open for users. The BL-14A is shared with EXAFS work, having a four-circle diffractometer and an Arndt-Wonacott oscillation camera with an imaging plate, while, at the BL-6A2, Sakabe's Weissenberg camera with imaging plate is fully used by world-wide protein crystallogaphers.

The Weissenberg camera data collection system at the Photon Factory consists of the Sakabe's Weissenberg camera for macromolecular crystallography [N. Sakabe (1983), J. Appl. Cryst. **16**, 542], a Fuji imaging plate (IP) as a two-dimensional detector, a Fuji image reader BA100, and a data reduction program [T. Higashi (1989), J. Appl. Cryst. **22**, 9]. Recently a full report has been published on this data collection system [N. Sakabe (1991), Nucl. Instr. Meth. **A246**, 572].

The reasons the unique Weissenberg geometry is employed at the Photon Factory are threefold. Firstly, a cylindrical cassette is convenient to collect higher angle data because of the less oblique incidence angle to the film. Secondly, spot density can be maximized by translating the cassette synchronized with a crystal rotation, reducing the number of films to be processed and, hence, reducing errors due to film scaling. In addition, this increases the chance that Bijvoet pairs are recorded on the same frame. Thirdly, the wider oscillation angle increases the ratio of the fully recorded reflections to that of the partial reflections.

On the other hand, there are some disadvantages in this geometry. The problem that the crystal-to-film distance is fixed to the radius of the cylindrical cassette is solved, to some extents, by using cassettes with different camera radii, of 143.25, 286.5, 430.0 and 573.0 mm. The accumulated background due to wider oscillation is not so serious when the camera is filled with helium gas and the relatively larger camera radius is used. Optionally, a multi-layer-line screen is usable for the further reduction of the background. A variation of absorption effect during wide oscillation is less significant when we use wavelength of 1.0 Å or shorter.

The excellence of the IP as an x-ray detector will be discussed by others at the meeting. The exposed IP of 200 × 400 mm is readout on a Fuji BA100 image reader with a pixel size of 100 × 100 μm. The intensity per pixel is in logarithmic scale, digitized upto 256 levels. It takes about 2 min to read an IP sheet and another 4 min to transfer data to magnetic tape.

In the normal use of the BL-6A2 station, the wavelength is 1.04 Å, monochromatized by an asymmetric-cut triangular bent Si(111) monochromator and calibrated by the Au LIII absorption edge. The sample crystal is aligned so as to make layer lines perpendicular to the crystal rotation axis, by two (1-4°) oscillation photographs taken 90° apart using polaroid film.

The shortest time to obtain a whole data set along one axis is 1.5 h, from crystal mounting to the end of the last IP exposure. Most users have collected three full data sets in a day except for data processing.

Accuracy of the obtained data is reasonable. A comparison of the Weissenberg data with four-circle diffractometer data for common low angle reflections [Y. Takeuchi, et al. (1988), Photon Phactory Activity report 6. 103] indicates that the quality of Weissenberg data is at least comparable to four-circle diffractometer data. The anomalous difference Patterson map clearly showed Hg-Hg vectors, where the wavelength was 1.00 Å, the occupancy of Hg atom was 0.4, and hence the contribution of anomalous scatterer to f'' was 4 electrons [N. Watanabe, et al. (1989), J. Boichem. **105**. 1]. Using the data collected on the Weissenberg camera, the structure of cytochrome C_{553} was solved by the multiple anomalous dispersion method [A. Nakagawa, et al. (1990), J. Biochem. **108**. 701].

Protein crystallography facilities at EMBL - Hamburg: present and future.

Jaap Pijpelink,
European Molecular Biology Laboratory,
Notkestrasse 85,
2000 Hamburg 52, Germany.

Till recently, EMBL had two beamlines available at the DORIS II machine, which were dedicated for protein crystallography. Because of a major reconstruction of the DORIS machine during the second half of 1990 and the first half of 1991, one of these beamlines, X11, had to be removed from the ring. This because previously, X11 was fed with radiation from the positrons running in the machine, and pointed in the opposite direction as the other beamlines. The machine has been upgraded to DORIS III, with the so-called Bypass project. In this project, one of the very long straight sections in which the former collision point for the Crystal Ball experiment has been, was replaced by a curved bypass with seven shorter straight sections. An overview is given of DORIS III, the existing beamline X31, the planned rebuild of X11, and the planning of a wiggler beamline with two branches.

The machine.

After the rebuilding, DORIS is still a high energy physics machine, but with only one experiment for high energy physics (HEP). It is an asymmetric machine, having a long straight section for the HEP experiment and seven straight sections used for insertion devices opposite. Six of these straight sections are four meters long, the central one is only 2.7 meters long. Because it is still a HEP machine, DORIS is running with both electrons and positrons for about 0.5 - 2/3 of the year. During this so called HEP-run, the energy of the electrons in the machine is about 5.3 GeV, while during dedicated synchrotron runs (SR), the energy is about 4.5 GeV. Table 1 gives the electron energy, maximum current in the machine and the critical wavelength of the radiation from a bending magnet for each of these two modes.

Table 1: Main parameters of DORIS III in High Energy Physics and Synchrotron mode.

	HEP run	SR run	
electron energy	5.3	4.5	GeV
maximum current	40	100	mA
bending magnet λ_c	0.46	0.74	Å

The value of 100 mA for the current during SR runs, has not yet been achieved. During the last weeks of beamtime for 1991, the maximum current for stable beam conditions has been about 45 mA.

Existing beamline.

The only beamline for protein crystallography EMBL had available during 1991-beamtime, was X31 in the old Hasylab experimental hall. The main parameters are given in table 2.

Table 2: Main parameters of bending magnet beamline X31.

- monochromator: channel cut Si-111 crystal, tunable from 0.6 to 2.5 Ångstrom
- toroidal shaped gold coated quartz mirror (8 segments) for focussing with a 1 : 1 demagnification
- Laue experiments possible
- Imaging plate scanner as data collection system
- 6×10^9 photons/sec/mm^2 @ 3.7 GeV and 100 mA
- focus size (2.3 σ) : 3.8 mm x 2.6 mm

Other bending magnet beamlines.
The second beamline EMBL had available for protein crystallography, X11, has been dismounted, and will be rebuilt in one of the new experimental halls, Hasylab V. Previously, it was fed by radiation from the positrons, in the future it will be fed by radiation from the electrons in the DORIS machine. This means an effective increase in available beamtime for this line. Another difference will be the distance from the source to the monochromator, which was 22 meters in the old setup, and will be changed to about 16 meters. The main parameters of X11 are given in table 3.

Table 3: Main parameters of bending magnet beamline X11.

- bent Ge-111 crystal with 7 degrees asymmetric cut as monochromator
- wavelength range variable between 0.9 (0.7) and 2.3 Ångstrom
- horizontal focussing with monochromator crystal
- bent quartz mirror (6 segments) as vertical focussing device with 4 - 5 : 1 demagnification
- Imaging plate scanner as data collection system
- $> 10^{11}$ photons/sec/mm^2 @ 5.3 GeV and 45 mA
- focus size (2.3 σ) : 1.2 mm x 0.64 mm

The numbers as are given in table 3 are for the previous setup, in which X11 could only be used during High Energy Physics runs.

A beamline which has been planned for the future, but which doesn't have a high priority, is X12, which is the straight through branch of line K. This line has not been used by EMBL in the past, but it will be activated as another protein crystallography line. Because it is still open, it can be dedicated to, for example, Laue work, or for MAD experiments, or it can be equiped with a channel cut monochromator and a toroidal mirror, and be used as an upgraded version of X31. How it will be, depends on requests from the user community.

The wiggler beamline.
The wiggler beamline EMBL will get in Hasylab V, will have two branches: one straight through branch, BW7A, and a sidewards deflected branch, BW7B. The source of radiation for this line is one of the new X-ray wigglers, which are installed in the DORIS-Bypass. The main parameters of the wiggler are given in table 4.

Table 4: Main parameters of Bypass Wiggler BW7.

- number of poles: 56
- total length 4 meters
- magnet field 1.01 Tesla
- minimum gap 30 mm
- deflection parameter K = 13.2
- critical energy 13.6 keV (0.91 Ångstrom) @ 4.5 GeV electron energy
- power density 118.4 W/mA,mrad^2
- total power 52.5 W/mA
- source size 5.1 mm x 1.3 mm (FWHM)
- divergence 3 mrad x 0.5 mrad (FWHM)

The front end of the wiggler beamline will be constructed by Hasylab, and will have standard components, as the other Bypass beamlines. The main components of the front end are for vacuum protection and radiation safety, as well as beam position monitors and a water cooled slit system. In the experimental hall, a plane premirror will be installed. This will be in first instance a metal mirror, which will be replaced in about one year from startup by a SiC mirror, which will have a rhodium coating. The premirror will be followed by carbon foils and a beryllium window. After

the Be-window, the beamline will be split into the two different branches. BW7A will be equiped with a double crystal monochromator (Si 111), and a toroidal mirror with a 3 : 1 demagnification. The monochromator will be tunable in a range from about 0.6 to 2 Å. This mirror will also have a Rh-coating. The side branch, BW7B, will have a triangular, bent Ge 111 or Ge 220 crystal as monochromator, followed by a segmented, bent mirror for vertical focussing of the beam. This monochromator will be tunable in the range from about 0.6 to 1.6 Å. BW7B will be constructed first, because this design is more straightforward than that of BW7A, and at least one of the lines should be in such a state that tests of the beamline are possible during late April 1992. All EMBL protein crystallography beamlines will have imaging plates as detector system.

The GBF/MPG Wiggler Beamline on DORIS III

Hans D. Bartunik
Max-Planck Research Unit for Structural Molecular Biology
c/o DESY, Notkestraße 85, 2000 Hamburg 52, FRG

The GBF/MPG wiggler beamline (BW6) will be used for applications in protein crystallography which require highly intense synchrotron radiation (see, e.g., Bartunik, 1991). These include native and derivative data collection at highest possible resolution from medium- and high-MW structures, experimental phasing by resonant diffraction techniques, and studies of structural kinetics by low-temperature and time-resolved techniques. Main users will be the GBF Braunschweig, the MPI for Biochemistry in Martinsried, the Max-Planck Research Unit at DESY and research groups from other Max-Planck Institutes. The beamline will also be accessible for groups outside the GBF and MPG. Beamtime may be requested on the basis of proposals which will be evaluated by a priorities committee.

The beamline BW6 includes a 56-pole wiggler with a field of 1 T; the length of the straight section is 4 m. At 4.5 GeV, the predicted source dimensions are (H x V =) 2.1 mm x 0.55 mm, the divergences 0.21 mrad x 0.21 mrad. The horizontal emittence will be 4.4×10^{-5}, the vertical emittence 1.2×10^{-6}. At wavelengths near 1.0 A, the spectral brightness will be 2.2×10^{13} photons/sec/mA/mrad^2/0.1% bandwidth, i.e., by nearly a factor 100 higher than at a bending-magnet beamline at DORIS.

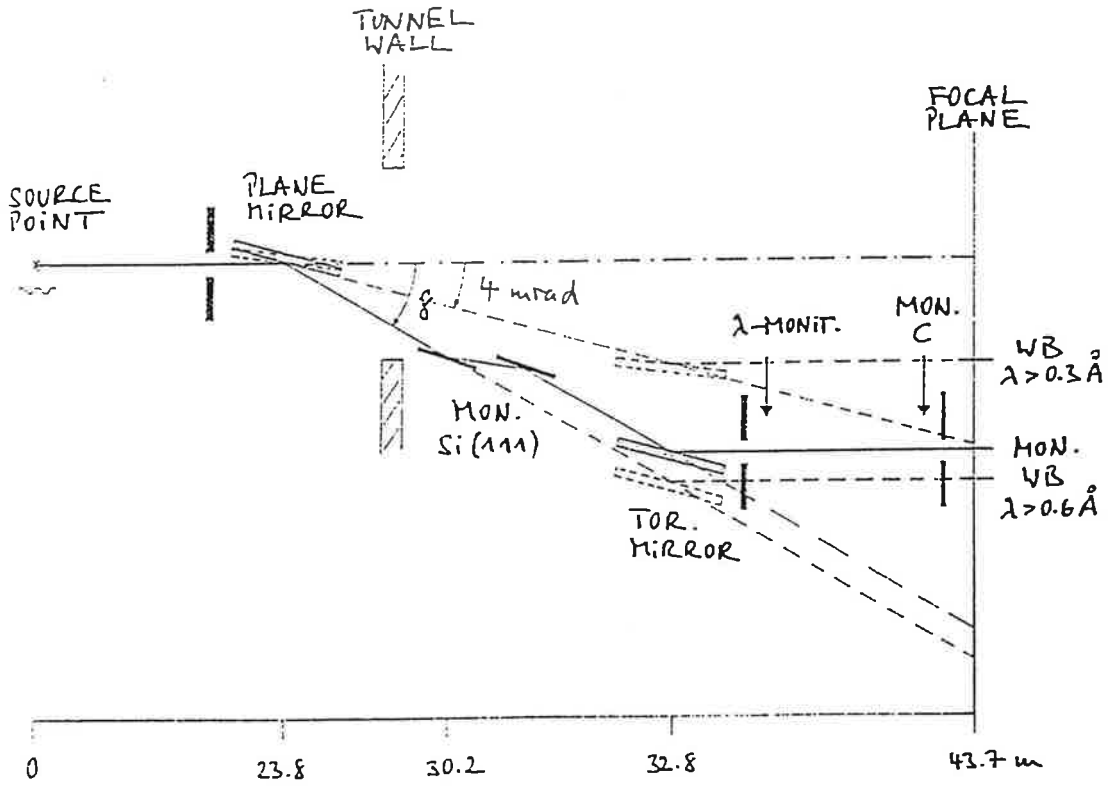

Fig. 1: Scheme of BW6 imaging geometry

The X-ray optics include a plane mirror as first optical element followed by a Si(111) double-crystal monochromator and a focussing toroidal mirror for 3:1 demagnifying imaging. The monochromator may be moved out for white-beam Laue experiments with wavelengths > 0.3 A (unfocussed) or > 0.6 A (focussed). A graphite double-monochromator may be inserted in order to define a 5% wavelength bandpass. Fig. 1 shows a scheme of the set-up.

The different modes of operation and the available diffraction conditions are summarized in Tables 1 and 2, respectively. During a first period starting in May 1992, only unfocussed modes may be used. This should provide suitable conditions for Laue diffraction experiments; optimum conditions for monochromatic diffraction data collection will only exist after installation of the toroidal mirror which is foreseen for end of 1992.

Table 1: Scope of applications / Techniques

application	monochrom. crystal rot.	Laue diffraction 5%	white-beam
high resol.	X		
anom. phasing	X		
high MW	X	X	X
time-res. kin.		X	X
low-T kinetics	X	X	X

Table 2: Modes of operation of BW6

mode	radiation	bandwidth	wavelength range
1 - foc.	monochromatic (Si)	0.01-0.1%	0.6-2.5 A
1 - unfoc.			0.3-2.5
2 - foc.	polychromatic (C)	5%	0.6-1.5
2 - unfoc.			
3 - foc.	polychromatic (WB)	white beam	0.6-2.5
3 - unfoc.			0.3-2.5

Fig. 2 shows the expected intensity distribution in the focal plane as derived from a ray-tracing calculation using the program SHADOW (F.Cerrina). For the full beam (without limiting slit apertures), the focal spot size will be ca. 1.1 mm x 1.6 mm at FWHM.

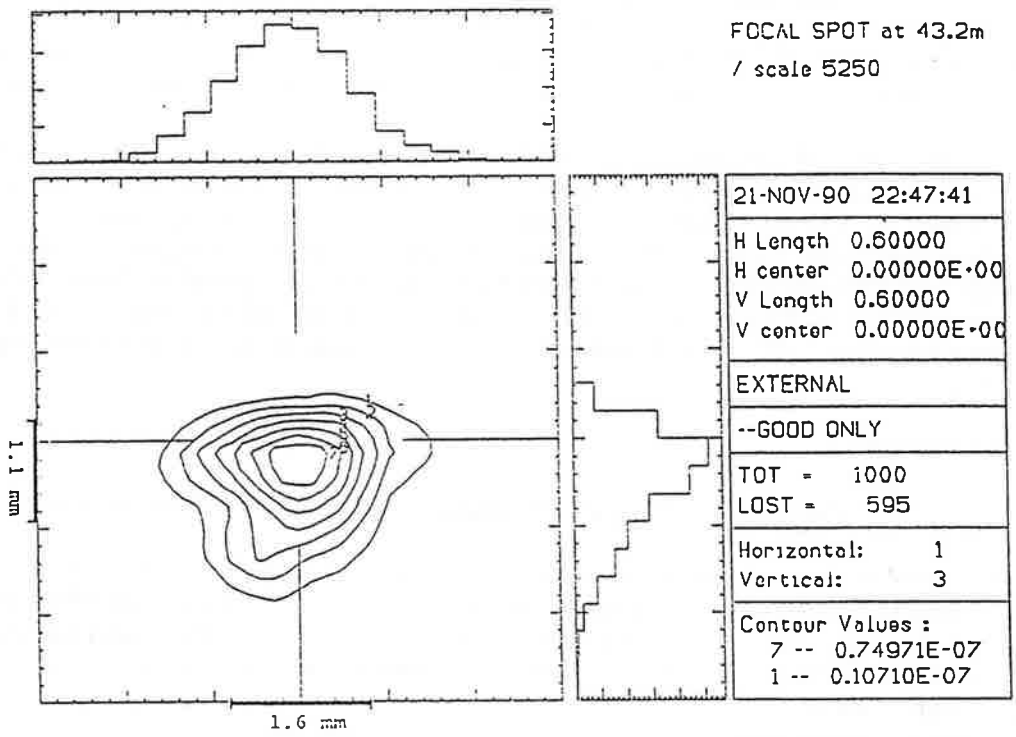

Fig. 2: Focal spot dimensions

For diffraction data acquisition, a 4-circle diffractometer (CAD4) equipped with a FAST area detector (ENRAF-NONIUS) and a 2-circle-goniometer with an on-line imaging-plate scanner (MAR-Research) are available for alternative usage. The beam incident on the sample will be monitored for fluctuations both in intensity and (under monochromatic conditions) in wavelength. Fluctuations will be automatically compensated in a similar way as previously described for rotation data collection (Bartunik et al., 1981). For data processing on VMS and ULTRIX workstations, MADNES (A.Messerschmidt and J.Pflugrath) and MOSFLM software (A.Leslie) may be employed in monochromatic and LAUEMAD (H.D.Bartunik and T.Borchert) in Laue applications. Auxiliary equipment includes cooling facilities (CRYOSTREAM) and flow cells for temperatures in the range from 80-300 K, lasers for excitation at 308 nm (excimer laser) or at 350-950 nm (dye laser), and an on-line diode-array microspectrometer for time-resolved transmission measurements in the range from 300-600 nm. Further, a rapid chopper may be used for sub-millisecond time-resolved X-ray diffraction.

Bartunik, H.D., Clout, P.N. and Robrahn, B. (1981). J.Appl.Cryst. 14, 134-136.

Bartunik, H.D. (1991). In: Handbook on Synchrotron Radiation, Vol. 4, pp. 147-197, eds. S.Ebashi, M.Koch and E.Rubenstein, Elsevier Science Publ.

Protein crystallography with long wavelength X-Rays.

M. S. Lehmann *, (ILL, Grenoble)
H.-H. Müller, H. Stuhrmann (GKSS, Geesthacht)

Using long wavelength X-rays ($\lambda \geq 5$Å) near the K-absorption edge of sulphur (or phosphorous), these atoms can in principle be used to phase protein diffraction data. The relative change in the structure factor is approximately $\Delta F/F \cong 1/\sqrt{2}\ \sqrt{N_S/N_p}\ f_S/f_p$, where N_S and N_p are the number of sulphur (phosphorous) atoms and atoms in the protein, respectively, and f_S and f_p are the corresponding formfactors. The value for f_S is in this case the variation in scattering power of the sulphur around the absorption edge (λ = 5.018 Å) which can attain about 8 electrons. With $f_p \cong 6.7$ electrons we thus get $\Delta F/F \cong 0.8\ \sqrt{N_S/N_p}$.

It is worth noting that $\Delta F/F$ is independant of the protein size, but only depends on the relative amount of sulphur. For the average protein, there is for example about 3,1 % cys (Dayhoff, 1976), which gives $\Delta F/F$ = 5.5 % (assumming 7 atoms per residue), so although the individual Bragg intensities will diminish with increasing protein size, the anomalous signal remains constant for a given sulphur content.

First experiments have now been done to show that X-ray diffraction at 5 Å wavelength can be observed.

The measurements were carried out at HASYLAB with the A1 instrument, using crystals of tetragonal hen egg-white lysozyme (TL) and hydrophobic protein from soy-bean (HPS). The X-ray beam is produced with a single Ge (111) monochromator, and three large position sensitive detectors allow observation of reflections up to a resolution of 2.9 Å. The total beam path is in vacuum and the crystals are mounted inside a humidity cell with a 10µ mylar window.

Observations were done on several crystals, varying scattering geometry and crystal size. To observe the anomalous scattering of sulphur two wavelengths were used, namely one for maximum f" and one 0.03 Å above the absorption edge. The quantitative analysis of the data is not yet finished, the measurement being completed only a fortnight ago, but the first conclusion is that both reflection and transmission geometry can be used, requiring though very thin (≤20 µ) specimens in the latter case. Crystal lifetime at room temperature was 12 to 24 hours for TL and 6 hours for MPS, and old crystals of TL seemed to be more radiation resistant than freshly made samples.

The signal is at present rather low, requiring scanning speeds of less than 2 deg./hours in order to observe most of the data (with a statistic of 3 to 5 %), so at least two orders of magnitude increase in photon flux is required for routine measurements. This is of course not impossible to aquire, so the burning question is whether the radiation damage due to the high absorption ($\mu \geq 100\ cm^{-1}$) will allow for sufficient crystal lifetime. An obvious remedy to the problem is the use of crystal cooling, and further studies are therefore planned to clarify this issue.

Acknowledgements: We are very thankfull to the groups of EMBL and MPI at HASYLAB for their help during the experiment.

* = Gastwissenschaftler at DESY

Ideas on Sources and Detectors - U. W. Arndt

For single-crystal data collection from protein and virus crystals the main requirement is for a primary X-ray beam of high intensity and small cross-fire (convergence or divergence). Synchrotron radiation beam lines satisfy both these requirements: even with today's beam lines the intensity is frequently greater than can be handled efficiently with the present generation of detectors. The small cross-fire with these sources is largely responsible for the cleanliness of the diffraction patterns as compared with conventional sources.

It is possible to generate intensities at the sample up to 50 times greater than with present-day rotating-anode X-ray generators with pin-hole collimation, and with a cross-fire at the sample of about 1 millirad, i.e. to produce a primary beam comparable, - at least at 1.54 Å, - with SR beams. The way of doing this is to use a focusing collimator which produces an image of the source at the sample. A high intensity requires that the collimator subtend a large angle at the source; since we also need a small convergence of the beam at the sample we need a large ratio of image distance to object distance, i.e. a large magnification of the source. With specularly reflecting toroidal mirrors the planar angle of collection at the source can be made a large fraction of the theoretical maximum which is $4\theta_c$, where θ_c is the critical angle for total external reflexion. For Cuk$_\alpha$ and a gold surface $\theta_c = 10$ millirad so that we require a ratio of image and object distances of 20-40. For a typical sample size of 300 μm, therefore, we can utilize a source size of only 7.5 to 15 μm. The permissible loading of an X-ray tube target is inversely proportional to the linear dimensions of the focus whereas the intensity of the beam is proportional to the square of the planar angle of collection, i.e. to the square of the magnification. Consequently, for a given cross-fire and an optimally loaded X-ray target, the intensity at the sample is linearly proportional to the magnification of the collimating system, i.e. in theory we can do 20 to 40 times better than with pin-hole collimators and conventional X-ray generators. In addition the total power loading of the target will be 20-40 lower.

The practical problems to be overcome are:

1. To achieve the required magnification we need a very short distance (~ 20 mm) between source and upstream end of the mirror.

2. The bore of the toroidal ellipsoidal mirror must be less than 1 mm.

3. The maximum roughness of the mirror must be below 20Å to achieve a reflectivity close to unity.

We have designed, and are in course of constructing, a magnetically-focused rotating-anode tube which satisfies the requirements. We believe that we can produce the necessary mirrors by making electro-formed replicas of a N.C. diamond-turned and polished mandrel.

An advantage is that the total power dissipated in the anode is less then 500 watts; this amount can be dissipated by radiation to stationary water-cooled baffles, so that our generator can dispense with rotating shaft seals.

Focusing becomes rapidly more difficult as the X-ray wavelength decreases, since θ_c is proportional to λ. However, there is some hope that Bragg reflexion at artificial multilayers (with varying spacing along the length of the mirror) instead of specular reflexion can be used for X-rays down to Mokα.

It should be noted that, by Liouville's Theorem, the above relations between source size, specimen size, angle of collection and cross-fire apply to any form of collimation which can be devised, such as X-ray zone plates, bundles of fibres or microchannel plates, concentrating monochromators etc.

An efficient use of any high-power X-ray source, of course, requires a detector with a high duty cycle, i.e. ratio of exposure to read-out time.

Combination of cryocrystallography and anomalous techniques.

Felix Frolow

Department of Chemical Services,

The Weizmann Institute of Science, 76100, Rehovot, Israel.

Introduction.

Last time cryothechniques were reintroduced to protein crystallography in the middle of 80's (1-2). Since then several protein and DNA structures were solved and refined using high quality data produced by cryotemperature diffraction experiments (4-11). However real advantage of cryotemperature experiments as complimentary technique to anomlous diffraction experiments was not yet used to our best knowledge. Here we would like to describe in short the essence of cryocrystallography, existing low temperature machines and exploring experiments of measuring anomalous diffraction signal using low temperature during experiment.

Protein cryocrystallography.

Also not always simple in their application. cryogenic temperatures experiments in protein cystallography posses an ability to diminish radiation decay and short range (on time scale) changes of the structure. For crystals of some proteins and DNA molecules the application of low temperature dramatically improve the resolution. for crystals of others it gives an ability to measure all effective initial resolution from one crystal.

In our laboratory we use two types of low temperature devices. One is based on Enraf_Nonius low temperature device, where the cold stream of LN2 is obtained by maintaining the constant pressure in the evaporator. This low temperature device was extensively modified, especially when the laminarity of a cold stream and the elimination of the frost formation on the crystal is considered. The alternative device

is produced by Oxford Cryosystems and is based on the heat exchanger approach. This device has the obvious superiority as it allows to control very stable stream of LN2 in large ranges of temperatures (from 300K to 78K). We use low temperature devices on~ all our diffractometers as well as on an area detector.

The essence of crystal mounting is very simple. We use 'flesh-cooling' approach in order to bring a crystal as fast as possible to a target temperature to prevent destructive phase transitions. Crystal is covered with some viscous substance (hydrocarbon oil, epoxy resin etc.) to prevent dehydration and is mounted on a top of a glass fiber. In some cases cooling give a raise to mosaicity. Subsequently we treat such crystals prior to mounting, soaking them in an antifreeze solution which is mimicking a mother liquor. Our experience with diffraction experiments using conventional laboratory sources of X-ray as well as synchrotron radiation show that even during measurements which last long time, radiation decay is not detectable.

The last statement leads us directly to possibility of measuring reliable anomalous signal using longer exposures and/or measuring redundant data. Recently we made an attempt to solve a structure of halophilic protein Ferredoxin from Halobacteria Marismortui using RAP (Resolved Anomalous Procedure) approach (12).

Exploring experiments.

Ferredoxin is small iron-sulfur protein, which consists of 128 residues, (among them 4 cysteins and 4 methionines) and Fe2S6 cluster (4 sulfur atoms belong to cysteins an 2 are inorganic). Our aim was to measure an anomalous signal accurate enough to be able to solve the structure. The experimental details of the anomalous signal measurement are outlined in Table 1. The anomalous Patterson map was clear and we were able to locate Fe atoms. Difference anomalous Fourier helped to locate sulfur atoms bonded to Fe. Position parameters as well as temperature and occupancy factors were refined against 3000 strongest anomalous differences giving a final R factor

38%, and averaged residual differences between calculated and observed anomalous signal close to averaged standard deviation of anomalouse signal.

Final parameters are presented in Table 2.

TABLE 2

Atom	X	Y	Z	S.O.F	B
FE1	0.13581	0.17032	0.14488	0.98	2.4
FE2	0.10619	0.19062	0.15172	0.94	2.8
S1	0.09381	0.15456	0.14275	0.84	6.8
S2	0.14877	0.20706	0.14275	0.56	4.3
S3Cys	0.13712	0.13900	0.15368	0.88	6.2
S4Cys	0.16160	0.17535	0.12971	0.94	6.2
S5Cys	0.10300	0.22142	0.14844	0.62	6.2
S6Cys	0.08867	0.21852	0.18133	0.84	6.2

Electron density map of refined iron-sulfur cluster is depicted on the Fig. 1. Presently we are trying to locate additional sulfur atoms using variouse techniques.

ELECTRON DENSITY MAP OF 2FE6S CLUSTER (1.9 A RESOLUT

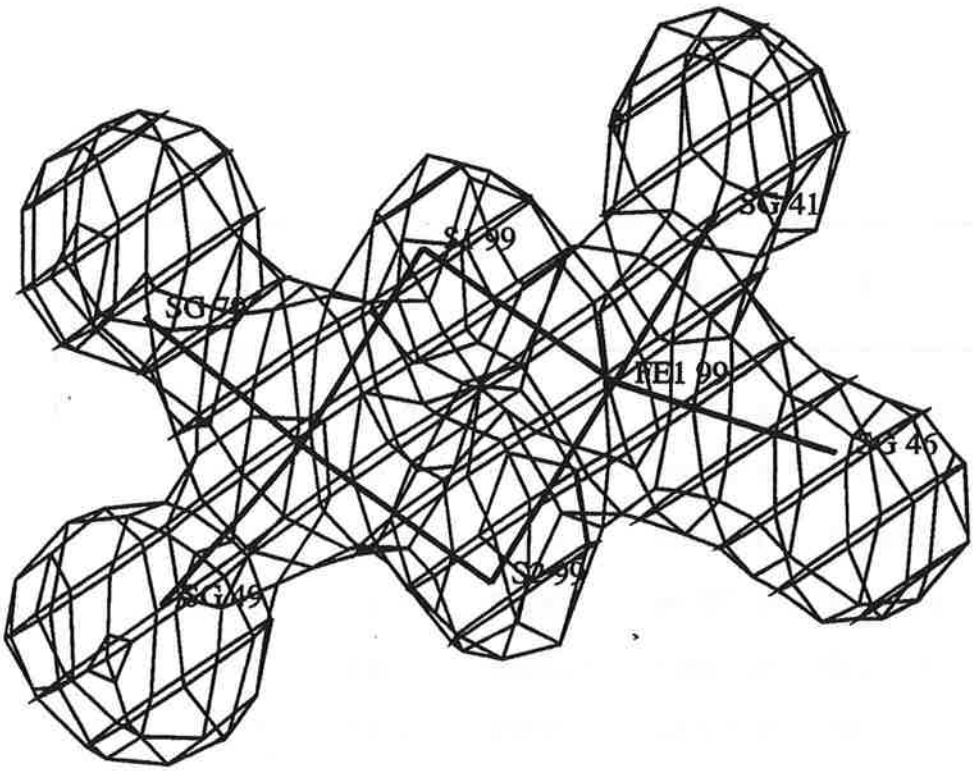

Fig. 1
Electron density of 2Fe6S cluster based on RAP phases.

References.

1. H. Hope.
Acta Cryst. B44, 22-26, 1988.

2. H. Hope, F. Frolow and J.L. Sussman.
The Rigaku Jurnal, 4, 1/2, 1987.

3. H. Hope, F. Frolow, K. von Bohlen, I. Makowski, C. Kratky, Y. Halfon, H. Danz, P. Webster, K. Bartels, H. Wittman, A. Yonat.

4. J. L. Sussman, M. Harel, F. Frolow, L. Varon, L. Toker, A. H. Futerman, I. Silman.
J. Mol. Biol., 203, 821-823, 1988.

5. M. Harel, C.-T. Su, F. Frolow, Y. Ashani, I. Silman and J. L. Sussman.
J. Mol. Biol., 1-10, 221, (1991).

6. U. Wagner, M. Werber, Y. Beck, J. Hartman, F. Frolow, J. Sussman.
J. Mol. Biol., 206, 787-788, 1989.

7. U. Wagner, M. Werber, Y. Beck, J. Hartman, F. Frolow, J. Sussman , M. Ludwig.
J. Mol. Biol., Sibmitted(1991)

8. M. Eisenstein, H. Hope, T. Haran, F. Frolow, Z. Shakked and D. Rabinovich
Acta. Cryst., B44, 625-628, 1988.

9. Z. Shakked, G. Guersstein-Guzikevich, M. Eisenstein, F. Frolow and D. Rabinovich.
Nature, 342, 6248, 456-460, 23 November 1989.

10. M. Eisenstein, F. Frolow, Z. Shakked and D. Rabinovich.
Nucleic Acids Research, Vol. 18, No. 11, 3185.

11. L. Joshua-Tor, D. Rabinovich, H. Hope, F. Frolow, E. Appella, J. L. Sussman.
Nature, 334, 6177, 82-84, 7 July 1988.

12. W. Hendrickson and M. Teeter
Nature, 290, 107, 1981.

X-RAY CRYSTALLOGRAPHY STUDIES ON GIANT BIO-ASSEMBLIES WITH SYNCHROTRON RADIATION

Or: Approaching Atomic Resolution in Crystallography of Ribosomes

Ada Yonath

Dept. Structural Biology, Weizmann Inst., Rehovot, Israel and Max-Planck-research-Unit for Ribosomal Structure, Hamburg, FRG

Of all organelles in the living cell, only the ribosome has thus far been crystallized. These are the supramolecular assemblies responsible for one of the most fundamental life-processes: the translation of the genetic code into proteins. A typical bacterial ribosome is of a molecular weight of 2.3 million daltons, sediments with a coefficient of 70S and is composed of 3 very long chains of RNA (with a total of about 5500 nucleotides) and 57 different proteins. These are arranged in two independent subunits of unequal size (m.w. of 1.45 and 0.85 million daltons) which associate upon initiation of protein synthesis.

Although ribosomes are notoriously unstable and flexible, we have obtained at least one diffracting crystal form from each ribosomal particle (Table I). Of particular interest is the fact that we have been able to crystallize the entire series of ribosomal particles. Furthermore, in addition to the crystals of the intact whole ribosomes and their subunits from this bacterium, we grew crystals of complexes mimicking defined stages in the process of protein biosynthesis, aiming at investigating the conformational changes which take place upon the association of ribosomes from their subunits and upon binding the components involved in biosynthetic process (e.g., m-RNA, t-RNA and fragments of nascent protein chain).

The crystals of the functional complexes are expected of be of extraordinary significance for the understanding of the function of the ribosome. Although they currently diffract to medium resolution, based on our previous experience, we expect that within a few years we shall be able to construct more defined complexes, mimicking several steps in the biosynthetic process, which should diffract to much higher resolution.

Due to the weak diffracting power and the large unit cells of our crystals, virtually all the crystallographic studies have to be performed with synchrotron radiation. Reasonable quality data were collected at various synchrotron-radiation facilities (EMBL/DESY, CHESS, SSRL, KEK/PF).

At ambient temperatures all ribosomal crystals decay upon exposure to X-ray irradiation. The damage is so severe and rapid that the reflections beyond Bragg spacings of 18 Å, which are typically very weak, decay before they can be irradiated for durations long enough to be detected. This extreme sensitivity

led us to underestimate the real resolution, to wrong assignments of the cell parameters and to numerous difficulties in data collection and evaluation. Therefore, a procedure was developed for data collection at cryotemperature from shock frozen crystals. Under these conditions, crystals can be irradiated for days or weeks with no measurable radiation damage.

X-ray crystallographic data have been collected with synchrotron radiation at cryotemperature (85 K) from the following systems: whole ribosomes; large subunits of wild-type and mutated bacteria; chemically modified large and small subunits (with specifically bound heavy-atom clusters); and complexes of ribosomal particles with components of protein biosynthesis, namely mRNA, tRNA and short nascent protein chains. As seen in Table I, the highest resolution recorded so far is 2.9 Å (Fig. 1). Data of a high quality have been recently collected at CHESS/F1, and at KEK/PF/BL6 on film and IP respectively. In both stations the geometry of the data collection facility imposed compromises: at CHESS data were collected from the shell: between 350 Å to 3.3 Å and at KEK between 40 Å to 3 Å.

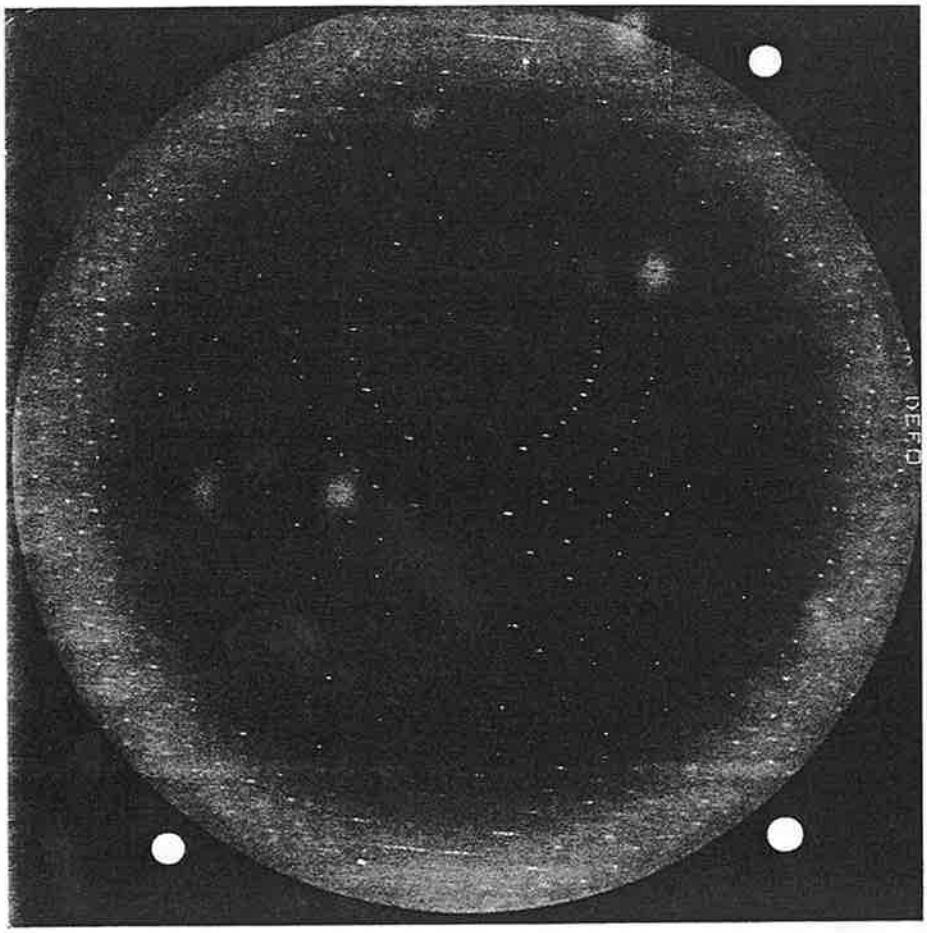

Figure 1. 1° rotation photograph of a crystal of 50S ribosomal subunits from Haloarcula marismortui grown within 6-12 days by vapor diffusion in Linbro dishes at 19°C from solutions of 1.2 M KCl, 0.05 M magnesium chloride, 0.001 M Cadmium chloride and 5-6% polyethyleneglycol (6000), at pH=5.6, equilibrated with 1 ml reservoir of 1.7 M KCl and all the other components of the drop. The pattern was obtained at 90 K at Station F1/CHESS, operating at 5.3 Gev and 50-80 mA. Crystal to film distance = 220 mm, collimator = 0.1 mm; wave length = 0.919 Å.

A monofunctional reagent prepared from a compact heavy-atom cluster, undecagold, has been used for quantitative, specific binding to an isolated ribosomal protein, which was in turn reconstituted into mutated ribosomes, lacking this protein. The modified 50S subunits have been crystallized, and yielded crystallographic data of reasonable quality. Despite a severe lack of common centric reflections, the low resolution (20 Å, a resolution range where the disordered solvent is expected to contribute a large amount of noise), the difference Patterson map showed distinct and correlated peaks, consistent with the expected four 50S subunits per asymmetric unit.

Approximate reconstructed models from tilt series of two-dimensional sheets examined by electron-microscopy were used in attempts to provide initial phasing of the crystallographic data. A few distinct packing arrangements with calculated R factors of around 45% were generated, after rigid-body refinement and solvent flattening the R factor of one solution has so far dropped to 29.8%.

We aim to determine the molecular structures of the whole ribosome and of its large and small subunits, as well as their functionally active complexes, their heavy atom derivatives and their mutants (Table I). Since four years were required to reach the current highest resolution (2.9-3 Å) for a particular crystal form, and since we estimate that about the same length of time will be required for obtaining well diffracting crystals from the other sources, we assume that within a few years we shall be able to measure high resolution data from crystals from other sources, listed in Table I).

It is clear that for obtaining meaningful results, especially for phasing, complete data sets of extremely high quality are essential. Our basic requirements are: "clean" and not fragmented beam of a high brilliance; an X-Y controlled collimator; a long bench (above 750 mm) with adjustable helium or vacuum path; a choice of data collection geometry (rotation camera, Weissenberg); a choice of efficient detectors (film, IP) of a size allowing data collection to higher than 3 Å from unit cells of dimensions larger than 500 Å coupled with proper scanners with fine rasters; devices for cryotemperature data collection; counting controlled rotations; a provision for very low resolution (below 200 Å) data collection; tunable wave-lengths; an on-line connection to interactive evaluation procedures to enable immediate estimation of crystal quality (e.g. mosaic spread, cell constants) and for the determination data collection parameters; adaquate space for crystal handling and mounting; reasonable facilities for data storage.

CHARACTERIZED THREE-DIMENSIONAL CRYSTALS OF RIBOSOMAL PARTICLES

Source	Grown Form	Cell Dimensions (Å)	Resolution(Å)
70S T.t	MPD *	524x524x306; $P4_12_12$	app. 20
70S T.t + m-RNA & t-RNA #	MPD	524x524x306; $P4_12_12$	app. 15
30S T.t.	MPD	407x407x170; $P42_12$	7.3
50S H.m.	PEG *	210x300x581; $C222_1$	3.0
50S T.t.	AS *	495x495x196; $P4_12_12$	8.7
50S B.st. ^	A *	360x680x920; $P2_12_12$	app. 18
50S B.st. ^<	PEG	308x562x395; 114°; C2	app. 11

* MPD, PEG, A, AS = crystals were grown by vapor diffusion in hanging drops from solutions containing methyl-pentane-diol (MPD), polyethyleneglycol (PEG), ammonium sulphate (AS) or low molecular weight alcohols (A).

A complex including 70S ribosomes, 1.5-2 equivalents of $PhetRNA^{Phe}$ and an oligomer of 35 ± 5 uridines, serving as mRNA.

^ Same form and parameters for crystals of large ribosomal subunits of a mutant (missing protein BL11) of the same source and for modified particles with an undecagold-cluster.

< Same form and parameters for crystals of a complex of 50S subunits, one tRNA molecule and a segment (18-20 mers) of a nascent polypeptide chain.

B.st = Bacillus stearothermophilus, T.t. = Thermus thermophilus, H.m. = Halobacterium marismortui

TOWARDS THE NORMALISATION OF VIRUS DATA COLLECTION

Elizabeth Fry[†], Derek Logan[†], Susan Lea[†], Stephen Curry[†$], Andrew King[$], Ekatherina Morgunova[‡], Albert Mikchailov[‡], Boris Vainshtein[‡], Keith Wilson[*], Zybszek Dauter[*] and David Stuart[†]

[†]Laboratory of Molecular Biophysics, Oxford, UK OX1 3QU.

[‡]Institute of Crystallography, Moscow, Russia.

[*] EMBL outstation, c/o DESY, Hamburg, Germany.

[$] AFRC Institute for Animal Health, Pirbright, UK.

The collection of reasonably complete sets of diffraction data from virus crystals has traditionally involved a lot of rather painstaking work. We show here that by combining the excellent source characteristics of a synchrotron (bright, parallel beam) with the detector characteristics of an image plate (large active area, good sensitivity, spatial resolution reasonably matched to typical beam diameter) it is possible now, given good crystals with favourable lattice parameters, to solve such a structure with a handful of crystals and to obtain an excellent difference map from a single crystal. There are still many virus crystals for which the spots are too closely spaced to allow high resolution data collection on the present generation of detectors. However larger image plate detectors are possible and using such devices we could look forward to collecting reasonably high resolution data from some of the most challenging systems. Such a detector would also serve the interests of the masses since it should provide significant improvements in the signal to noise ratio for weak high resolution data from proteins by allowing increased crystal to plate distances.

We give below brief accounts of an *ab initio* structure determination and a difference map study

The structure determination of carnation mottle virus

Carnation mottle virus (CMtV), a small spherical virus ($\approx$ 300Å diameter), represents the first virus structure to be determined crystallographically using data collected on a imaging plate. Cubic crystals of the virus of maximum dimension 0.7-0.8mm were grown from ammonium sulphate and used for data collection using the Hendrix-Lentfer image plate system at the EMBL outstation, Hamburg, beamline X11(λ=0.96Å). The space group was confirmed as I23, a=382Å with one-twelfth of the virus particle in the crystallographic asymmetric unit (5-fold non-crystallographic redundancy). Four crystals were used in total, one to collect low resolution data.

Virus crystals are renowned for their susceptibility to radiation damage and combined with the necessarily long exposure times, it is unusual to achieve more than a couple of shots per crystal, though it has been found that the use of wavelengths <1Å offers a signicant reduction in radiation damage (Acharya *et al.*, 1989). To date film has been the only recording medium able to provide the resolution required for data collection with a unit cell >300Å . However, with a centred cell, data can be collected to 3.2Å on this image plate (diameter 220cm, pixel size 180μ) and the increased efficiency of this recording device enabled a 90% complete data set to be collected in two 12 hour shifts from four crystals. Further, the data processing required only two days compared to the usual timescale of weeks. The data were also unusually well measured (Rsym=7.5% on intensities).

Of the small RNA plant virus structures already determined, CMtV is closely related to tomato bushy stunt virus (TBSV) and turnip crinkle virus (TCV). The protein capsids of these viruses contain 180 subunits and exhibit T=3 icosahedral symmetry. Each subunit comprises an R domain (which interacts with the RNA), a shell (S) domain and a protruding (P) domain. Refined 2.9Å coordinates were available for TBSV (Olson *et al.*, 1983), thus it was chosen as a starting model for a molecular replacement analysis. 33% of the residues in the S domain were identical in sequence and in similar positions between CMtV and TBSV and the equivalent figure for the P domain is 14%. These figures are low for the usual molecular replacement method.

A cross rotation function verified that the CMtV and TBSV coordinates were similarly orientated in the I23 cell. Starting phases to 6Å were based on the TBSV coordinates. Calculated structure factors for TBSV scaled to the observed CMtV data with an R-factor of 57%, little better than random. These phases were improved by iterative averaging (Bricogne, 1976) and solvent flattening using the automatic envelope determination procedure and protocol developed for the structure determination of FMDV (to maximize the phasing power with only five-fold non-crystallographic redundancy). Phase-extension to 3.5Å proceeded in small steps (300 cycles) with repeated envelope determinations. The marked differences between CMtV and TBSV were reflected in the slow convergence of the phasing procedure. The final averaging statistics were however excellent (R-factor 11.8% and correlation coefficient 0.961 on all data to 3.5Å).* The map was extremely clear and allowed an atomic model for the three icosahedrally distinct subunits to be built rapidly using FRODO. This model produced a starting

---

*

$$R = \frac{\sum_h |(|F_{h,obs}| - |F_{h,calc}|)|}{\sum_h |F_{h,obs}|} \times 100$$

$$C = \frac{\sum_h (< F_{obs} > - |F_{h,obs}|)(< F_{calc} > - |F_{h,calc}|)}{[\sum_h (< F_{obs} > - |F_{h,obs}|)^2 \cdot (< F_{calc} > - |F_{h,calc}|)^2\ ]^{1/2}}$$

F_{obs} is the observed structure amplitude of reflection h.
F_{calc} is the calculated structure amplitude of reflection h
as a result of back-transforming the averaged and modified electron density map.

R-factor of 0.35 on all the data from infinity to 3.5Å . Refinement using XPLOR reduced the R-factor to 17% with no manual intervention and no simulated annealing required. No water molecules are included in the model, however, two sulphates and a calcium ion were included in the refinement. The power of the averaging/flattening procedure is demonstrated by the fact that the mean phase change from the starting values was 67°, corresponding to a figure of merit of 0.4.

The overall architecture resembles other 'T=3' icosahedral plant and animal viruses. Comparison with closely related plant viruses reveals differences in the subunit contacts and most significantly the lack of the β-annulus elements around the 3-fold icosahedral axes proposed to form a scaffold for the assembly of the coat proteins. The structure suggests an alternative assembly pathway.

Conformational modulation in foot-and-mouth disease virus

We have found that serotype O of foot-and-mouth disease virus appears to use a disulphide bond to modulate the conformation of a major antigenic site on the virus. In order to understand the relevence of this effect to the *in vivo* situation we have investigated the conformation of the virus as a function of reoxidation time.

Crystals of O_1BFS 1860 were grown at the AFRC Institute of Animal Health, Pirbright by the method of Fox *et al.* (1987). The crystals were first reduced for 18 hours in 10mM DTT. They were then passed through a series of oxidizing solutions. The total reoxidation period before data collection was approximately 6 days.

Data were collected at Station 9.5 of the Daresbury SRS using the MARResearch imaging plate detector. The parameters relevant to data collection are listed in Table 1.

crystal to plate distance	325mm
oscillation range/image	0.5°
exposure time/image	750 - 1050s
resolution at edge of plate	3.35Å
no. crystals exposed	1
no. images	33

Table 1.

The crystal exposed was larger than average (0.4mm in the largest dimension). However, the dramatic increase in the amount of data available from a single crystal can be attributed to the sensitivity of the imaging plate at short wavelengths relative to film. The total exposure time required for each image was similar to that used to record a film on Station 9.6 in spite of the factor of 10

reduction in flux. The 33×0.5° images were 'spaced' at 1° intervals in order to sample a large volume of reciprocal space. This resulted in a data set 87% complete to 3.38Å (see below) from a single crystal. To define the detector origin and crystal to detector distance an image was recorded containing 'powder' rings from a sample of paraffin.

The data images were processed using the programs of the MOSFLM version 4.22 package (Dr. A. G. W. Leslie, L.M.B., Cambridge). Detector origin and crystal to detector distance were determined using a modified version of the WAX program supplied by the Daresbury laboratory. No still images were taken and the orientation matrix was derived from the first image using REFIX (Kabsch,1988), a solution was found by limiting spot-finding to the central 60mm of the detector. This orientation matrix was iteratively refined using IDXREF on spots from pairs of images (images 1 and N, where N was successively 3, 5, 10, 20 and 33), allowing refinement over a continuously expanding angular range. Final refinement was carried out using images 1, 15 and 33. Reflections were profile-fitted using MOSFLM. A tangential offset of -0.23mm satisfactorily modelled the slight mechanical misalignment of the Daresbury image plate scanner. After data reduction postrefinement was performed. The input value of the mosaic spread (0.08°) was a deliberate overestimate and thus mosaicities have refined to very small but consistant positive values and reclassification of reflections is overwhelmingly from partially to fully recorded. After postrefinement reflections more than 75% recorded were scaled up to 100% and the data merged (Rmerge 8.4% on intensities) to give a set of 82801 unique data in the range 24.3–3.38Å (cf 72589 before postrefinement). The data set is 87.3% complete to 3.38Å and of high quality.

Icosahedrally averaged difference maps were calculated against native (oxidized) and reduced data sets. These splendid maps show that even after some 6 days of reoxidation 30% of the disulphide bonds remain unmade, suggesting that this process may produce a long term modulation of the antigenic structure of the virus.

References

Acharya R., Fry E., Stuart D., Fox G., Rowlands D. and Brown F. Nature 327: 709-716 (1989).

Bricogne G. Acta Crystallogr. A32: 832-847 (1976).

Fox G., Stuart D., Acharya R., Fry E., Rowlands D. and Brown F. J.Mol.Biol. 196: 591-597 (1987).

Olson A.J., Bricogne G. and Harrison S.C. J. Mol. Biol. 171: 61-93 (1983).

Kabsch W. J. Appl. Crystallogr. 21: 67-71 (1988).

Current and Future Facilities at CHESS

Steven E. Ealick, Cornell University, Ithaca, New York 14853

CHESS (Cornell High Energy Synchrotron Source) is a synchrotron radiation laboratory that runs in parasitic mode from the CESR 8 GeV storage ring. CESR is currently running at 5 GeV with typical currents of 80 mA. The storage ring operates with 7 almost equally spaced bunches of of positrons and electrons. The ring has an average radius of about 122 meters and the circulation time is 2.56 us. A fill last for one hour and an ideal 24 hour running period would receive about 19 fills.

CHESS has five beam lines. Beam lines A,B and C are fed from the electron currents while beam lines D and F are fed from the positron currents. Five caves are the first chambers to receive the raw synchrotron radiation passed through two 10 mil berylium windows that separate the laboratory from the CESR machine vacuum. The A,C,D and F caves contain monochromators that supply diffracted radiation to the experimental stations. The experimental hall is a radiation area accessible to the experimenter during injection and when beam is stored in CESR. The experimental hall is divided into two area, CHESS East and CHESS West, that are separated by the high energy physics detector CLEO. Seven experimental stations (A1,A2,A3,B1,B2,C1,C2) are located within CHESS West and four experimental stations (D1,F1,F2 and F3) are located within CHESS East. Three beam experimental stations, A1,B2 and F1 are of particular interest to macromolecular crystallographers.

The A1 experimental station receives 2.0 milliradians of synchrotron radiation from a 6-pole wiggler. The radiation is monochromated by the (111) planes of a bent, water cooled germanium crystal. The beam, approximately 3.0 cm wide at the monochromator, is focussed to 1.5 mm at the experimental station. Upon leaving the monochromator the beam is reflected from a 60 cm long rhodium coated mirror that can be bent to provide a 0.3 mm high image of the source. The fixed wavelength (1.55A or 8 keV) provides about 3 x 10 12 photons/s in a size of 1.5 mm by 0.3 mm at a convergence angle of 2.0 mradians horizontally and 0.4 mradians vertically. The hutch contains a remotely controlled optical table. Standard station equipment includes an oscillation camera for single crystal X-ray diffraction experiments.

The B2 station receives 1.5 mradians of bending magnet radiation and is located from 13 to 15 m from the source. The station contains a dedicated monochromator box at the upstream end of the hutch. An optical table is located at the downstream end of the hutch. The station has a bench camera for oscillation or Laue crystallography. The user can make use of the B2 radiation in one of three modes: (1) use the direct white beam, (2) use a wide bandpass beam created by using a quartz mirror to impose a high energy cutoff and absorbers for a low energy cutoff, (3) use a monochromatic beam generated from a silicon or germanium crystal mounted inside the monochromator box. The B2 station was designed as a general purpose diffraction station. It has been primarily used for Laue protein crystallography and X-ray standing wave experiments.

F1 is a doubly focused, tunable X-ray station with exceptionally high flux. F1 also provides the capability to handle biohazardous materials at the BL-3 level. F1 accepts half of the radiation from a 25 pole 1.2 Tesla wiggler magnet. The station is designed to be tunable from 6 to 14 keV with (111) crystals. A vertically focusing mirror is available downstream from the monochromator. A flux of 6 x 10 12 photons/s has been observed in a focal spot of 2 mm by 0.3 mm at 13.6 keV. The combination of high flux with low beam divergence has made F1 ideal for studies of small protein crystals with large unit cells and short lifetimes such as virus crystals. To enhance the capabilities fro diffraction at energies close to an absorption edge a channel cut silicon crystal can be inserted between the first monochromator and the mirror. This arrangement maintains the horizontal and vertical focussing but increases the energy resolution to between 1 and 2 eV for a 13 keV beam energy. This energy resolution is suitable for MAD phasing experiments.

In addition station A2 has been used for Laue crystallography during the dedicated undulator runs. Two one month undulator runs have been previously funded. Funding is available for on additional undulator run that will be scheduled sometime in the future.

The laboratory provides two darkrooms, one located within the F1 experimental station and one located just outside of the experimental hall. A Kodak storage phosphor scanner is also available for processing X-ray diffraction patterns. Other equipment include various oscillation cameras and a complete low-temperature system for flash-cooling crystals. A second image plate scanner is currently under discussion.

Future developments include addition of a 25-pole wiggler on the beam line A. Addition of a vertically focusing on F2 which is equipped with a pair of parallel monochromators should make that station ideal for MAD phasing experiments. Detector development projects will include a collaboration with Sol Gruner of Princeton University to develope a CCD based X-ray detector.

Support for macromolecular crystallography at CHESS is provided through an NIH research resource, MacCHESS. The purpose of this resource is to (1) construct specialized apparatus for macromolecular crystallography, (2) provide support and training for users during their stay at CHESS and (3) conduct core research that expands the horizons of the field of X-ray crystallography. Steve Ealick has recently assumed responsibility as Director of MacCHESS replacing Don Bilderback who served as interim director during the past 18 months. Don Bilderback will remain as co-PI for the MacCHESS grant and continue to serve as Associate Director of CHESS.

Beam time at CHESS is awarded through one of three modes: (1) regular beam time applications, (2) feasibility studies and (3) A1 express mode proposals. Regular proposals are solicited about twice a year. Beam time is awarded based on a peer review process. Proposals for feasibility studies and A1 express mode beam time can be received anytime. The proposals are reviewed by committees to facilitate rapid decisions. Feasibility studies are short experiments designed to demonstrate whether or not a full study is justified. Express mode proposals are only used to allocate no more than 48 hours of beam time on beam line A1. At any one time about 15-25 MacCHESS proposals are active. About 8-10 express mode proposals are approved each year. During the past year a total of 125 outside scientists from 22 user institutions carried out experiments though the support of MacCHESS.

Long term plans at Cornell will be influenced by the current proposal to construct a B-factory. The purpose of the B-factory is to study the decays of B and anti-B mesons. Under this proposal the current 8 GeV ring would be replaced by two rings, one operating at 8 GeV and the other 3.5 GeV. The 8 GeV ring would be designed to store 1 A currents while the 3.5 GeV ring would be designed to store 2 A currents. Under this proposal a CHESS-B facility would be constructed with five beam lines on the 8 GeV ring and 3 beam lines on the 3.5 GeV ring. Three beam lines on the 8 GeV ring would

receive radiation from bending magnets while the other two beam lines would receive radiation from undulators. Two of the beam lines on the 3.5 GeV ring would receive radiation from separate 25-pole wigglers and the third beamline would receive radiation from a soft X-ray undulator. A comparison of the proposed CHESS-B undulator to the APS undulator A shows that CHESS-B would have 9.7 times the flux, 3.4 times the brightness and 0.53 times the brilliance of the APS undulator line. Currently the Cornell B-factory proposal has passed a fiscal review and will undergo scientific review this spring. If funded B-factory construction would not occur for several years.

Oscillation data reduction program

Zbyszek Otwinowski

Department of Molecular Biophysics and Biochemistry, Yale University and Howard Hughes Medical Institute

Program Denzo allows data reduction of single crystal oscillation images. Diffraction data are indexed, cell and detector parameters are refined and reflections are integrated by a weighted profile fitting algorithm. The dependence of the precision of the integrated data on the assumptions made in data reduction programs is described.

The program Denzo has been written to integrate reflections from single crystal diffraction data measured on film or phosphofluorescence Image Plate (IP) detector. The program has been used to reduce data from four different types of off-line scanners and two types of on-line scanners.

The design and implementation of such a computer program involves compromises among three areas: ease of use, accuracy of the output data, and range of data formats, data collection geometries and strategies acceptable to the program. Accuracy of the scattering intensities calculated by data reduction program depends to a large extend upon validity of simplifying assumptions made by the program about the collected data. Every crystallographic data reduction program was initially tailored to the characteristics of a particular type of detector. Often the programs (or particular formulas used in the programs) were later extended to include more detector types. Such extension of the programs sometimes resulted in non-optimal treatment of the data. The history of the profile fitting method demonstrates the need for a critical re-evaluation of how to reduce data from each new type of detector.

Crystallographic area detector produces an image of 3-dimensional reciprocal space. Such image is collected as a series of 2-d images, each of them representing different (curved) slice of the reciprocal space. The target of the measurement is in reciprocal space, but what we see is a distorted image. Part of the distortion is geometric and easy to invert, for example,

projection of the Evald sphere on the detector surface. More problems introduce other effects like: (1) convolution of the projected image with crystal dimensions, beam divergence, wavelength spread and detector resolution, (2) histogramming (reduction of the image into discrete pixels), (3) spatial distortions and (4) non-uniform absorption and detector response. The magnitude and types of the image distortion of the reciprocal lattice vary dramatically between detectors. For example, multiwire counters (MWPC) have large high frequency spatial distortions that manifest in non-uniform pixel size. Resulting image has Scotch plaid appearance even if the detector has uniform absorbion. In contrast, TV detectors have large but stable variations in detector sensitivity that have to be calibrated. Imaging Plate and film have one to two orders of magnitudes more spatial pixels (and better spatial resolution) than MWPC. Counters compensate by having in principle infinite resolution in the time domain. The slow readout speed of current IP scanners requires that individual 2-d images represent large oscillation sectors and result in a poor image resolution in the corresponding direction.

Slow detectors are used in the data collection mode where most of the diffraction spots are fully recorded, while fast detectors spread out reflections over a number of frames. Existing programs can only process data acquired in one of these modes. The programs BUDHHA, MADNES, the UCSD package, XDS and XENGEN integrate time resolved spots. Programs DENZO, FILME, MOSFLM and OSC represent a group of programs that process large oscillation sectors. Most of the following discussion will be based on experience with the program DENZO, written by the author.

The integration program starts with an approximate indexing. DENZO can accept an orientation matrix from autoindexing programs like REFIX. Alternatively, the user can determine the approximate orientation by an iterative process resembling that used for aligning precession photographs, except that the predicted pattern is being adjusted, rather than the diffraction image. The manual indexing is helped by graphics feedback. The interactive indexing process is also helped by the ability of the program to define the current orientation relative to any (principal or higher order) zone being in the center of the image. This is particularly useful

in centered space group and in characterizing unknown lattices. The ability to overlay the boundaries of the integration areas on the intensity (or color) coded diffraction image allows for quick and accurate visual feedback of the integration process. Visual inspection of the data is one of the most important parts of the data reduction process. Graphics is also invaluable in debugging the program.

The initial crystal and detector orientations require refinement. This can be simple for a series of images collected with an on-line detector or quite involved if both the detector and the crystal orientation are only crudely known. The refinement strategy is fully under user control and can consist of several steps. In each step the user defines the resolution limits and parameters to be fitted. Both detector and crystal parameters are fitted together by the fast converging least squares method. Program Denzo refines all parameters using only data from one image. This is of primary importance when crystal slips during data collection. Refinement can be unstable due to high correlation among parameters, in such case eigenvalue filtering removes the most correlated components from refinement. If eigenvalue filtering becomes active, users are encouraged to fix some of the parameters to known, even if approximately, values. Fortunately, if a parameter cannot be precisely determined from a diffraction image, use of an incorrect value will not significantly affect the prediction of the diffraction pattern. In such case integration can proceed without hindrance.

One could think that integration of spot intensity requires only its approximate coordinates, as the summation of the peak area is not affected by its imprecise placement. However, accurate prediction of spot positions is often necessary for spot integration. In many cases detector is placed as close as possible to the crystal consistent with complete separation of diffraction spots. In such cases small errors in spot prediction would make one diffraction peak to intrude upon the predicted background of the next peak. The most important reason for accurate position prediction results from the application of profile fitting. Profile prediction calculates an average of profiles shifted by the predicted separation between spots. If the predicted positions have errors, the average profile will be broadened and/or displaced from the

actual profile of the reflection. The consequences of this effect on calculated intensity will be quantified later.

Errors in the prediction of spot position affect the accuracy of the summed intensity by a different mechanism. If predictions do not match the peak position exactly, one has to enlarge the expected spot area to sum the intensity of the whole spot. Enlargement of the predicted spot area increases the total background to be subtracted. Larger background has larger variance that adds to the measurement variance. Auto centering of the spot area can compensate for errors in the prediction, but it only works for strong spots and if applied individually to every spot would seriously bias the calculated intensity. Some programs do auto centering by averaging the local deviations between observed and predicted position. This is not done explicitly in Denzo, however, the profile prediction algorithm used in Denzo has a similar effect.

The detector and crystal parameters are refined by a least squares method that minimizes deviation of the reflection centroids from their predicted positions. Such refinement is seriously deficient when applied to a single oscillation image, since one crystal rotation parameter is undefined and others are highly correlated and/or poorly defined. To overcome this problem Denzo adds another term, in which the intensity of partial reflections is compared to the predicted partiality times an average intensity in the same resolution range. This residual is very similar to the one used in postrefinement, except that the error in the predicted fully recorded intensity is very large, equal to the expected intensity. Concomitant position and partiality refinement used in Denzo is stable and very accurate. A major benefit is uniform treatment of detector and crystal variables in the whole refinement process. The most important effect of combined residual refinement is in reduced correlation between detector and crystal parameters.

Correct understanding of detector geometry is essential to accurate positional refinement. Unfortunately most detectors deviate from perfect flat or cylindrical geometries. These deviations are detector specific. Primary sources of error include misalignment of the detector position sensors (MAR, R-AXIS), non-planarity of film or IP during exposure or in the scanner, inaccuracy of the wire placement and distortions of the position readout in MWPC, optical

distortion (can also be due to magnetic field acting upon image intensifier) in the TV or CCD based detectors. If the detector distortion can be parametrized, then these parameters should be added to the refinement. For example, in the case of the MAR scanner there are two parameters describing the end position of the scanning head. In the perfectly adjusted scanner these parameters would be zero. In practice, they may deviate from zero by as much as 0.5mm. Such misalignment parameters can correlate very strongly with other detector and crystal parameters. If the program does not have ability to describe detector distortions, other parameters such as unit cell and detector to crystal distance will be systematically wrong. With film and IP handled manually in cassettes, the biggest problem is in keeping the detector flat during exposure and subsequent scanning. In manual systems it is much harder to model the possible departures from ideal flat or cylindrical geometry, and most programs make limited attempts to correct for such distortions. Non-ideal film/IP geometry is one of the main factors behind variable quality of data collected with manual systems.

Denzo accepts the diffraction data formatted in any rectilinear coordinate system. Denzo maps reciprocal space on the detector coordinates flexibly, so any detector geometry, flat or cylindrical can handled. The detector can be in any point in space and in any orientation. In particular, for cylindrical geometry, there is no requirement for the crystal to be on the cylinder axis, nor that the scanning coordinate system be parallel and perpendicular to the cylinder axis. All detector parameters can be refined. They are described as series of rotations, translations and scale factors rather than as one transformation matrix. This allows for each of the detector parameters to be individually fixed or refined according to user specification.

Correction for non-linear function of detector to the photon flux is applied internally in the program so that it can read original data without the need for any transformations (this does not yet apply to the spiral data from the MAR scanner). Pixel values can represent two special cases: no measurement or detector overload. Overloaded pixels are assumed to be close to the center of gravity of the diffraction spots, as such they are used in determining spot centroids. Pixels that are either overloaded or had no measurement are ignored in calculating the spot

intensity, but the existence of such pixels in the spot area is flagged by negation of the sigma estimate. Profile-fitted intensities seem to be reliable independent of existence of such pixels in the spot area. Denzo does not attempt itself to determine an active area of the detector, but it is supplied with a small separate program that looks for the cassette and the beam stop shadows. The position of the cassette shadow can be used as a substitute for the fiducial marks. This option has been very useful with manually loaded cassettes at synchrotrons where there was no option to take a direct beam exposure. On-line scanners do not require fiducials, as they have a fixed relation between the scanned and exposed positions.

To calculate the diffraction intensity background has to be estimated and then subtracted from the reflection profile. The standard method to estimate the background is to calculate an average detector signal in the neighborhood of a specific spot. Some programs assume that background is a linear function of detector coordinates. Denzo makes the simpler assumption, that the background is constant. This usually does not affect intensity measurements, as the background is measured symmetrically around each spot. With symmetrical background areas and spot area shapes, to the first approximation the effect of linear background variation is zero. However, profile fitting is slightly affected by linear background variations. Non-zero effect can be also due to background editing removing pixels asymmetrically from background measurement area. Denzo removes pixels from the background area in two cases: when they have been flagged as no measurement by an auxiliary program or when they are in the spot area of another nearby reflection. Removal of pixels is based on predicted, rather than measured, spots positions.

Profile fitting is two steps process: First, the profile is predicted based on the profiles of other reflections. Second, the observed profile M_i is describes as sum of the background B_i and the predicted profile p_i times a constant (index i represents all pixels in 1,2 or 3-dimensional profile). If the predicted profile is normalized $\sum_i p_i = 1$, then the constant is the fitted intensity I.

The calculation of the fitted intensity has an equivalent but simpler explanation: each pixel

provides an estimate of spot intensity $\frac{M_i - B_i}{p_i}$ with variance $\frac{V_i}{p_i^2}$. Variance is a function of expected signal in a pixel, in the case of a counting detector $V_i = \langle M_i \rangle = Ip_i + B_i$. A profile fitted intensity is then simply a weighted average of all observations:

$$I = \frac{\sum \frac{p_i^2}{V_i} \frac{(M_i - B_i)}{p_i}}{\sum \frac{p_i^2}{V_i}} = \frac{\sum \frac{p_i (M_i - B_i)}{V_i}}{\sum \frac{p_i^2}{V_i}} \qquad \text{(Eq. 1)}$$

This approach was first implemented by Diamond in 1969 for the 1 dimensional case. However, in 1974 Ford proposed a simplified formula where V_i is constant. This was based on mistaken idea that variance of the optical density value of the X-ray exposed film is independent of the degree of X-ray exposure. Equation 1 become simpler:

$$I = \frac{\sum p_i (M_i - B_i)}{\sum p_i^2} \qquad \text{(Eq. 2)}$$

Most of the subsequent programs followed the formulation of Ford rather than of Diamond, even when applied to data collected with counters or IP. The unweighted formula proposed by Ford works quite well where peak spot intensity is not much higher than background intensity. This happens more often with data collected on film, which has a high intrinsic background, or when crystals have low scattering power due to a very large unit cell, high solvent content or disorder. The unweighted profile fitting improves accuracy (compared to straight summation) of weak reflections but at the cost of reducing the accuracy of the strong ones. This observation did lead to a partial solution based on taking a weighted average between profile fitted and summed intensity, where the weight is function of reflection intensity.

The weighted formula (eq. 1) used in Denzo does not deteriorate the accuracy of strong, low resolution reflections. Thus, the that observed problem with the unweighted formula is in weighting, rather than in the accuracy of the predicted profile.

The prediction of the spot profile has been based on three approaches: modeling of the spots in detector coordinates by an analytical function, averaging of spot profiles in detector coordinates, and averaging of the spot profiles in reciprocal space coordinates. None of these

approaches has an intrinsic advantage over others, what is more important it is how well the detailed assumptions about profile shape and its variability match what happens during data collection. Denzo is based on the averaging of profiles in detector coordinates. It is different from other programs in that it averages profiles separately for each spot. This approach has two main advantages: first, it chooses only nearby spots, ones with most similar profiles: Second, additional shifts by a single pixel can be introduced to make the average profiles center on the predicted one eliminating the need for interpolation.

The profile prediction is never exact. Predicted profiles can be of different shape and displaced from the measured spot profile. Diamond analyzed the case of one dimensional Gaussian profiles and unweighted profile fitting formula. The important parameters are: w - root mean square (rms) width of the actual profile, f - root mean square (rms) width of the predicted profile, d - displacement of the predicted profile. We can define $\Delta^2 = \left(f^2 - w^2\right)/w^2$. For no displacement the fitted intensity will be wrong by a factor (Diamond):

$$\sqrt{1+\frac{\Delta^2}{2+\Delta^2}} \qquad \text{eq 3.}$$

The averaging of profiles adds $r^2/3$ (r - raster size) to the f^2. The interpolation broadenes profile by a factor dependent upon position of the predicted reflection relative to the pixel boundries. This term, that also adds to f^2, is between zero and $r^2/2$.

CCD Detector Developments

Nigel M. Allinson
Department of Electronics, University of York, England

Introduction

The work described here forms part of a current EC Science Plan Grant (Reference SC-1-0269-CA) on protein crystallographic research and development using synchrotron radiation.

Diffraction experiments place stringent requirements on the two-dimensional imaging system – namely, large aperture, high local count rate, high resolution (small psf) and high sensitivity over a wide energy range[1]. For solid-state detectors to be accepted as a research tool, they must match, or surpass, the performance of photographic film – with the additional advantages of on-line observation and digitisation of patterns and short integration times for time-resolved investigations. The demands of Laue diffraction can be turned into an advantage, as such studies are an excellent tool for characterising imaging systems since, for a known crystal structure, a large number of well-defined spots of known energy, intensity and position are obtained. From one pattern, it is possible to determine accurately the efficiency, spectral response and spatial resolution of the detector.

The experiments described are concerned with the application of Laue methods, however the reported detector developments have implications for standard data collection especially at short wavelengths. The majority of the results presented in this paper have been obtained in the last few months, and so full analysis is not yet available.

Experimental Details

A schematic of the Laue experimental arrangement is given in Fig. 1. This system was installed at Station 9.5 on the wiggler line of the SRS. The detector is mounted on a motor-driven X-Z stage. A fast solenoid x-ray shutter is employed to control beam exposure time of the ccd detectors to the diffracted beam (minimum open period 20 ms). This shutter is directly controlled by the host computer. When an exposure is initiated, the asynchronous ccd camera begins its integration time and the shutter opens. The shutter is closed 10 ms before the end of the set integration time, in order to ensure a *clean* transfer of the image to the read-out register of the ccd. All read-outs are performed at standard tv rates and the signal digitised to 8-bits. The integration period is fully programmable. Data capture is performed by a Matrox image acquisition and processing board set mounted in a 386-PC computer. The deep memory can be employed for image summation, so that long effective integration times can be achieved without the need to cool the detector. All the equipment (e.g., stepper-motors, camera control signals, etc.) are controllable via a remote control rack and parameters set via a Windows 3 interface on the PC. Two modified EEV asynchronous cameras were used – one for the direct-detection and scintillator-coated ccds, and the other for the phosphor-coupled detection experiments. This second camera possesses a First Generation single-stage image intensifier with an 18 mm diameter fibre-optic input faceplate.

The range of wavelengths over the whole pattern ranges from ≈0.5 Å (25 keV)– ≈0.9 Å (14 keV) for the test crystal, and ≈0.5 Å (25 keV) – ≈2.0 Å (6 keV) for the concanavalin sample. The incident flux is estimated to about $10^5 h\nu\ s^{-1}$ for a typical pattern spot (an intense reflection may be 100x higher).

Phosphor-coupled Detection

There have been a number of systems have been developed using phosphor coupling to ccd imagers[2,3]. Most recent attempts have employed micro-channel plate intensifiers. There are a number of advantages in the older First Generation intensifiers, as they possess (for diffraction studies) superior noise performance (i.e., less impulsive noise components). The geometric distortion, generic to such devices, can be corrected, and very high pre-storage gain does nothing to improve overall system signal-to-noise performance and can result in saturation

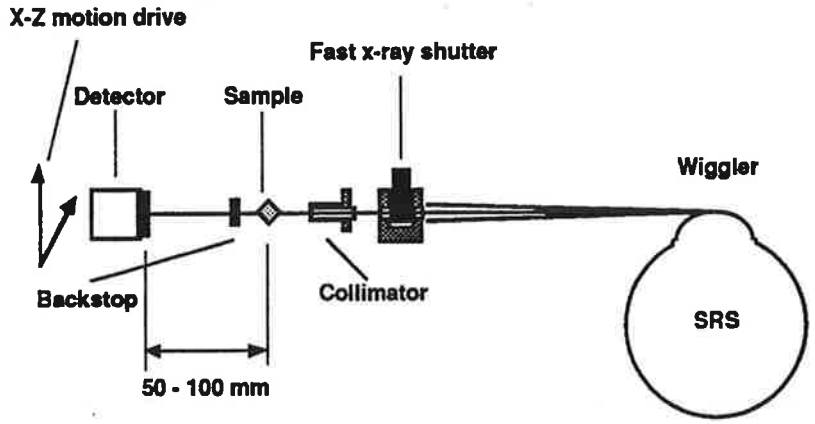

Fig. 1 Schematic of Laue experiment

of the ccd[4]. Dynamic range is in many situations more important for integrating detector systems than are noise floor levels.

The phosphors investigated in this study were Gd_2O_2S and ZnCdS – each at 10 mg/cm^2 and 20 mg/cm^2 thicknesses. The profile plots of Fig. 2 indicates the relatively poor psf of these relatively thin phosphors. Fig. 3 shows the variation in sensitivity for a transverse scan across the phosphor (for this measurement the attenuated direct beam was used, and the phosphor-coated faceplate moved relative to the stationary and *in-line* beam and a photo-amplifier. Another major difficulty with phosphors, especially for time-resolved experiments, is their relatively long decay times.

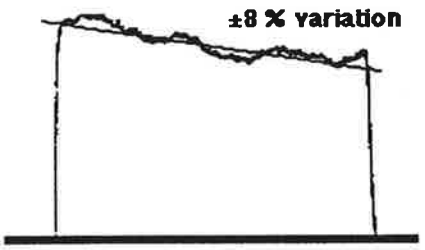

Fig.3 Sensitivity scan for a Gadox phosphor (20 mg/cm2)

Direct Detection

We have previously reported results using the direct bombardment of x-rays into deep depletion ccds[5]. The soft x-ray window for ccds is centred about the Si K-edge (E = 1.84 keV), and extends from about 1 keV to 10 keV with an extension up to about 25 keV for deep depletion devices. The devices used are fabricated on 1000 Ω cm wafers, which results in an estimated depletion depth of 30 μm. Earlier work reported a DQE of 5.6% at the Mo$K\alpha$ line (E = 17.5 keV), and merging R factors, on intensity, for strong reflections of 3%[6] – these are comparable with film. Full mosaics with apertures of 33 mm x 32 mm, and an exposure time is 100 ms per frame, have been recorded. Fig. 2 shows a typical single spot profile for direct detection (collimator diameter is 200 μm, that is about 10 pixels on the final image). It is possible to resolve *overlapping* spots. Fig. 4 indicates the relative sensitivity of direct detection with respect to film (in terms of integrated spot intensities). The usefulness at the longer wavelengths of this method is apparent.

Direct detection not only offers excellent resolution (if very deep depletion layer devices are used in order to extend the high energy range, then this may not hold), but also overcome the temporal problems associated with phosphors. The high internal gain of the ccd relaxes the demands on low-noise amplification of the resulting signals and device cooling. Detection is essentially photon noise limited. The oft quoted objection to direct detection is that of radiation damage to the ccd itself. An extensive investigation of such damage for soft x-rays has been undertaken previously[7], and annealing techniques for the full recovery of devices developed[8].

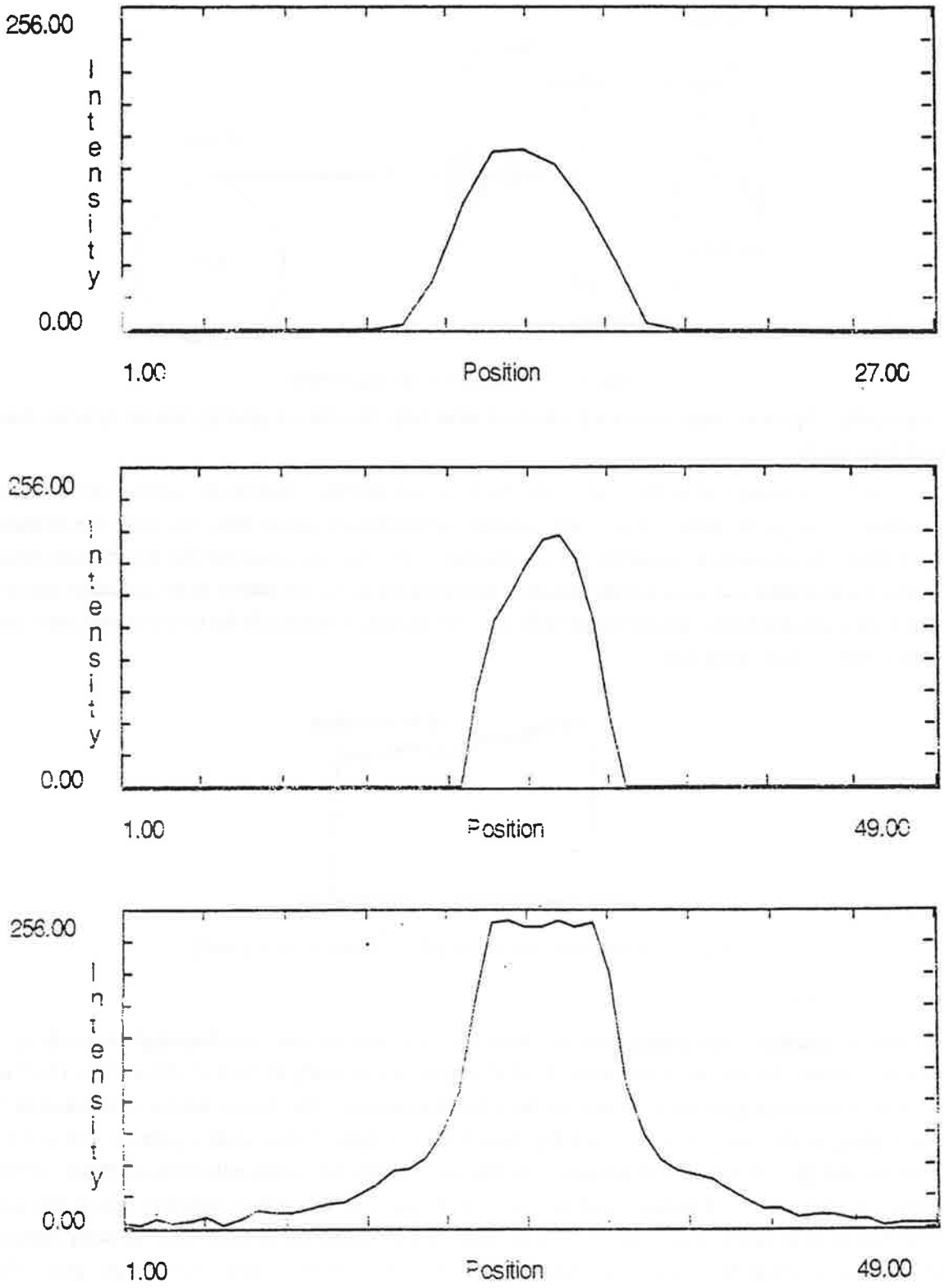

Fig. 2 Typical spot profile

a) Phosphor-coupled

b) Direct

c) Scintillator

(Same reflection in each case)

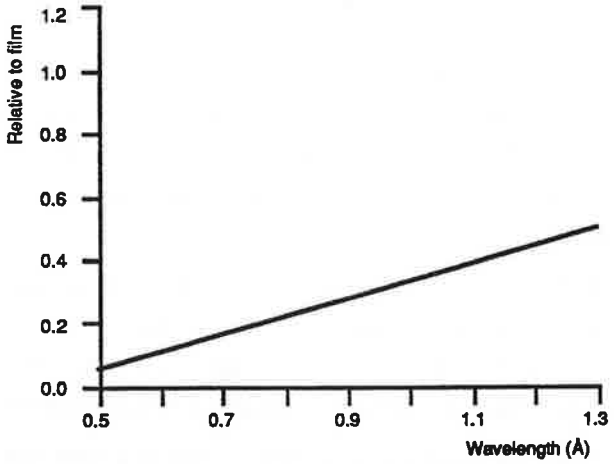

Fig. 4 Relative sensitivity of direct detector

Scintillator-coated Detection

Scintillators can offer superior temporal performance to phosphors, and provide higher efficiency (especially at shorter wavelengths). The choice of scintillator depends on a number of factors including the nature of the incident radiation, spatial and temporal resolution, compatibility with the spectral range of the integral visible sensors and environmental considerations. For the work described here, a 100 μm layer of CsI(Tl) was deposited directly on the surface of the ccd. Vacuum evaporated CsI(Tl) forms a columnar structure orthogonal to the substrate (about 10 μm diameter crystallites – function of deposition conditions). Peak emission from CsI(Tl) is 560 nm, which matches the responsivity curve of the ccd. Fig. 5 shows a typical single spot profile (Notice the long tail to the psf – this is due to the initial random ordering of the CsI(Tl) growth). The sensitivity of the scintillator improves towards the higher energy range. At the lower energies, where the CsI(Tl) is more transparent, then there will be a contribution due to direct-detection by the ccd. Fig. 6 shows the relative sensitivity of CsI(Tl) coated detector relative to film.

Though such scintillators appear to offer improved performance (certainly over phosphors), there remains the problems of radiation damage and environmental considerations. The light output of CsI(Tl) falls by approximately 30% after exposure to 10^4 rads (due to the formation of colour centres)[9]. These figures are for single crystals and their is some evidence that evaporated layers are about 100x harder[10]. This damage will, to some extent, recover after a period of time. The hydroscopic behaviour of this type of scintillator, also, implies special environmental considerations.

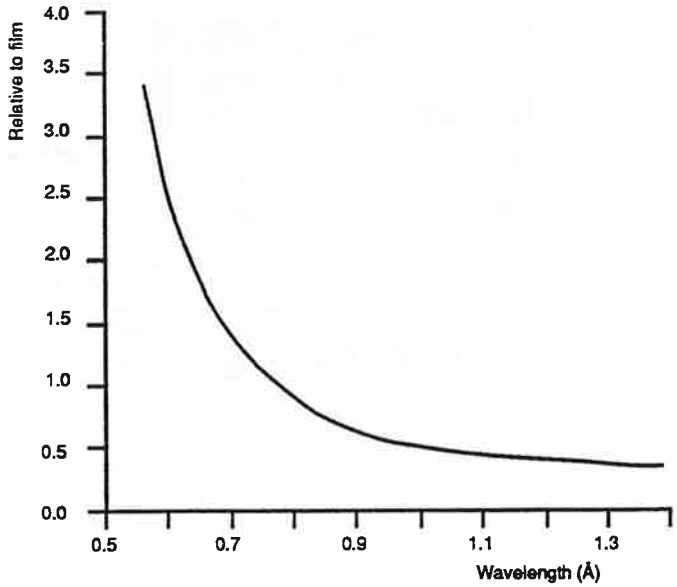

Fig. 6 Relative sensitivity of CSI(Tl) detector

Future Developments

Further effort will concentrate on detailed characterisation of the various detection topologies, and the development of a large area ccd camera[11] that will be capable of producing full-frame images and time-slices (at a minimum periods of about 200 μs). A schematic view is given in Fig. 7. This camera will possess a full aperture eight times that of the current camera. Hence, millisecond temporal resolution will be feasible for the monitoring of reaction events.

Further, more fundamental, research will be undertaken on scintillator types and topologies (i.e., direct-coating and use of fibre-optic couplers). Important aspects of these investigations are quantification of radiation damage (and possible annealing) and modification of scintillator layers to optimise internal dqe in order to maximise overall system dynamic range. This work will be in cooperation with commercial companies.

Second generation instrumentation is nearing completion – VME rack with 68040 processor, bank of 128 KB memory boards, 2K x 2K display, 750 MB hard disc (with 5 Mbaud SCSI interface), and tv standard auxiliary frame store for real-time display and video recording; fully programmable camera drivers (will permit use of a range of ccds – e.g., Ford and Kodak), and digital filtering of chip signals. Schemes for very high speed shutters have been developed. Current mechanical shutters can provide the short exposure times (~ 1ms), but they suffer from very variable latency periods.

References

1. J R Helliwell (in press), *Macromolecular Crystallography with Synchrotron Radiation*, Cambridge University Press, 584 pp.
2. R H Templer, S M Gruner and E F Eikenberry (1988), *Adv. Elect. Elect. Phys.*, **74**, 275-283.
3. M G Strauss, I Naday, I S Sherman, et al. (1987) *IEEE Trans. Nucl. Sci.*, **NS-34**, 389-395.
4. N M Allinson (1989), *Nucl. Inst. Meth.*, **A275**, 587-596.
5. N M Allinson, R Brammer, J R Helliwell, et al. (1989), *J. X-ray Sci. Tech.*, **1**, 143-153.
6. N M Allinson, P D Carr, M Colapietro, et al. (in press), *Phase Transitions.*
7. N M Allinson, D W E Allsopp, A L Quayle and B G Magorrian (1991), *Nucl. Inst. Meth.*, **A310**, 267-272.
8. B G Magorrian and N M Allinson (1988), *Nucl. Inst. Meth.*, **A273**, 599-604.
9. M Kobayayashi and S Sakuragi (1987), *Nucl. Inst. Meth.*, **A254**, 275-261.
10. I Fujieda, G Cho, J Drewery, et al. (1991), *IEEE Trans. Nucl. Sci.*, **38**, 255-262.
11. N M Allinson, M Colapietro, J R Helliwell, et al. (in press), *Rev. Sci. Instrum.*

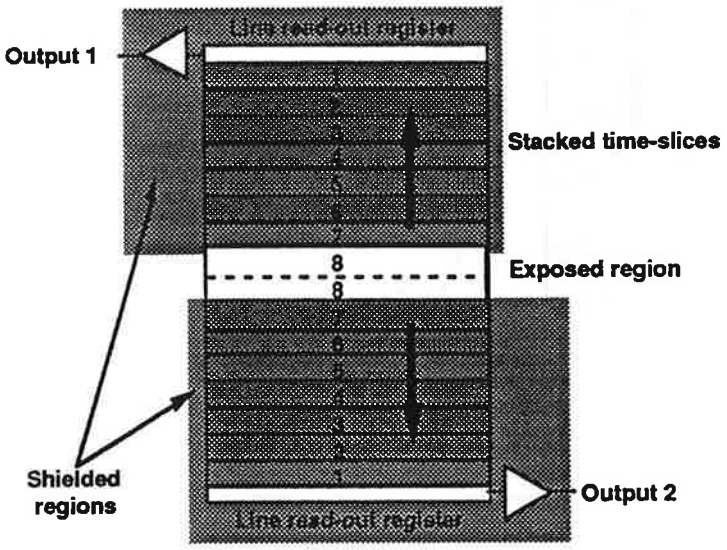

Fig.7 Time-slicing detector

European Workshop on X-Ray Detectors for Synchrotron Radiation Sources at Aussois: a summary (restricted to applications in bio-crystallography).

R. Fourme, LURE, B209D, Université Paris-Sud, 91405 Orsay Cedex, France.

It is clear that to satisfy the increasing demand of users of synchrotron radiation sources in the area of diffraction, spectroscopy and imaging studies, a new generation of detectors must be developed. In this context, a workshop was organised by A. H. Walenta (University of Siegen) and held from september 30 to October 4, 1991 at Aussois (France) with about a 100 participants. The goal was to bring together scientists from the synchrotron user community to describe in detail their requirements as well as groups developing detectors and experts in electronics and data acquisition systems associated with these detectors.
This brief summary will be limited to the specific field of macromolecular crystallography. On the basis of discussions with colleagues from the LURE team, I presented an introductory talk on this topic, attempting to outline the "Target characteristics of an area detector for the crystallography of biological macromolecules using third generation, high energy synchrotron radiation sources" (R. Fourme, A. Bahri, R. Kahn & R. Bosshard, Proceedings of the Workshop). The bulk of my presentation concerned data acquisition with monochromatic radiation. The general context of data collection with monochromatic radiation was presented on the basis of table 1 and the conclusion of the talk was a list of specifications (summarized with a few modifications in table 2). Important features are the capability of handling short wavelengths (0.3-0.5Å), a pixel size which is relatively large (governed by the crystal size), a good point spread function (PSF) with limited wings, a rather extended surface (by surface, we mean the actual sensitive area in the case of a gas or an image plate detector, or the first converting screen in other cases), a good detection quantum efficiency (DQE), a high count rate and a good duty cycle. In table 3 it is shown that, even in normal beam geometry, such a detector would allow data collection to a quite respectable resolution for a wide range of unit cell dimensions. (In general, there are no objections to incline the detector with respect to the X-ray beam, in order to collect data to higher resolution. The normal beam geometry may be preferred in some cases; for instance, when using a spiral scanning image plate detector, it ensures that any decay of luminescence during scanning will equally affect the intensities of all reflexions in a given shell of resolution). These specifications were not significantly modified by the subsequent discussions (there were in fact very few protein crystallographers in the audience!) and their technical feasibility was discussed during parallel sessions devoted to various types of detectors.

1/ Image plate detectors

The main drawback of current systems is the dead time between two exposures due essentially to laser scanning and erasing (in a typical example, about 120 sec for a circular plate with 1200 pixels per diameter). As a consequence, to preserve a reasonable duty cycle, the oscillation range per frame cannot be made in practice as small as would be required to optimise the S/N ratio. The PSF has a good FWHM, but fairly extended wings requiring relatively large integration boxes. Other features, including simplicity and ease of use, are very attractive. For the use with third generation sources, the good DQE at short wavelengths and high count rate capability are crucial. This type of detector is still in its infancy, and their performance can be improved in several respects (new phosphors, better scanners); the importance of collaboration with companies making equipment for medical radiography was underlined.
(During the Hamburg meeting discussions, the importance of image plates for bio-crystallography at the ESRF was emphasized, in particular for the most demanding applications such as virus crystallography (D. Stuart). A detector perhaps twice as large as current detectors while keeping about the same dead time would be a basic tool for these applications. I note that such a detector would have the capability of 240-300 diffraction orders and would have several important specifications close to those in table 2).

2/ Gas detectors

Gas detectors are photon counters, which have a duty cycle close to 1 and a good DQE, allowing the use of small angular ranges per frame and kinetic studies. When properly designed, they can produce very accurate measurements. Detectors which are currently available at synchrotron radiation facilities for bio-crystallography are based on multiwire proportional chambers (MWPC), sometimes coupled with an electrostatic device for parallax suppression. The global count rate of these detectors is limited by the dead-time of the single position encoder and the local count rate is limited by the physical processes which occur in MWPC. From the various presentations and discussions during the workshop, it became clear that there are solutions to improve by one and perhaps two orders of magnitude both local and global count rate capabilities of gas detectors, using in particular microstrips or pads instead of wires, and parallel position encoding, thus approaching specifications in table 2. Nevertheless, the target characteristics should be defined in a realistic way, in order to keep both cost and complexity in reasonable limits (In this respect, during the Hamburg meeting, it was pointed out by C. Nave that a gas detector with even a modest 10^6 cps capability would be a very useful instrument).

One of the outcome of the Aussois workshop was that several European groups are on the way to join their efforts in order to make a scientific and technical proposal for a state-of-the art gas detector and associated electronics.

3/ Other detectors

Solid state devices with a rather large sensitive surface directly exposed to X-rays do not appear as a realistic possibility in the near future for various reasons, including development costs. Several teams, such as the ESRF detector group, are working on detectors with an indirect detection by a CCD. In these devices, the primary process is a conversion of X-rays into either visible photons or electrons and the last stage is imaging by the CCD. These detectors might combine short wavelengths and high flux capabilities with a good duty cycle. In practice, the DQE, the point spread function and the stability (both for position and intensity response) may be degraded by the cascade of processes involved in the detector. In the context of bio-crystallography applications, these systems will certainly require a careful settling and evaluation.

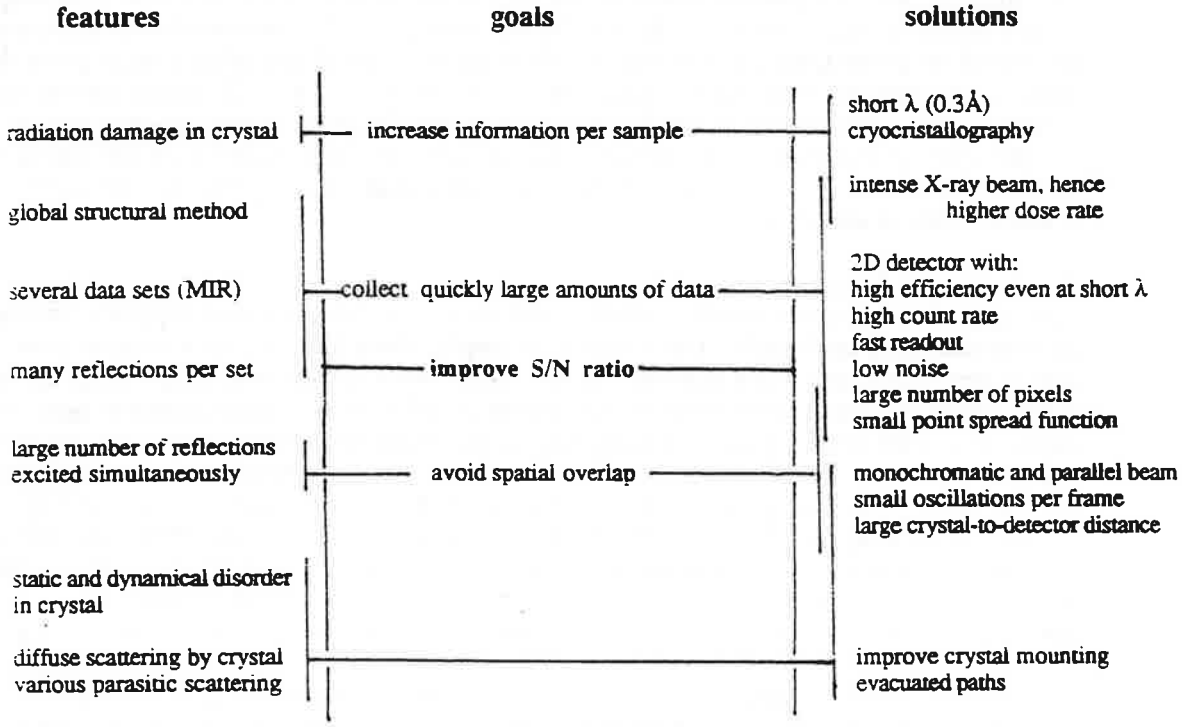

Table 1. Data collection using a monochromatic X-ray beam

useful sensitive area (or area of first converter)	
shape	e.g. disk or square
point spread function (fwhm)	150 microns
pixel size	200-250 microns
number of pixels on edge or diameter	1800
typical edge of integration box	5-6 pixels
max. number or orders	300
dynamical range (max. obs. signal/min. obs. signal)	5 decades
detector noise level	1 equivalent quantum per pixel
detection quantum efficiency $((SNR_{out}/SNR_{in})^2)$	0.5 (λ range 0.3Å-2Å)
total (local) count rate	10^8 (10^6)
rms deviation between obs. and calc. Bragg spot position (mapping function or correction table)	0.3 pixel
uniformity of intensity response (possibly with correction by flood field table)	at least stable in time to 10^{-3}
duty cycle (exposure time/ total elapsed time)	0.5
monitoring of X-ray beam intensity (linearity and stability)	10^{-3}

Table 2. Target characteristics of an area detector for bio-crystallography with a third generation, high energy synchrotron radiation source (monochromatic beam)

cell parameter (Å)	resolution (Å)	distance D (cm)
100	1.71	7.5
	1.00	16.6
	0.71	50
300	2.61	22.5
	2.14	50
	2.02	150
600	4.35	45
	4.07	100
	4.01	300

Table 3. Maximum resolution and crystal-to-detector distance for a detector in normal beam geometry, with a disk-shaped sensitive area and characteristics as in table 2, for various cell parameters and wavelengths of respectively 2.0, 0.9 and 0.3Å.

Data collection using short wavelength radiation

(Z. Dauter, Meeting in Hamburg, 12-13 Dec. 1991)

Our experience with collecting diffraction data using short wavelength X-rays is exclusively related to the use of the Imaging Plate Scanner. In contrast to film, the sensitivity of imaging plates remain practically unchanged over a wide range of X-ray wavelengths. This property of imaging plates makes them very useful not only when collecting anomalous data at desired absorption edges, but for routinely recording data at short wavelengths as we have done in EMBL Hamburg during the last two years. The advantage of using a detector which is effective at short wavelength results from the minimisation of errors related to absorption effects, prolonged life time of the crystals and minimisation of the secondary diffraction by air. The performance of our Imaging Plate Scanner is illustrated by the following examples. They range from the large structure of a virus, when most important is prolongation of crystal life-time, to a very small inorganic salt, when short wavelength makes it possible to obtain very high resolution data at minimal crystal to detector distance.

The diffraction data from the crystals of Carnation Mottle Virus (CMV), in cooperation with A. Mikhailov and K. Morgunova (Moscow) were collected on the beam line X11 using 1 Å radiation. The structure has now solved and refined in Oxford in collaboration with the group of David Stuart. With the use of film and 1.5 Å radiation these crystals allowed the collection of one or two oscillations per specimen, whereas using the IP Scanner only four crystals were used to obtain 90 % complete data set at 3.2 Å resolution. The overall R(merge) was about 7.5 % with rather high redundancy. The crystals are cubic, space group I23, with cell dimension 382 Å. The first crystal was used to collect the 6 Å data, 97 % complete, from 35 oscillations of 1° each, with short exposures. Three more crystals were used to obtain 3.2 Å data, with about 20 oscillations of 0.5° each before substantial crystal damage was observed. More than 15,000 reflections were present on each image. The crystals diffracted to a higher resolution than 3.2 Å, and that limit was selected to avoid problems with spot overlap during

data processing. In such cases, of well diffracting crystals with large cell dimensions, a larger (about two times) imaging plate would be desirable.

The example directly illustrating the effects of absorption on the quality of data is the experience of Gideon Davies (York University) with the collection of data from the plate like monoclinic crystals of a protein of about 30 kDa using both the Cu (1.54 Å) and Mo (0.71 Å) sealed tube source and the IP Scanner. In both cases data to beyond 2 Å were collected with 180° of total rotation. The merging of the Mo data set resulted in an overall R(merge) of 6 % with all contributing images having approximately the same individual R(merge) values. The Cu data set merged within 7.5 %, but the images corresponding to the flat crystal in approximately horizontal orientation, when the beam path in the crystal is maximal, had individual R(merge) values of above 12 %. This effect was observed for several crystals of native protein and for derivatives as well. The exposure times necessary to collect data on the Mo source were about two times longer than in case of the Cu source.

The use of the shortest possible wavelength radiation to collect very high resolution data was necessary in the case of rubredoxin, an electron transfer protein with 52 amino acids, undertaken in cooperation with Larry Sieker (Seattle). This structure has previously been refined against the data from a diffractometer and Cu source at 1.5 Å resolution. The use of Imaging Plate Scanner on the EMBL synchrotron beam line X31 with 0.65 Å wavelength allowed the collection of data to 1.0 Å from two crystals, and recently a better quality data from one crystal extending to 0.92 Å, giving an overall R(merge) of 3.8 % and completeness of 98 %. These data served to refine the structure anisotropically to an R factor below 10 %, and to less than 8 % using a 2σ cutoff in cooperation with George Sheldrick (Goettingen) using his program SHELX99. It was possible to solve this structure with the SHELX classic direct methods approach in spite of there being about 480 independent atoms in the asymmetric unit. The structure could be successfully refined without restraints with the exception of about 7 disordered or highly mobile side chains.

The other case illustrating how powerful is the combination of an Imaging Plate detector with a strong short wavelength synchrotron radiation is β-cyclodextrin. This structure consists of about 90 independent atoms and is typical for medium size organic crystals, which often behave

like proteins, with the diffraction falling off rapidly at high resolution and with substantial degree of disorder in the structure of the molecule and especially in the regions filled by solvent. This structure was previously solved using diffractometer data and refined to 7.3 %. The data collected using the 0.65 Å synchrotron beam and the 0.71 Å Mo sealed tube source combined to give a 0.87 Å resolution set with R(merge) being a flat function of resolution at about 3.5-4.0 %. These data allowed us to refine the structure and to model the disordered atoms using a graphics display station to an R factor of 3.2 %.

Two data sets from crystals of medium size structures were collected in collaboration with E. Pohl and G. Sheldrick from Gottingen, a cyclosporin derivative and SMS, a linear octapeptide crystallising with three molecules in the asymmetric unit. For SMS on the diffractometer (even at the low temperature of -80°C) it was only possible to collect data with less than 30 % of intensities above the 2 σ(I) limit in the high resolution data shell beyond 1.2 Å. At least 50 % seems to be necessary to be able to solve the structure by direct methods. The IP Scanner and 0.65 Å synchrotron radiation produced high quality data sets with more than 70 % of the reflections above the 2 σ(I) limit in the 1.0-1.1 Å resolution shell, which made it possible to solve the structures routinely with the SHELX program.

Experience with collecting data on cobalamin derivatives with G. Faerber and Ch. Kratky (University of Graz) also stressed the advantage of collecting data on medium size crystals using the oscillation method and the combination of an Imaging Plate Scanner with an Mo sealed tube source or synchrotron radiation. On the diffractometer to collect the 1.0 A data set with about 30 % amount of observed reflections at the highest resolution shell required about a week. In contrast, using the oscillation method even with two or three data sets merged together at high, medium and low resolution to cover strong as well as weak reflections, required about a day using the Mo sealed tube and about 5 hours using the synchrotron source, with substantially higher percentage of observed reflections at highest resolution of 1.0 (Mo Kα) or 0.8 Å (SR).

The last example is data collection on crystals of aluminium selenium phosphate (cooperation with A. Cheetham, Santa Barbara) with cell dimensions 5 x 5 x 11 Å and the point group P321, possibly the smallest ever cell for which data were collected by the oscillation method

and strategy of data collection and processing developed for protein crystals. 18 images of 10° oscillation were collected twice, with exposure times differing by about 30 times. The diffraction pattern was highly pseudosymmetric, with even-l reflections very strong and odd-l reflections very weak. The data collected on the X31 beam line and 0.65 A wavelength merged with R(merge) of 4 % to give 252 unique reflections of which only 2 were unobserved, i.e. below the 2 σ(I) limit. 12 reflections are missing from this 0.8 Å data set of which 6 are systematically absent along the 00l axis.

A report on the European Synchrotron Radiation Facility made at the Facilities Workshop held in Hamburg December 13–14 1991
by J.R. Helliwell, Department of Chemistry, University of Manchester and SERC, Daresbury Laboratory

The European Synchrotron Radiation Facility (ESRF) is under construction in Grenoble, arguably Europe's "Science City". The ESRF represents a cooperation of Europe's nation states to keep Europe at the forefront of a field in which it has excelled in the last 15–20 years. It is a so–called 3rd generation machine being dedicated to synchrotron radiation (SR) science with the SR emanating for a variety of insertion devices (undulators and wigglers) as well as its bending magnets. The ESRF will be the first such 3rd generation machine to come on–line in the world but being closely followed by similar machines in the USA (the "Advanced Photon Source (APS)", under construction at Argonnne National Laboratory, near Chicago) and in Japan (the "Super Photon Ring"running at 8 GeV, Spring–8, under construction in Nishi–Harima).

The ESRF machine installation has passed key installation and operational milestones under the energetic leadership of the Machine Director, J.–L. Laclare and his deputy, G. Mülhaupt and the dedication of the Machine Division staff. Both the LINAC and Booster are now operational. In November 1991 the Booster reached 6 GeV and 5 mA. The installation of the lattice on the main ring is well underway. Overall the whole machine complex is 6 months ahead of schedule. This feat brought commendation for the Grenoble team from the Machine Advisory Committee (MAC), an international group of machine experts, at its last meeting.

Pressure on the Experiments Division and the scientific community is intense now to be ready to exploit the fantastic specification of this machine at an earlier than expected turn on date. The first seven insertion device beamlines are

proceeding as quickly as possible. The designs have required pioneering experiments on high heat load optics and are pushing the limits of commercial mirror technology. In addition to the insertion devices the bending magnets offer a superb brilliance with emission into the hard X–ray range (λ's $\approx$ 0.5Å and less).

Macromolecular crystallography (MX) has a strong interest in two of the beamlines in Phase I namely lines 3 and 4. Line 3 is a multipole wiggler line offering white beam (Laue) and a monochromatic mode; the "Beamline Responsible" is Michael Wulf and the guideline split is 70% for MX and 30% for high pressure materials science. Line 4 is an undulator beamline offering unprecedented brilliance especially suited for large unit cell data collection; the Beamline Responsible is Peter Bosecke and the guideline split is 50% MX and 50% small angle scattering (there will be separate hutches for each).

Criticism of the volume of beam time for MX and ESRF has led to general acceptance 'that further facilities for MX are required. As a result line 19 fed by a bending magnet is being developed jointly by ESRF and EMBL in Grenoble primarily for multi–wavelength experiments (especially MAD); the Beamline Responsible is Andy Thompson. It has also been agreed by ESRF management and the Scientific Advisory Committee (SAC) that line 20 should be developed and dedicated for high brilliance MX fed by an undulator. Its target operational date is 1996 and when it comes online then beamline 4 would become dedicated to small angle scattering. It has also been agreed by ESRF management and the SAC that for the full exploitation of the above beamlines a full cooperation between ESRF and EMBL is to be welcomed. Amongst other things the existing infrastructure and facilities of the EMBL Outstation in Grenoble for diffraction experiments and for detector development specific to MX gives ESRF, Grenoble an important lead over its counterparts in the USA and Japan. Detector development activity for MX has to be increased however; fortunately Europe has

strengths in MWPC's, CCD's and (now) IP's on which to build. The massive potential of ESRF for MX has also been recognised by the establishment of the Institute of Biological Structure (IBS), by French Government Agencies, adjacent to the ESRF (and of course to ILL). A bending magnet beamline is being developed by IBS for a variety of techniques including MX, EXAFS and diffuse scattering; the Beamline Responsible is Michel Roth. A close cooperation between all bending magnet developers is essential and facilitated by a CRG (Collaborating Research Group) bending magnet club. Also, of interest for MX is the Swiss/Norwegian beamline, comprising two branches with different optics; the Project Leader is Phil Pattison.

Input from the MX community to ESRF is coming via ESRF User's Information Meetings, a Diffraction Advisory Group (including Keith Wilson, Roger Fourme, J.R. Helliwell) and the Scientific Advisory Committee (which includes J.R. Helliwell). In addition to these and the people mentioned earlier, other familiar contacts for the MX community are Carl Branden (Science Co–Director from 1/4/92) and S. Cusack (EMBL Outstation Director). As well as detailed input on the above beamlines several general factors are being stressed. The need for an appropriate volume of beamtime allocation to the MX field has been stressed (spearheaded by Ada Yonath). Also, our strong interest in long lifetime beams and a stable source has been stressed. The Machine Division have plans to implement a positron option, after an initial phase using electrons, which will help both these factors. They also have an extensive scheme of insertion device beamline feedback control of position and angle. Anxieties remain for us with respect to two main areas. Firstly, the GRAAL experiment, involving firing a laser beam through the electron beam to produce gamma rays, is expected to reduce the beam lifetime by 20% when operational. But really how did such a proposal get so far since it will deleteriously affect all the SR science on

our premier European source?! A second anxiety, hopefully very temporary, is the current settling of the site at values of microns per day.

Matters facing ESRF and the MX Community at present largely involve forward planning and organisation. The challenge from the USA and Japan is potentially strong. Fortunately our field is noted for its skills of cooperation. Hence, the outside challenge will bring out the best of what we have to offer science as well as the community at large, who perceive the utility of this research.

Footnote

Useful units and definitions of the source are the flux, brightness and brilliance where

[Flux] = photons s^{-1} $(0.1\%\ \delta\lambda/\lambda)^{-1}$

[Brightness] = photons s^{-1} $(0.1\%\ \delta\lambda/\lambda)^{-1}$ $mrad^{-2}$

[Brilliance] = photons s^{-1} $(0.1\%\ \delta\lambda/\lambda)^{-1}$ $mrad^{-2}$ mm^{-2}

Brilliance is a particularly useful definition for experiments with small samples whilst also requiring a well collimated beam. These definitions are the so–called European ones (i.e. used in the ESRF Red Book). There are alternative definitions (but are not given here).

Current plans for collaboration between EMBL and the ESRF.

Stephen Cusack, EMBL Grenoble Outstation.

The ESRF Red Book (1987), in its brief discussion of the special needs of biology at the ESRF contains the sentence (p529) "A fuller scientific back-up for biological sciences at ESRF will be discussed with the Director General of the European Molecular Biology Laboratory with a view to considering the role of the present EMBL outstation at the Institut Laue-Langevin". Such discussions on the role of EMBL at the ESRF have been going on ever since and despite difficulties, have recently resulted in a draft agreement (outlined below), which has been accepted by the EMBL Council and is still under discussion by the ESRF Council.

The **Grenoble Outstation of EMBL** was established in 1976 under Dr. Andrew Miller as a biological service laboratory for visitors to the high-flux neutron reactor at the Institut Laue Langevin (ILL). The Outstation was substantially devoloped under Dr. Bernard Jacrot in the new building ILL20 on the ILL site. The roles of the Outstation are:

(a) Provision of biochemical and biophysical service facilities for biologists visiting the ILL for neutron experiments.

(b) Provision of complementary structural techniques for both in house researchers and visitors (electron microscopy, dynamic light scattering, image processing, X-ray scattering, deuteration laboratory) to permit good physical characterisation of samples and preparation of complicated experiments.

(c) Development of new neutron techniques (usually in close collaboration with ILL scientists):

- low resolution neutron diffraction of crystals of biological complexes (nuclesome, viruses, tRNA-synthetase complex, membrane proteins, ribosome). The dedicated low resolution neutron diffractometer DB21 was built in a 50% collaboration with the ILL for this purpose.
- use of inelastic neutron scattering to study protein dynamics and directly test molecular dynamics calculations,
- design of a quasi-Laue neutron diffractometer for high resolution protein crystallography (Clive Wilkinson and Morgens Lehmann (ILL)).

(d) Integrated in-house research programmes in structural biology, necessitating both molecular biology and biophysical techniques (e.g. viral proteins, aminoacyl-tRNA synthetases, super-coiled DNA).

(e) Development of multi-wire gas detectors for X-rays (André Gabriel).

With the coming of the ESRF, EMBL saw an excellent opportunity to extend its facilities at Grenoble and become a major international focus for the application of both neutron and X-ray diffraction to structural biology. In keeping with its philosophy towards the ILL however, EMBL wishes to do more than just provide wet biochemical facilities for visitors to the ESRF; it wishes for a direct involvement in the design, construction and running of dedicated beamlines for structural biology. In addition there should be in-house research programmes orientated towards use of synchrotron radiation in biology. The experience at the Hamburg Outstation of EMBL has shown that such an approach is a good basis for the provision of forefront synchrotron facilities for the benefit of scientists all over Europe. It should be stressed that EMBL is by no means seeking a monopoly on structural biology at the ESRF. Indeed it sees colloboration with other interests (e.g. the French Institut de Biologie Structurale (IBS), the various national CRGs and of course any biologists at the ESRF) as vital for the success of the effort in Grenoble. However being an international laboratory it can have a special role in representing the interests of the large European biological synchrotron radiation user community.

To these ends, EMBL has proposed the following, as the basis of a collaboration with the ESRF:

(a) Appoint a scientist to be responsible for the design of a bending magnet beamline dedicated for anomalous scattering in protein crystallography (BL19). Construction would be in collaboration with the ESRF. Andrew Thompson has been appointed to this position (see his contribution).

(b) Appoint a scientist to be responsible for the protein crystallography station on the ESRF undulator BL4 which is currently shared with small angle scattering. This is to ensure the optimal set up for measurement of weakly diffracting macromolecular crystals (e.g. large unit cells, frozen micro-crystals).

(c) Work with the ESRF on the design and construction of a dedicated undulator beamline (BL20) to replace BL4.

(d) Prepare a proposal for an EMBL-funded beamline (CRG).

(e) Appoint initially 2 engineers/technicians and 3 scientists to aid in design, construction and running of the beamlines.

(f) Provide biochemical laboratory facilities for short and long term ESRF visitors.

(g) Establish a biophysics group to develop applications of intense synchrotron beams (e.g. Laue, time-resolved studies and MAD).

(h) These expanded facilities will be housed in an extension of about 850 m^2 to the current Outstation building.

These proposal are the basis of the draft agreement signed by the Director Generals of EMBL and ESRF in October 1991.

BEAMLINE 4 OF THE ESRF: A HIGH-BRILLIANCE BEAMLINE FOR MACROMOLECULAR CRYSTALLOGRAPHY AND SMALL-ANGLE X-RAY SCATTERING

Peter Bösecke, ESRF, B.P. 220, F-38043 Grenoble Cedex

The ESRF Beamline is an undulator beamline at a high-β section of the storage ring (Table 1). The beamline is dedicated to X-ray studies on macromolecular structures with large internal dimensions (unit cells): a) Time resolved small angle X-ray scattering (SAXS), b) biological macromolecular crystallography. It will be available in the course of the year 1994 (see also [1]).

The beamline will provide high flux of monochromatic photons with low divergence through a sample cross section of typically 100 μm × 300 μm. It will preferably be used around 0.1 nm wavelength (12keV). Three insertion device segments of each 1.6 m length can be installed. At the beginning only one undulator segment with 46 mm period will be installed. A second segment with 26 mm period is proposed (Table 2). Only the 46 mm type will be mentioned here. A 500μm thick cooled Be-window at the interface between the storage ring and the beamline will absorb wavelengths longer than 0.25 nm. In the central radiation cone the remaining power density is 20W/mm^2. The total beam power will be in the order of 100 W. A cryogenically cooled silicon monochromator can withstand this power load without severe broadening of the rocking curve [2]. The optics will therefore consists of a Si(111) double crystal monochromator followed by a double focusing mirror with total reflection for wavelengths longer than 0.73 nm (Table 3). It must be removed for work at smaller wavelengths. Because of the small beam divergencies the focusing parameters (curvature) are fixed. The expected parameters of the beam at the source at 65 m are listed in Table 4. The experiments hutch is devided into two parts (Fig. 1). One part between 50 m and 55 m from the source will be used for crystallographic experiments .In this distance the beam has its smallest size (Fig. 2). The small-angle X-ray scattering hutch follows immediately afterwards (55 m - 71 m). The sample is always located at 57 m. The range of scattering angles can be chosen by changing the distance between detector and sample. A sample-detector distance of about 10 m should give the best small-angle scattering-resolution (vertically about 1000 nm). No refocusing of the beam to the new detector position will be necessary. The expected beam size at the sample position is shown in Table 5.

Because the ideal detector does not exist yet different types of detectors will be available. The crystallography experiment will be equipped with a goniometer and an image plate system.

Figures

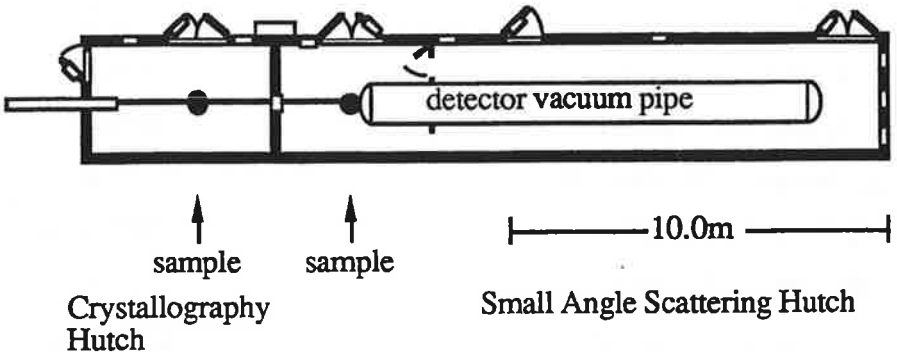

Fig. 1: Experiments Hutches

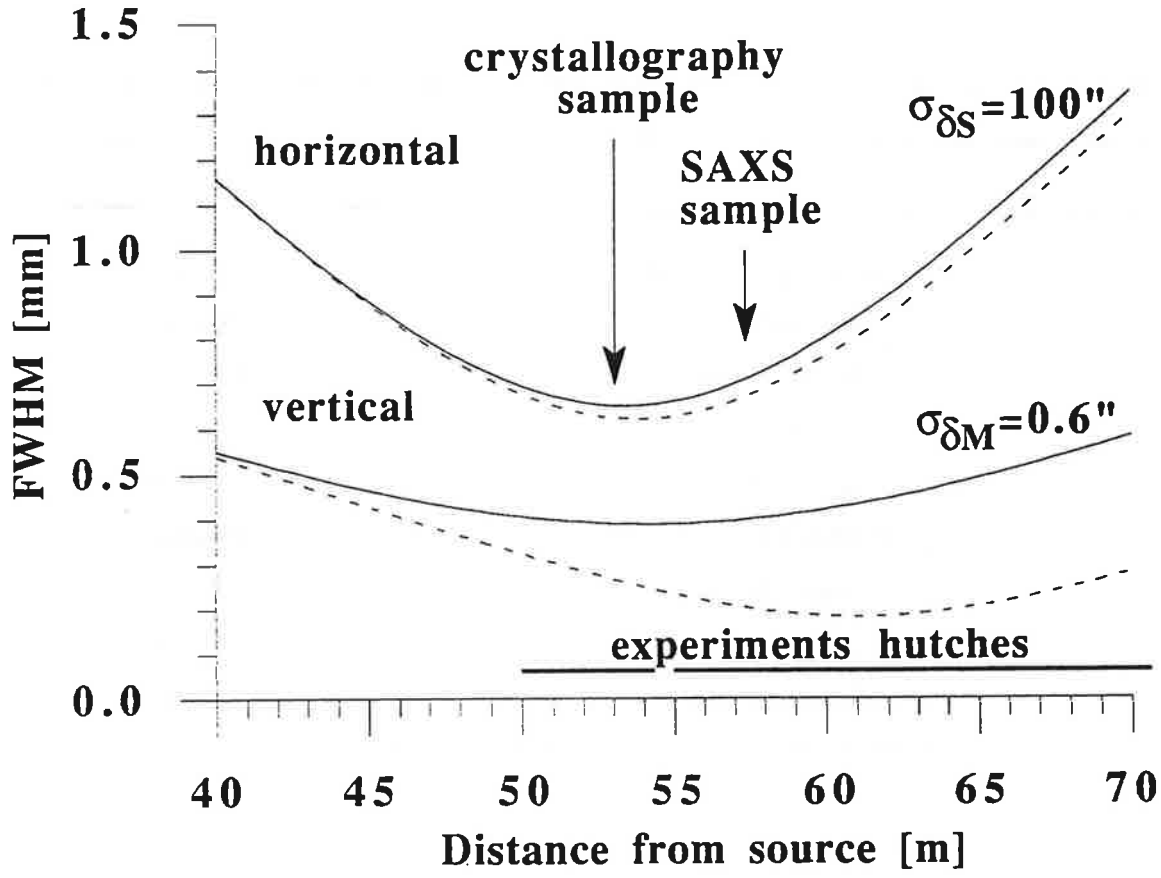

Fig. 2: Beamsize along the experiments hutch of the High-brilliance beamline: full line: including slope errors ($\sigma_{\delta S}$: sagittal RMS slope error, $\sigma_{\delta M}$: meridional RMS slope error), dashed line: ideal mirror without slope errors.

Table 1

Electron beam parameters of the high-β section of the ESRF storage ring at which the insertion device of the beamline will be installed (x: horizontal, z: vertical direction).

E_e (electron energy):	6 GeV
I_e (electron current):	100 mA
β_x (horizontal β-function):	27 m
ε_x (horizontal emittance):	$7 \cdot 10^{-9}$ m·rad
β_z (vertical β-function):	11 m
ε_z (vertical emittance):	$7 \cdot 10^{-10}$ m·rad

Table 2

Parameters of the undulators. Three undulator segments of 1.6 m length can be installed. Initially only segment A will be available.

B_r (remanent magnetic field):	1.1 T
d_g (gap width):	≥20 mm
L_u (undulator length):	1.6 m
segment A	
X-ray wavelength range	$\lambda \leq 0.25$ nm
λ_u (undulator period):	46 mm
segment B	
X-ray wavelength range	0.1 nm
λ_u (undulator period):	26 mm

Table 3

Optical setup of the ESRF High-brilliance Beamline (BL 4)

Position	Device
0 m	insertion device (Table 2)
24 m	cooled beryllium window (500 μm thick)
29.6 m	Si(111) double-monochromator (50 mm vertical displacement, first crystal cryogenically cooled)
32.5 m	toroidal mirror (Rh-coated, length 400mm, vertical reflection angle ϑ=3.9 mrad, $\lambda \geq$ 0.073 nm)
50 m - 55 m	crystallography hutch
53 m	goniometer
53 m - 55 m	image-plate detector
55 m - 71 m	small-angle scattering hutch
57 m	sample stage
57.5 m - 67.5 m	2d-detector
71 m	end of hutch

Table 4

Properties of the beam at 12 keV (absolute flux values of the source calculated with RADIA [3], focus parameters calculated with SHADOW [4] for an ideal mirror).

position	at the source (0 m) (central undulator cone)	at 65 m $\Delta E/E=2\cdot10^{-4}$
flux characteristics	$1.42\cdot10^{17}$ Ph/s/0.1%/mm^2/mrad^2	$8\cdot10^{12}$ Ph/s
$FWHM_x$	1.03 mm	0.95 mm
FWHMx'	0.043 mrad	0.069 mrad
FWHMz	0.21 mm	0.21 mm
FWHMz'	0.027 mrad	0.025 mrad

Table 5

Beam sizes around the sample position (55m, 12keV).

	$FWHM_x$ (horizontal size)	$FWHM_z$ (vertical size)
unfocused	2.6 mm	1.3 mm
focused (ideal mirror)	0.6 mm	0.2 mm
focused (0.6" RMS-slope error)	0.7 mm	0.4 mm

References

[1] Peter Bösecke, *The High-flux Beamline at the ESRF*, to be published in Rev. Sci. Instrum. 63 (1992),

[2] G. Marot, et al., *Cryogenic Cooling of X-ray Monochromators*, to be published in Rev. Sci. Instrum. 63 (1992),

[3] P. Elleaume, RADIA ESRF, Grenoble 1989

[4] F. Cerrina, B. Lai, F. Cerrina, *SHADOW*, Nucl. Instr. and Meth. A246 (1986), pp. 337.

The ESRF MAD Beamline .

Andy Thompson (EMBL Grenoble)

An ESRF beam line for MAD is to be built on a bending magnet in collaboration with the EMBL. Some initial design considerations are presented. These are the basis for discussion amongst the PX community, and a workshop for this purpose is to be organised in Feb/Mar 92 .

1. The ESRF Bending Magnets as a Source for PX.

Even with the predicted beam size increase (due to 'mechanical instabilities') of 30% vertical, 9% horizontal [1] , the source size (0.14 x 0.13 mm sigma), critical wavelength (0.6 A) and collimation of the source is extremely attractive for macromolecular crystallography. The intensity gain over station 9.5 of the Daresbury SRS varies between 32 and 40 (see table 1) covering the wavelength range over which the Daresbury mirror reflects well. Clearly several points have to be borne in mind with this type of comparison :-

a) The ESRF is a new machine, and may not achieve high currents initially. Currents of > 300 mA are regularly achieved at Daresbury, whereas 100 mA is initially expected at ESRF.

b) Longer mirrors ,and hence larger vertical acceptances, can be considered at the ESRF as there are no space limitations.

c) The ESRF gains at wavelengths lower than 0.6A are much larger . The choice of mirror grazing angle is also imporatnt here.

2. Exploitation of the Properties of the ESRF for MAD.

The experimental requirements for MAD are well documented (see for example [2] and [3]), and can be summarised as:-

Narrow (10e-4) bandpass, wide wavelength range, rapidly tuneable, stable beam conditions, 'full' goniometry, sample cooling, automated data acquisition.

In addition, 'typical' samples which are candidates for the MAD technique will have neither an extremely large unit cell, nor an extremely small physical size . Taking these factors and the ESRF source parameters into consideration one can say that:-

a) There is no real requirement for either a very tiny focal spot size or extremely good collimation (though the possibility of the latter should be preserved if possible). The option of using the optical system focussed or slightly defocussed (in order to de - emphasise possible source movements) should be left open.
b) The monochromator is the 'work horse' on which the success of the station depends. The accuracy of angular positioning of the monochromator can be regarded as a solved problem with modern encoder/feedback systems, but the additional complications to the design (such as constant beam output height, offset of harmonics and sagittal focussing) should be approached with caution given the extreme reproducibility required.
c) The vertical collimation of the source makes a long mirror (or a segmented mirror?) attractive.
d) The grazing angle of the mirror can be chosen to reflect the hard wavelengths, to give a range of (say) 0.3 - 2 Angstrom.

3. Data Collection Protocol.

The choice of a data collection protocol is closely tied to the station design. Typically (in order to avoid temporal errors in beam and radiation damage) data are recorded for 4 wavelengths sequentially in narrow angular ranges (a few degrees). Three of these wavelengths are in the immediate vicinity of the absorption edge, the fourth is generally removed by 0.1 - 0.3 A to the harder side of the edge (to reduce radiation damage). The adoption of this protocol makes the choice of a sagitally focussing monochromator inadvisable, as the collection of the 4th wavelength will require the reoptimisation of the sagittal focus and the beam position (figs 1 and 2) - both mechanical operations prone to backlash and similar positioning error. If the requirement for collecting all 4 wavelengths simultaneously is relaxed, then careful reoptimisation for the collection of all the off edge data is a sensible option. (Here it should be borne in mind that a monochromator for MAD is NOT continuously scanning as , for example, an EXAFS monochromator - the rapid jumping from one wavelength to another makes things more difficult, not easier!)

4. Data Collection.

The detector is, of course, another crucial element of the whole

station. Indeed, it is only recent improvements in detector technology (notably the ip with its high dynamic range) that have made the MAD technique more tractable. The quality of MAD data coming out of facilities using ip systems should be carefully evaluated. In addition, the repetitive nature of the experiment makes it an ideal 'target' for automation ie computerised detector readout, crystal positioning, wavelength adjustment etc. As data is collected, there is a clear requirement for 'on line' evaluation - any poor quality data can then be recollected with the same sample , difficulties due to beam or optical instability (or poor sample!) will be immediately apparent. The minimum requirement for data storage and (realistic) on - line data evaluation should be considered part of the station development.

5. Conclusions.

The ESRF bending magnet offers an opportunity to build a MAD station with extended wavelength range into higher energies (Iodine K edge) whilst preserving good intensity and collimation in the focal spot. Two popular designs for achieving this exist (cylindrical mirror/sagittal focussing monochromator, toroidal mirror/channel cut or constant output height monochromator) - either can produce a small focal spot size, and both produce satisfactory resolution. The choice of one or the other is dependent on data collection protocol. Additional complications to the monochromator should be avoided IF POSSIBLE - for example harmonic rejection can be easily achieved with a post - mirror. The existing image plate systems are likely to prove satisfactory detector elements, but this should not preclude efforts to develop detectors specifically for MAD work. The requirement for on line data processing is a neccessary part of the station design.

TABLE 1

Wavelength (A)	Gain (BL19/9.5)
1.5	32 - 44
0.9	38 - 52
0.6	43 - 58
0.3	Not reflected by 9.5 mirror > 200

Note - The comparison is for a 75 cm Pt coated mirror, graze angle 3mr object distance 18m for the SRS (1.3:1 focussing); graze angle 2mr object distance 23.5m for the ESRF(1:1 focussing). The range of

gain covers zero beam blow up to predicted beam blow up. The comparison is on the basis of photons/sec/mm**2/mrad horiz/mA/0.01% bw vert. integrated into the mirror acceptance.

REFERENCES

1. P. Ellaume - ESRF User Meeting Handbook (July 91) p 6.
2. R. Fourme - Synchrotron Radiation for X Ray Crystallography (Notes of International School of Crystallography, Erice 1986)
3. W. Hendrickson and R. Fourme - in Synchrotron Radiation and Biophysics (ed Hasnain) J. Wiley 1991.

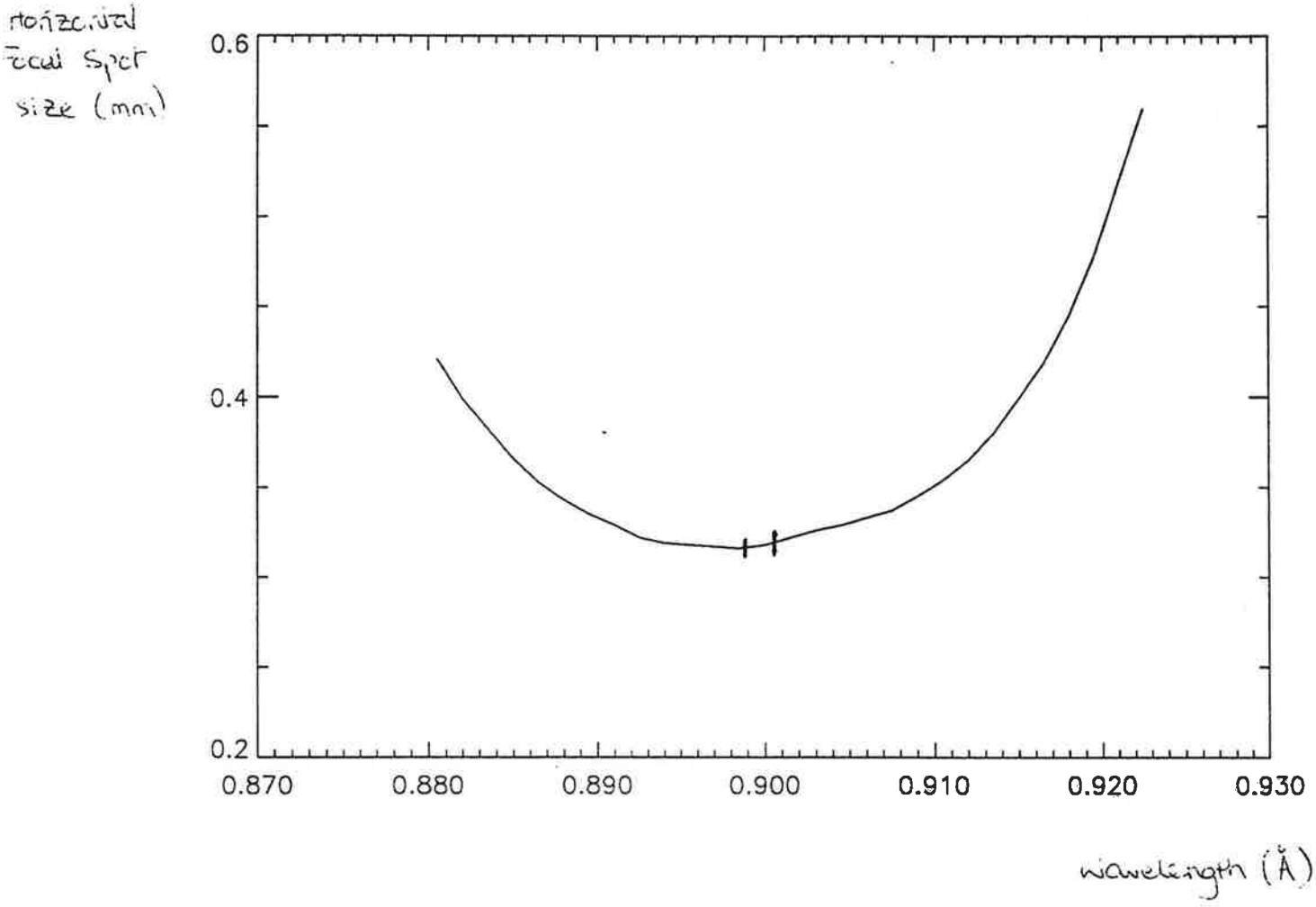

VARIATION OF SPOT SIZE WITH λ, SAGITTAL CURVATURE FIXED ESi (220) Mono

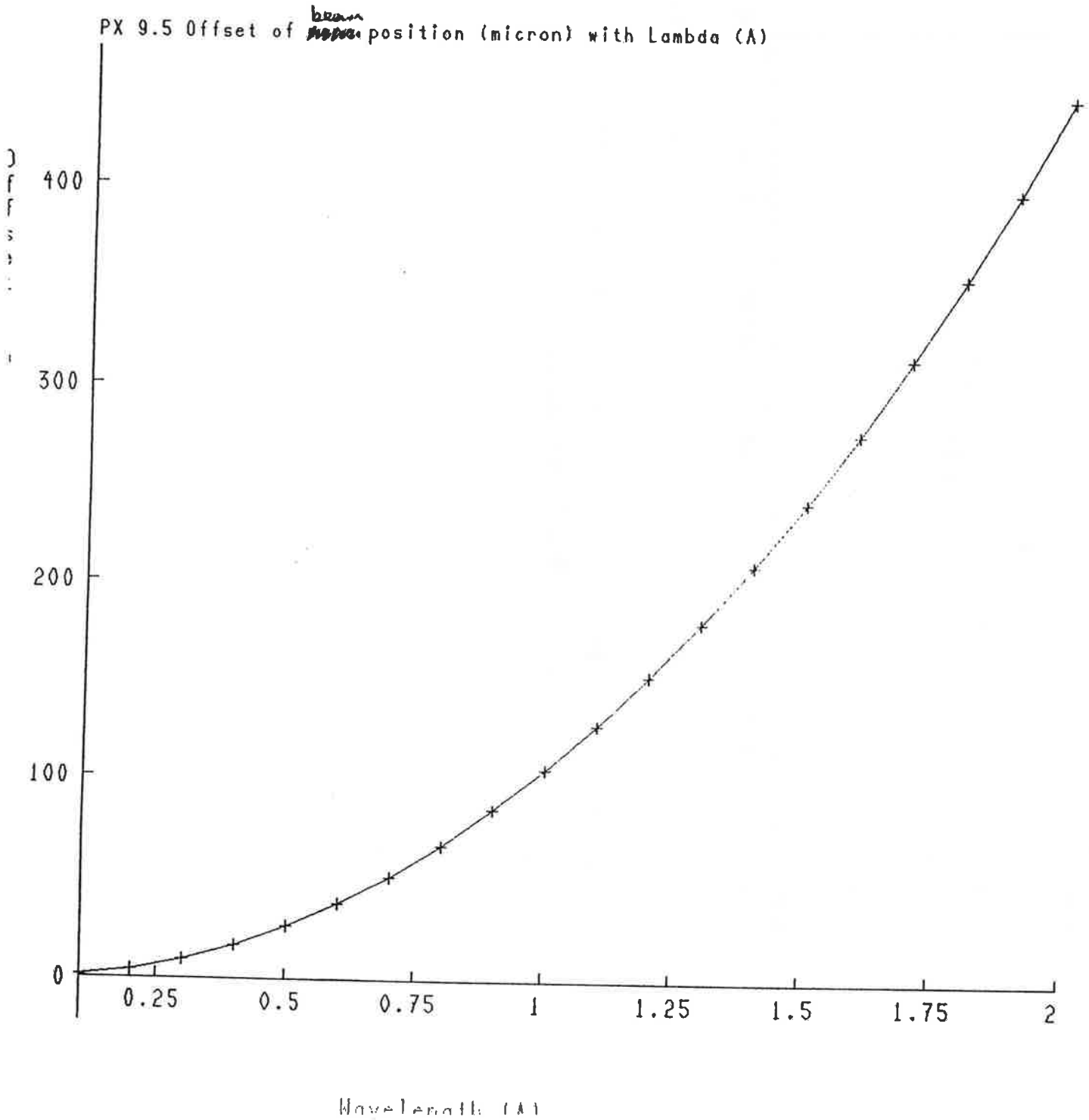

offset of double crystal channel cut monochromator

- crystal gap 5mm

Si(111) mono

The Swiss-Norwegian Beam Line at the ESRF

by

P. Pattison and H.-P.Weber, Institut de Cristallographie, Université de Lausanne, CH-1015 Lausanne, Switzerland

The Swiss-Norwegian Beam Line will be an independent experimental facility operating within the European Synchrotron Radiation Facility (ESRF) in Grenoble. It will take the synchrotron radiation supplied by an ESRF bending magnet source and, using various optical elements for energy selection and beam focussing, it will deliver the beam beam onto a number of different types of experimental equipment. These include apparatus for materials science and macromolecular studies on single crystals, a powder diffractometer, an EXAFS rig and a white beam topography camera.

The synchrotron radiation beam provided by the ESRF will emerge in a 6mrad horizontal fan through a Be window and shield wall about 23m from the bending magnet source (Dipole 1). The resulting beam cross section is approximately 140mm wide and 3mm high. An arrangement of cooled slits and absorbers will split the beam into two parts immediately after the shield wall. A vacuum pipe will deliver a 1mrad fan of radiation directly into an experimental hutch (**Station B**) situated about 10m further downstream. A water-cooled flat double crystal monochromator will select the appropriate wavelength for either a powder diffractometer or absorption (EXAFS) spectrometer. Both instruments can be permanently installed within the hutch. A camera for white-beam topography can also be installed in this area, in which case the monochromator would be driven out of the beam.

On the other side of the beamline, a 2.5mrad fan will first be vertically collimated by a primary mirror. This will produce a highly parallel beam incident on a double crystal monochromator, enabling both high through-put and narrow energy resolution to be achieved. The first crystal of the monochromator will be water-cooled, while the second crystal will be sagittally bent for horizontal focussing. Finally a secondary mirror will provide vertical focussing, resulting in a point-to-point focus. The focus will be inside a second hutch (**Station A**), in which a single crystal diffractometer will be installed. The mirrors, the monochromator and the beam pipe will all be under high vacuum. A control system will be developed to monitor and control the beamline vacuum, beam shutters, valves etc, as well as the movement of the optical components and the acquisition of data. The second hutch will be equipped both for high resolution single crystal diffraction (for measurements on inorganic or small molecule crystals) and with an area detector suitable for macromolecular crystallography. Sufficient space will be provided in the hutch to allow non-standard equipment to be installed behind the diffractometer, for other experiments which may later take advantage of the focussed synchrotron radiation beam.

THE *INSTITUT DE BIOLOGIE STRUCTURALE* (IBS) AND THE CRG/D2AM BEAM-LINE IN GRENOBLE, FRANCE.

by M.ROTH, DSV/DIEP/LCCP, Centre d'Etudes Nucléaires, BP85X, 38041 Grenoble.

The IBS, a French Institute supported jointly by the CEA (Commissariat à l'Energie Atomique) and the CNRS (Centre National de la Recherche Scientifique), Director Professor J.P.Ebel, is going to regroup about ten groups or laboratories specialised in different domains of structural biology: structural enzymology, protein folding, protein-protein assembly, protein-nucleic acid interaction, cytoskelet proteins, protein engineering. Most of the technics currently used in structural biology are going to be represented at IBS: macromolecular X ray crystallography, nuclear magnetic resonance (400 and 600 Mhz), electron microscopy, analytical biochemistry and peptide synthesis, mass spectrometry, and other structural biophysics techniques.

The IBS will open the doors in 1992, in a new building of nearly 5000m^2 (3500m^2 laboratories), located next to the ESRF/ILL ground. About 1000 m^2 will be available for X ray crystallography and crystal growth biochemistry.

The main activity of the IBS will be in house research, but an additional function will be also the welcoming and assistance to future ESRF and ILL beam-line users or user groups.

The current involvement of the IBS with respect to ESRF, is first its contribution to the construction of the D2AM beam-line at the ESRF (0.8T bending magnet), as a member of the French Collective Research Group (CRG) D2AM. This task has been undertaken since 1 and 1/2 year now by the "Synchrotron Group" of one (CEA) of the two X ray crystallography groups which are going to join the IBS in 1992.

Beside the D2AM beam line construction work, software for the treatment of the anomalous diffraction data, is currently developped, following the W.A.Hendrickson methodology, and the user interface of this software on Workstation, as well.

In a completely different domain, an experimental setting for LAUE diffraction experiments is currently in preparation, in the same group, for using the future ESRF LAUE diffraction station which will be available rather soon for test experiments.

Description of the D2AM beam line.

The beam-line is designed according to the following characteristics:

1. Point focusing of the beam on the crystal at fixed sample position,
2. High energy resolution: 2 - 5 eV

3. High Q resolution: $2\ 10^{-3}$ Å^{-1}

4. Accessible wavelength range: 0.5 - 2.5 Å i.e.25 - 5 keV

5. High rate of harmonic rejection: 10^{-4}

The optics will be constituted by a two crystals monochromator between two symmetrical cylindrical parabolic mirrors in a compact arrangement, with double focusing. This design should provide maximum intensity and great flexibility in use.

Bending magnet beam characteristics are:

* intensity at the source ~ 10^{13} photons/sec.mrad-of-horiz.-divergence.0.1%δE/E
* vertical size of the source : σ_v = 0.13 mm i.e. FWHM =0.3 mm,
* vertical divergence at the source(FWHM) between 0.11 mrad and 0.25 mrad
* horizontal divergence used: 3 mrad (out of 6 mrad available),

According to SHADOW simulations, the beam at sample position will have: resolution: 2.5 eV at 12.5keV (Si[111]) i.e. $\delta\lambda/\lambda \sim 2\ 10^{-4}$, intensity ~ 10^{12} photons/sec/mrad, size ~ 0.3x0.3 mm^2.

The different elements of the beam-line are now defined, and their realisation (detailed studies and construction by private companies) will begin in early 92. The beam-line will be constructed on the ESRF site during the first half of 93, including the installation of the main optical elements. The second half of 93 will be devoted to tests and alignements. The line will be open for public use in July 94.

A (relatively) small X ray crystallography lab (~ 40m^2) will be installed on the site, behind the experimental SR station, for crystal preparation, tests and pre-alignement. In this lab, the beam-line users will also find extensive computing facilities for data evaluation.

Synchrotron radiation from PETRA II, the electron booster storage ring of HERA

Jochen R. Schneider
Hamburger Synchrotronstrahlungslabor HASYLAB at
Deutsches Elektronen-Synchrotron DESY
Notkestr. 85, D-2000 Hamburg 52, FRG

Recently the storage ring PETRA has been reconstructed to an electron and proton booster storage ring for HERA, the new superconducting hadron electron storage ring at DESY. The expected lifetime in HERA is 3 hours for electrons, and 12 hours for protons. Between injections PETRA II could be used effectively as a storage ring for the production of synchrotron radiation without deterioration of its quality as a booster for HERA.

For synchrotron radiation users an electron beam of 10 to 15 GeV and undulators with a length of about 5 m would be desireable. To fulfil the magnetic requirements for this scenario the undulators have to be closed to a gap of 10 to 15 mm. However, the protons need a vacuum aperture of 30 to 40 mm. In order to make these different requirements compatible a bypass for synchrotron radiation experiments at PETRA II has been suggested (**W. Brefeld** and **P. Gürtler**, *Proccedings of the Particle Accelarator Conference*, Stanford, 1991).

At 13 GeV the existing electron booster optics of PETRA II provides an emittance of 79 nmrad. The photon beam divergence would be $\sigma_{x'}$ = 0.053 mrad horizontal and $\sigma_{z'}$ = 0.012 mrad vertical, the source size would be of the order of $\sigma_x \sim 1.5$ mm horizonal and $\sigma_z \sim 0.25$ mm vertical. At the experiment, in a distance of 100 m from the undulator, the beam dimensions would be 12 x 2.7 mm^2. Fig.1 shows the spectral brightness calculated for an undulator in hybrid technology with a period of 3.35 cm and a gap height of 11 mm, operated at an electron energy of 14 GeV. By opening the gap the energy of the photons from the fundamental can be tuned between 20 and 40 keV with almost constant intensity. Including third and fifth harmonic the energy range from 20 to 200 keV is covered by one device.

The total radiation power emitted by the proposed undulator is 13.7 kW and extreme heat load problems are expected at first glance. However, the spectral power distribution of the proposed undulator, shown in Fig.2, demonstrates, that in the energy range up to 5 keV only 130 W are emitted, in the range up to 15 keV the emitted power is 880 W. Therefore the heat load problem can be solved by applying proper absorber systems.

Compared to DORIS III, for X-rays with energies above 20 keV the gain in brightness is tremendous. With respect to the design values of the ESRF gain factors between 10 and 1000 can be expected. The longer term prospects of PETRA II are even better, because the electron optics can be improved to provide an emittance of approximately 10 nmrad at 14 GeV electron energy. Synchrotron radiation from undulators installed in a PETRA II bypass will open exciting new fields in research, including structural biology, inelastic scattering experiments with 5 meV resolution, Mößbauer spectroscopy, and high energy photon scattering.

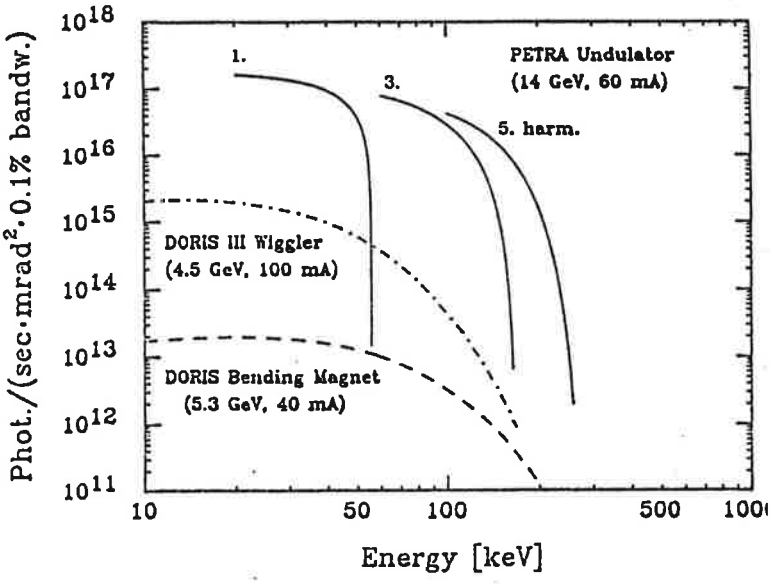

Fig.1 Central brightness of a PETRA II bypass undulator for the existing electron booster optics.

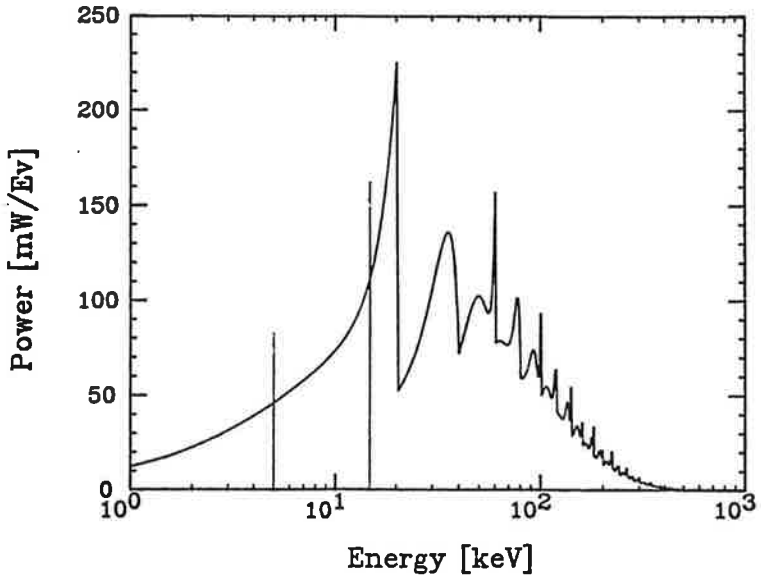

Fig.2 Spectral power distribution for the PETRA II undulator characterized in Fig.1.